SEMI-FLUORINATED CORE-SHELL LATEXES AND MODEL RANDOM POLYAMPHOLYTES

By

BALJINDER KAUR

Bachelor of Science
Punjab University
Chandigarh, India
2001

Master of Science in Organic Chemistry
Punjabi University
Patiala, India
2003

Submitted to the Faculty of the
Graduate College of the
Oklahoma State University
in partial fulfillment of
the requirements for
the Degree of
DOCTOR OF PHILOSOPHY
July, 2010

SEMI-FLUORINATED CORE-SHELL LATEXES

AND MODEL RANDOM POLYAMPHOLYTES

Dissertation Approved:

Dr. Warren T. Ford

Dissertation Adviser

Dr. K. Darrell Berlin

Dr. Richard A. Bunce

Dr. Jeffery L. White

Dr. Gary Foutch

Dr. Mark E. Payton

Dean of the Graduate College

PREFACE

Polymer colloids are the dispersed polymer particles in liquid media that stay dispersed indefinitely. Cationic polymer colloids can act as phase transfer catalysts (PTC) for the decomposition of toxic organic compounds. A PTC is a catalyst which facilitates the migration of a reactant in a heterogeneous system from one phase to another where reaction can take place. This results in the reaction of charged reactants, often insoluble in oil, with uncharged reagents. The objective of the first research project was to synthesize semi–fluorinated core-shell polymer colloidal phase transfer catalysts in water, for the decontamination of chemical warfare agents.

Polymer colloids were prepared with different compositions of 2,2,2-trifluoroethyl methacrylate and 1H,1H,2H,2H-perfluoroalkyl methacrylate by shot-growth emulsion polymerization of 2-ethylhexyl methacrylate (EHMA), vinylbenzyl chloride (VBC), (vinylbenzyl) trimethylammonium chloride, 2,2,2-trifluoroethyl methacrylate and 1H,1H,2H,2H-perfluoroalkyl methacrylate in aqueous media. Polymer colloids were quaternized by the reaction of VBC with trimethylamine to give quaternary ammonium ion colloidal particles. The colloidal particles and the coatings made from them were used as phase transfer catalysts for the hydrolysis of *p*-nitrophenyl hexanoate and Paraoxon, which are simulants of chemical warfare agents. Catalysis with the particles was fast when compared to the catalysis on the coatings.

The objective of the second research project was to synthesize model random polyampholytes in order to test the modern theory of polyampholytes. Polyampholytes contain both negatively and positively charged functional groups on different monomer units. They may be either neutral or have a net charge of one sign. The behavior of neutral polyampholyte is quite different from the charged polyampholyte. Addition of salt increases the viscosity of the nearly charge-balanced aqueous solutions of polyampholytes, and lowers the viscosity of the solutions with large net charge. The behavior of polyampholyte in aqueous solution is governed by coulombic interaction between anionic and cationic species located on different monomer units.

A series of random terpolymer was made with composition of 80(SMA):10(DMAEMA):10(tBMA) and 60(SMA):20(DMAEMA):20(tBMA) with degree of polymerization of 300 and 1000. The terpolymers were converted into water soluble random polyampholytes by reaction of DMAEMA with methyl iodide followed by acid catalyzed deprotection of SMA and tBMA to form glycidyl methacrylate, trimethylaminoethyl methacrylate and methacrylic acid repeat units. The compositions of the polyampholytes were confirmed by ^{1}H NMR spectra. The molecular weights, as measured by size exclusion chromatography, were close to the theoretical molecular weights.

ACKNOWLEDGMENTS

I would like to take this opportunity to thank the Almighty God for His kind blessings throughout my life.

Next, I would like to express my deepest appreciation to my research adviser, Dr. Warren T. Ford, for his excellent guidance, understanding, patience, motivation, and support throughout my research. I also wish to extend my appreciation to the dissertation committee members, Dr. K. Darrell Berlin, Dr. Richard A. Bunce, Dr. Jeffrey L. White, and Dr. Gary Foutch, for their continuous support, guidance, and helpful comments.

I would like to give my special appreciation to my husband, Jagjit Singh Saini, who always stood by me and provided continuous encouragement and motivation throughout my graduate studies. I would like to give my appreciation to my parents, Mr. Harkishan Singh and Mrs. Shanti Devi, for their kind wishes and their belief in me. I wish to say thank you to my sister and two brothers for their inspiration and love throughout my life.

Finally, I would like to acknowledge the Department of Chemistry for providing me a teaching assistantship during my graduate studies. I would like to thank Defense Threat Reduction Agency via the US Army Research Office, and the National Science Foundation for financial support as a research assistant during the course of my studies at Oklahoma State University.

TABLE OF CONTENTS

LIST OF TABLES

Chapter II

Table Page

Chapter IV

Table Page

LIST OF FIGURES

Chapter I

Figure Page

Chapter II

Figure Page

Figure Page

Chapter III

Figure Page

Figure Page

Chapter IV

Figure Page

LIST OF SCHEMES

Chapter I

Scheme Page

Chapter II

Scheme Page

Chapter III

Scheme Page

Chapter IV

Scheme Page

Scheme Page

CHAPTER I

POLYMER COLLOIDS

INTRODUCTION

Polymer colloids are complex heterogeneous systems having diverse applications. They are used widely in synthetic rubbers, paint and adhesives and as binder in non-woven fabrics and in paper-coatings. They also find application in medical diagnostics and as phase transfer catalysts. Polymer colloids have attracted much attention due to the environmentally friendly nature of the water-based synthetic approaches used. To reduce pollution by organic solvents, government environmental regulations make it necessary to substitute solvent-borne systems with water-borne systems. Water-based synthetic approaches in polymer colloids reduce the need for solvent recycling and disposal. Polymer colloids generally have viscosities almost like that of water. It is easy to synthesize polymer colloids with narrow particle size distributions in which all the polymer particles are the same size and carry the same amount of charge. As a result, all particles repel each other forming regular three-dimensional arrays. Catalytic functional groups can be introduced in polymer colloids during emulsion polymerization. Application of functional polymer colloids as phase transfer catalysts will be discussed in detail later in this chapter.

1.1 Polymer Colloids

A polymer colloid is a dispersion of submicron size polymer particles in liquid media (mostly water). They are also known as synthetic latexes due to their resemblance to the milky sap of rubber trees (known as latex). The size of colloidal particles in a dispersion ranges from 10 nm – 1000 nm in diameter. They are stable against gravitational forces due to electrostatic repulsions of charged sites in the polymer particle imparted by charged surfactant, charged initiator, or ionic monomer[1] as well as Brownian motion of the particles.

1.2 Synthesis of Polymer Colloids[2]

Polymer colloids can be synthesized by emulsion polymerization or by dispersion polymerization of vinyl monomer(s). Polymer particles of uniform size can be synthesized by emulsion polymerization with or without emulsifier.[3-7] Emulsion polymerization with emulsifier involves the emulsification of the hydrophobic monomer in water by a surfactant followed by an initiation reaction with a water soluble initiator or oil soluble initiator. During emulsion polymerization a large oil-water interface is generated. This intensifies the need for ionic and non-ionic surfactant which can be adsorbed physically or incorporated chemically onto the surface of a growing particle to prevent coagulation in the interactive latex particles. Emulsion polymerization is a complex process because nucleation of the particles, along with their growth and stabilization, depends upon free radical polymerization mechanisms and various colloidal phenomena. The key factors that control the particle growth stage in emulsion polymerization with or without emulsifier are: transport of monomer(s), free radicals, and

surfactant to the growing particles, and their partition among continuous water phase, monomer reservoir, monomer swollen polymer particles, and oil-water interface.

A typical emulsion polymerization formulation is comprised of water, water-soluble initiator, water-insoluble monomer(s), and a surfactant, which above its critical micelle concentration (CMC) forms micelles with the monomer(s). A monomer-swollen micelle is converted into polymer particles via free radicals, generated thermally in aqueous media. A small fraction of the hydrophobic monomer is present in the micelles or dissolved in water. Most of the monomer molecules are in monomer droplets. Submicron latex particles are generated by the capture of free radicals in micelles. Since micelles have a large oil-water interfacial area as compared to the surface area of the monomer droplets in aqueous phase, monomer droplets cannot compete with micelles in capturing free radicals generated in aqueous phase. Monomer polymerized in continuous water phase forms oligomeric radicals which become so hydrophobic that they enter monomer-swollen micelles and continue to propagate inside the micelles. Thus, monomer-swollen micelles are converted into particle nuclei. These nuclei continue to grow by absorbing more monomer(s) from monomer droplets and monomer-swollen micelles. The particle nucleation stage (also called Interval I) ends with the exhaustion of micelles. After the nucleation stage, the number of latex particles remains constant towards the end of polymerization. Monomer droplets serve as a reservoir to supply monomer to the growing particles. In the particle growth stage (also called Interval II) the majority of monomers is consumed and this stage ends when monomer droplets disappear from the polymerizing medium. Thus, emulsion polymerization proceeds during Interval II until all the monomer droplets disappear. In Interval III, the latex particles become

monomer starved and concentration of monomers continues to decrease towards the end of the polymerization. Hence, polymerization initiated in the micelles continues until all the monomers are consumed. The micelle nucleation model is illustrated schematically in Figure 1 below.

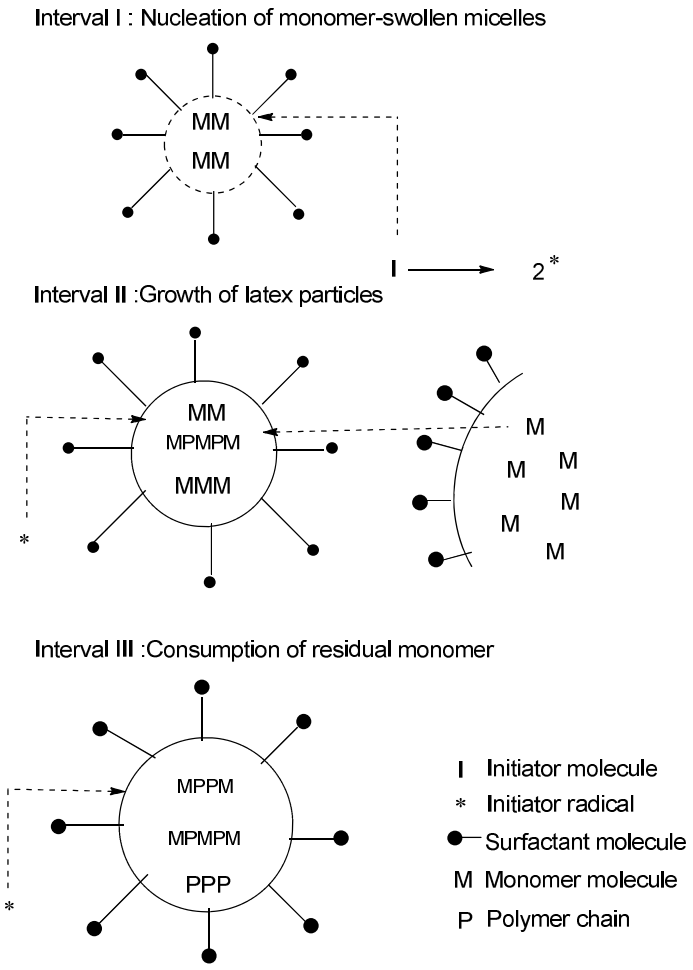

Figure 1. A schematic representation of the micelle nucleation model.[2]

Emulsion polymerization in the presence of an emulsifier or a surfactant is the most common method employed for the synthesis of a polymer colloid. The characteristics of the resulting polymer particles such as particle morphology, uniformity in the particle size, and stability of the colloid are strongly dependent on the type and the concentration of emulsifier or surfactant in the reaction mixture. Coatings or films made from polymer colloid lose their stability due migration of the emulsifier to the surface of the film. To overcome this problem the emulsifier must be polymerized where a chemical linkage can binds the emulsifier to the polymer particle and therefore, its migration to the surface can be prevented. This can be achieved by employing emulsion polymerization in the absence of an emulsifier.

1.3 Emulsion Polymerization without Emulsifier

Polymerization without emulsifier can be carried out in presence of small amounts of ionic monomers[8] (such as sodium styrenesulfonate and sodium salt of 2-sulfoethyl methacrylate), an ionic initiator[9] (such as potassium persulfate), a hydrophilic monomer[10] (such as carboxylic monomers) and amphiphilic high polymers or oligomers[11] which act as substitutes for an emulsifier or surface active compound. Ionic monomers below their critical micelle concentration (CMC) do not form micelles and are highly soluble in aqueous phase in the polymerizing mixture. The primary radical formed after decomposition of initiator in aqueous phase reacts with ionic monomers and organic monomer in the aqueous phase first, and then they propagate to form oligomeric free radical chains. On attaining the critical length, the chains coil up to form particles which absorb more organic monomer from the mixture and grow by chain propagation. As the

polymerization proceeds, the particles grow to a certain size and adsorb ionic monomer on their surface. When most of the water-soluble monomer is consumed and particles have been nucleated, the radicals formed in water no longer form new particles but are all trapped by existing particles. An advantage of this polymerization is in the preparation of polymer colloids that are used in making films or coatings in which no migration of emulsifier or surfactant occurs during the film formation, which leads to more stable films or coatings. In addition, it also provides polymer colloids of monodisperse particle size distribution and good shear stability.[10-12]

The dispersion polymerization differs from emulsion polymerization in being a homogeneous (rather than a heterogeneous) mixture of monomer(s), initiator, and a steric stabilizer that is a polar polymer such as poly(N-vinylpyrrolidone) or poly(vinyl alcohol). The function of steric stabilizer is to keep the insoluble polymeric particles dispersed in the reacting media by adsorption on to the surface of the growing particle.[13]

1.4 Applications of Polymer Colloids

1.4.1 Industrial Applications[14-16]

Polymer colloids synthesized on an industrial scale by emulsion polymerization find applications in various industries such as coating application in paints, as a binder for paper coatings, as rubber in tire manufacture, and as adhesives. Synthetic latexes were used as latex paints in the 1950s. Polymer particles in such paints have a low glass transition temperature (T_g) and as water evaporated from the applied paint, polymer particles coalesced to form a continuous film. Synthetic latexes are produced worldwide

on a large scale for a variety of applications. Aqueous latexes are synthesized at the atmospheric pressure and at a temperature in the range of 40-60 ^{o}C. The above reaction conditions make it a relatively safe process which is easy to conduct in standard stirred tank reactors. The simple batch-mode polymerization, in which all ingredients are mixed together at the beginning, is the preferred method for synthesizing latexes. The latexes are produced on an industrial scale by emulsion polymerization owing to its simplicity and because of possible synthesis of the high molecular weight polymers at low viscosities. Many industrial coatings still use solvent-based formulations to achieve desirable properties from the coatings. There is an environmental need to reduce the amount of solvent use in these syntheses. A possible solution to address such an environmental issue is the use of polymer colloids made by emulsion polymerization in water. Desirable properties can still be maintained in coatings by using polymer colloid blends in which one component has film-forming composition and other have high modulus polymer composition. For example, rubberized concrete is formed by mixing cement and sand with a rubbery latex (such as polystyrene/butadiene, which contains water) instead of mixing with water. The resultant concrete has the cement particles held together in part by the synthetic rubber which improves the flexibility and thermal expansion properties of the concrete.[15]

1.4.2 Applications of Functional Polymer Colloids[14-16]

Functional groups can be introduced onto the colloidal particles by the use of functional monomers in emulsion polymerization. The development of functional

polymer colloids led to the applications of polymer colloids in biomedical fields[17] and they are also studied as media for heterogeneous catalysis.[18-22]

Polymer colloids serve as heterogeneous catalysts because of high surface area, moderate surface hydrophobicity and controlled particle size. Associated colloidal dispersions such as anion exchange resins,[23-25] polyelectrolytes,[26-29] and latexes[18,19]catalyze the reaction between anion in aqueous media and organic compounds in organic media. The use of latexes as phase transfer catalyst showed a significant enhancement in the rates of reaction of anions with uncharged organic compounds. The enhancement in rate of reaction is due to high local concentration of ionic and organic substrate in a small volume fraction of polymer.[21]

Another potential application of polymer colloids acting as phase transfer catalysts is to hydrolyze p-nitrophenyl hexanoate (PNPH) and diethyl *p*-nitrophenyl phosphate (Paraoxon), which are simulants of chemical warfare agents.[30] A polymer colloid, as a phase transfer catalyst, facilitates the migration of reacting anions from one phase (aqueous phase) to another (organic phase). Thus, the heterogeneity of a polymer colloid offers the advantage of carrying out the reactions in aqueous media and transfer of reacting anions from aqueous phase into organic phase.

In order to understand how a polymer colloid acts as a phase transfer catalyst, we need to understand the term phase transfer catalyst and its mechanism. The next section explains the term phase transfer catalyst and its working mechanism. Subsequent sections discuss the application of polymer colloid as phase transfer catalyst in heterogeneous media.

1.5 Phase Transfer Catalyst

A phase transfer catalyst catalyzes the reaction between the anion in ionic compounds usually soluble in aqueous phase and the organic substrate soluble in the organic phase. The common examples of phase transfer catalysts are crown ethers[31], cryptates[32] and quaternary ammonium ions.[20,21] Figure 2 below shows the working of a phase transfer agent.[33]

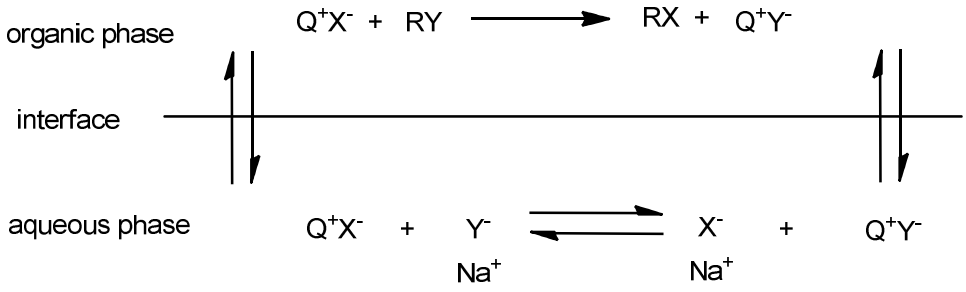

Figure 2. Mechanism of quaternary ammonium ion phase transfer catalysis.

In a quaternary ammonium-anion ion pair (Q^+ X^-) the alkyl chains provide an organophilic character to carry the anion from aqueous phase to organic phase. The anion in the organic phase reacts with the organic substrate (RY) as shown in Figure 2. The corresponding quaternary ammonium-anion ion pair (Q^+ Y^-) equilibrate with the aqueous phase. If the aqueous phase is enriched with reacting anion X^-, the quaternary ammonium ion associates with anion X^- and another cycle is initiated by the generation of (Q^+ X^-).

1.6 Prior Literature on Polymer Colloids as Phase Transfer Catalysts

Cationic polymer colloid possessing quaternary phosphonium and ammonium ionic sites have been synthesized and studied as phase transfer catalyst in the past in our laboratory.[17-20,29] Latex particles of (chloromethyl)styrene and divinylbenzene having a diameter in the range of 0.08-0.2 μm have been synthesized by emulsion polymerization. The structure of the polymer colloid is shown below in Figure 3.

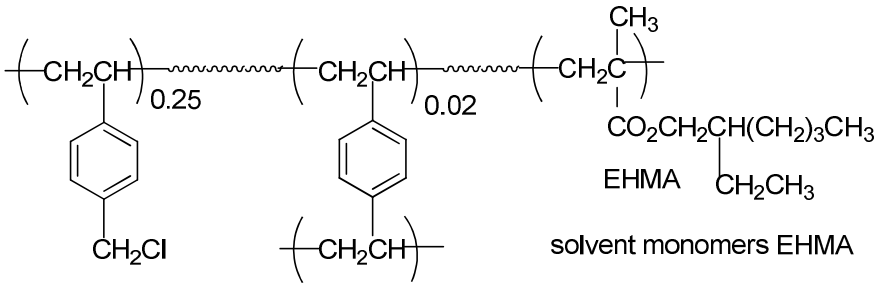

Figure 3. Structure of polymer colloid.

The insoluble copolymer was converted to insoluble polystyrene-bound benzyl(tri-n-butyl)-phosphonium ion phase transfer catalyst for nucleophilic displacement reaction.[17] A series of monodisperse latexes of styrene, styrylmethyl(trimethyl)ammonium chloride, divinylbenzene and (chloromethyl)styrene were synthesized by shot growth emulsion polymerization and were converted to quaternary ammonium ion exchange phase transfer catalysts for the decarboxylation of 6-nitrobenzisoxazole-3-carboxylate (NBIC).[18] Similarly cross-linked polystyrene latexes containing quaternary ammonium ion exchange sites were used to accelerate *O*-iodosobenzoate (IBA) catalyzed hydrolysis of *p*-nitrophenyl diphenyl phosphate (PNPDPP). Cationic polymer colloids,[19] cationic polymer colloid of styrene, 2-ethylhexyl

methacrylate (EHMA), 25 wt% of vinylbenzyl chloride (VBC), 1 wt% of divinylbenzyl, and 1 wt% of styrylmethyl(trimethyl ammonium chloride) were used to catalyze hydrolysis of *p*-nitrophenyl hexanoate (PNPH) at 30 ^{o}C,[20] and anion exchange latex particles of EHMA, VBC and cationic surfactant in a mixture of basic aqueous solution and fluoro solvent HFE-7200 (mixture of perfluorobutyl and perfluoroisobutyl ethyl ether) were used as phase transfer catalysts for the hydrolysis of PNPH and Paraoxon.[29]

1.6.1 Polymer Colloid as Phase Transfer Catalyst for Nucleophilic Displacement Reactions[17]

Polystyrene linked benzyltri-n-butyl-phosphonium ion latex particles were used to catalyze the reaction of aqueous sodium cyanide with 1-bromooctane in toluene as shown below in Scheme 1.

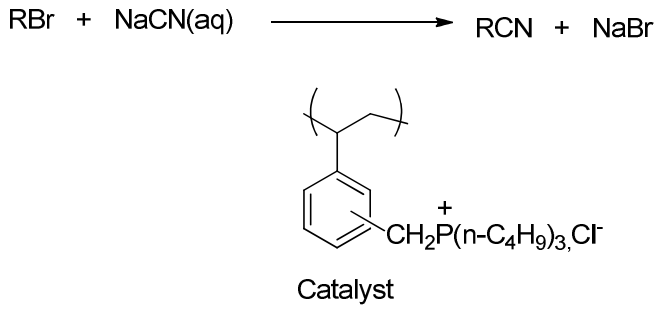

Scheme 1.

The most active latex catalyst was the one containing 2% divinylbenzene and having particle size in the range of 0.12-0.27 µm. The rate constants for the reaction containing 2 mol% of active catalyst were high and independent of stirring speed in the range of 510-670 rpm. Higher activity of a polymer bound phase transfer catalyst was obtained in a very fast reaction by using catalysts having much smaller latex particles

rather than larger particles 20-250 µm in diameter that were made by suspension polymerization. The enhancement in the rate of reaction is due to a shorter path for inter-particle diffusion of the reactant from polymer-supported phase transfer catalyst.

1.6.2 Cationic Polymer Colloid for the Decarboxylation of 6-Nitrobenzisoxazole-3-Carboxylate (NBIC)[18]

Polystyrene latexes with quaternary ammonium ion exchange sites were used to catalyze the decarboxylation of NBIC in aqueous dispersion as shown in Scheme 2. The rate constant for the decarboxylation was 21,000 times the rate constant in water using colloidal particles having 24 mol% of poly(styrylmethyl-tri-n-butylammonium chloride) repeat units. This was the largest rate enhancement reported at 25 ^{0}C for the decarboxylation of NBIC in colloidal medium. Lesser hydration of the reactant in polymer latexes than in water is the reason for rate enhancement.

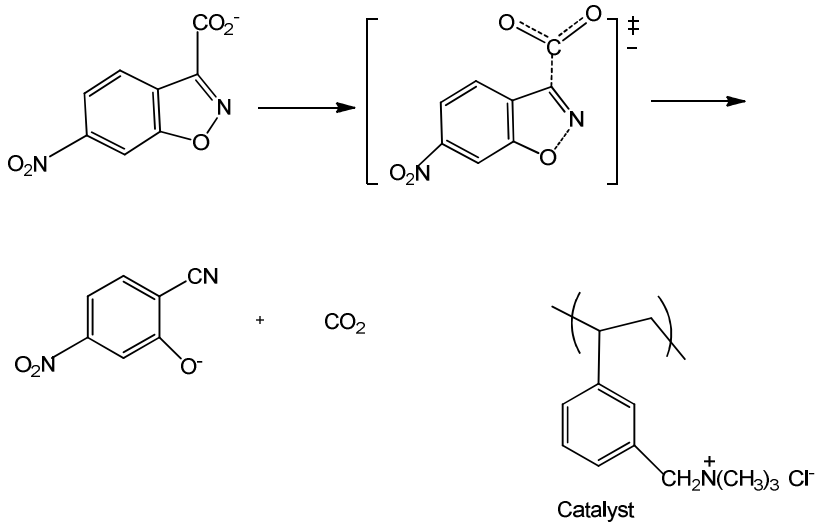

Scheme 2.

1.6.3 Acceleration of *O*-Iodosobenzoate (IBA) Catalyzed Hydrolysis of *p*-Nitrophenyl Diphenyl Phosphate (PNPDPP) by Cationic Polymer Colloids[19]

Series of monodisperse polymer colloids of poly(chloromethylstyrene) were prepared by emulsion polymerization to study the reaction of the nucleophilic catalyst IBA bound to the surface of colloids. Generally, the rate of such reactions in the presence of polymer bead catalysts is less than in a polymer colloid because of small surface area of polymer beads causing diffusion limitations. However, diffusion limitations can be overcome if such a reaction is carried out in the presence of polymer colloids. Polymer colloids, owing to the small size and greater surface area per unit mass of colloids, overcome the diffusion limitations. Cationic polymer colloid derivatives of poly(chloromethylstyrene) were used for the hydrolysis of *p*-nitrophenyl diphenyl phosphate as shown in Scheme 3 below.

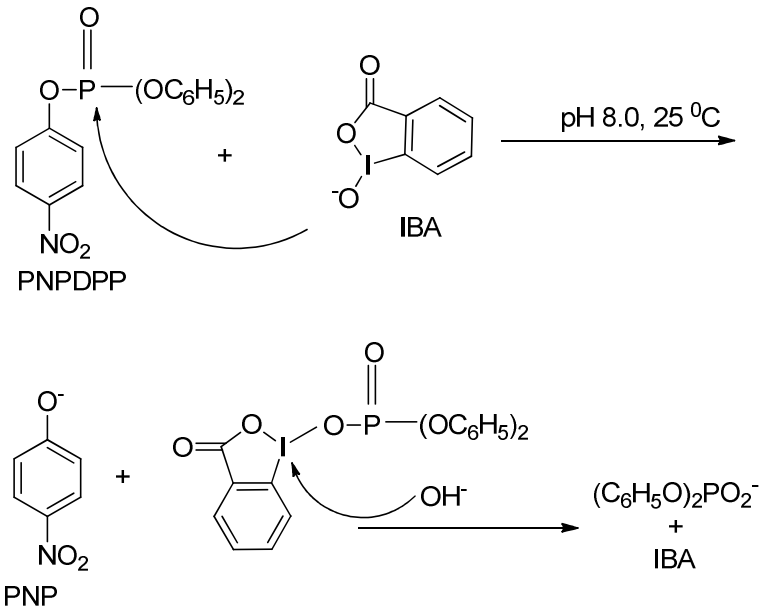

Scheme 3.

The hydrolysis of PNPDPP is a prototype or simulant for the hydrolysis of toxic organophosphate insecticides and chemical warfare agents. There was up to 6,300 times rate enhancement for the hydrolysis of PNPDPP by colloidal particles containing 24 mol% of (styrylmethyl)tributylammonium chloride repeat units.

1.6.4 Hydrolysis of *p*-Nitrophenyl Alkanoate[20]

Cationic polymer colloid containing copolymers of styrene, 2-ethylhexyl methacrylate (EHMA), 25 wt% of vinylbenzyl chloride (VBC), 1 wt% of divinylbenzene, and 1 wt% of styrylmethyl(trimethyl)ammonium chloride were used to catalyze hydrolysis of *p*-nitrophenyl hexanoate (PNPH) at 30 ^{0}C. Hydrolysis of PNPH is shown in Scheme 4 and the structure of active catalyst is shown in Figure 4 below.

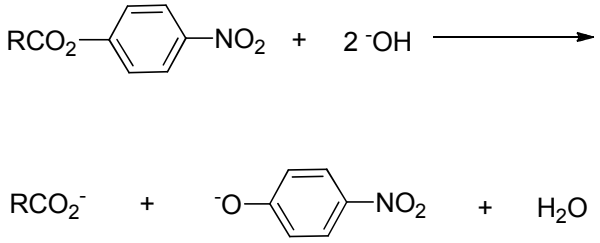

Scheme 4.

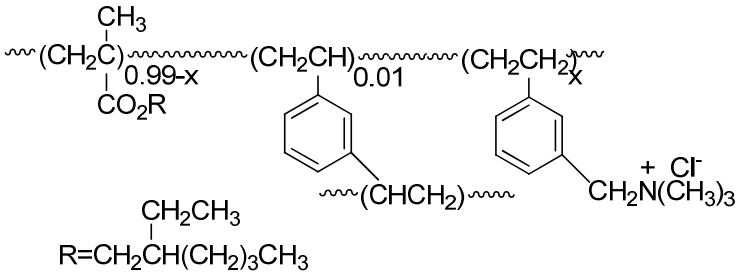

Figure 4. Structure of EHMA latex catalyst.[6]

The rate of reaction for the hydrolysis was 2.3-16.5 times faster in presence of 1.2 mg mL^{-1} of quaternary ammonium ion latex than in water alone. Quaternary ammonium latexes containing 75 wt% of EHMA and 25 wt% of VBC were further tested for the decarboxylation of 6-NBIC in aqueous media. The observed rate of reaction was 10,400 times larger than in water alone. Faster intra-particle rate constant and favorable partitioning of reactant into the latex results in higher rate of reaction.

1.6.5. Hydrolysis of PNPH and Paraoxon in Water and Fluoro Solvent[29]

Hydrolysis of PNPH and Paraoxon was studied using anion exchange latex particles and cationic surfactants in a mixture of basic aqueous solution and fluoro solvent HFE-7200 (mixture of perfluorobutyl and perfluoroisobutyl ethyl ethers) as shown in Scheme 5.

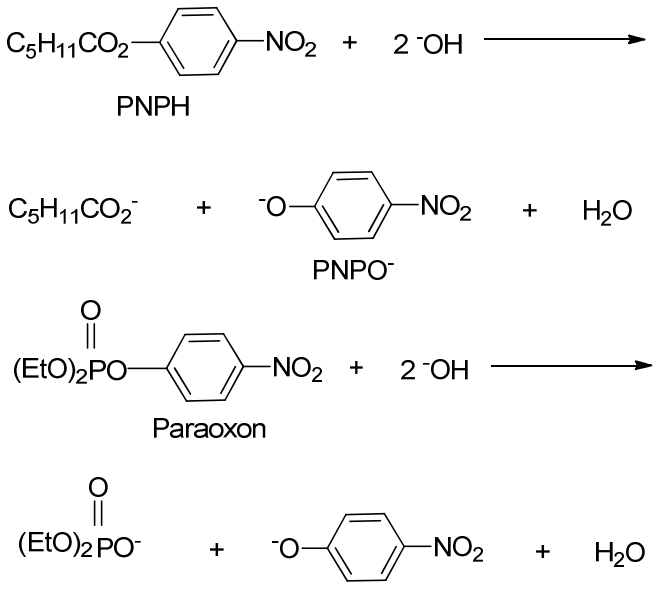

Scheme 5.

In borate buffer solution at pH 9.4, aqueous colloidal particles of cross-linked copolymer of EHMA and styrylmethyl(trimethyl) ammonium chloride were the most active catalyst for the hydrolysis of PNPH in HFE phase. Aqueous colloidal particles and hexadecyltrimethylammonium bromide (CTAB) in aqueous phase were the most active catalysts for the hydrolysis of Paraoxon in 0.1 M NaOH.

1.7 Objective of Research

The objective of this research project is to understand the decontamination of simulants of chemical warfare agents in cationic polymer colloids as phase transfer catalysts. Latex copolymers containing either EHMA or styrene and styrylmethyl(trimethyl) ammonium chloride units and cross-linked with DVB had been employed in the past for the hydrolysis of toxic organophosphate and organoesters which are simulants of chemical warfare agents. Most of the research had been done on cationic latexes based on polystyrene and EHMA in aqueous media and in fluorinated media.[17-20,29]

The aim of the current research is to synthesize cationic polymer colloids as a phase transfer catalyst (74 wt% EHMA, 25 wt% VBC, and 1 wt% vinylbenzyl trimethyl ammonium chloride) for the decontamination of simulants of chemical warfare agents in aqueous media using fluorinated monomer such as 1H,1H,2H,2H-perfluorobutyl ethyl methacrylate, 1H,1H,2H,2H-perfluorooctyl methacrylate, and 2,2,2-trifluoroethyl methacrylate. We prepared a colloidal dispersion having cationic sites to decontaminate toxic organophosphate (Paraoxon) and organoesters (PNPH). The latex can be applied to a surface as a coating having a resistant fluoro surface of fluorinated monomers in the

latex particles. The semi-fluorinated core shell latexes as described above were synthesized by shot-growth emulsion polymerization. The dispersions were successfully tested for the hydrolysis of PNPH and Paraoxon.

References

1. El-Aasser, M. S.; Sudol, E. D. *In Emulsion Polymerization and Emulsion Polymers*; Lovell, P. A., El-Aasser, M. S., Eds.; Wiley: Chichester **1997**,pp 37-55.
2. Chern, C. S. *Prog. Polym. Sci.* **2006**, *31*, 443–486.
3. Ono, H.; Jidai, E. *Colloid.Polym. Sci.* **1976,** *254,* 17-24.
4. Taner, T.; Oguz, O.; Cetin, S. I. *J. Appl. Polym. Sci.* **1996**, *61*, 485-493.
5. Xu, Z.; Ford, W. T. *Macromolecules* **2002**, *35(20),* 7662-7668.
6. Pei, Li.; Junmin, Z.; Panya, S.; Harris, F. W. *J. Dispersion Sci. Technol.* **2003**, *24*, 607-613.
7. Shunchao, Gu.; Hiromitsu, A.; Daisuke, N.; Yoshio, K.; Mikio K. *Langmuir* **2004**,*20*, 7548-7951.
8. Juang, M. S.; Krieger, I. M. *J. Polym. Sci., Polym. Chem. Ed.* **1976**, *14*, 2089-2107.
9. Goodall, A. R.; Wilkinson, M. C.; Hearn, J. *J. Appl. Polym. Sci.* **1977**, *15*, 2193.
10. Ceska, G. W. *J. Appl. Polym. Sci.* **1974**, *18*, 427.
11. White, W. W.; Jung, H. *J. Polym. Sci. Polym. Symp.*, **1976**, *45*, 197.
12. Kawaguchi, H.; Ohtsuka, Y.; Sugi, Y. *J. Appl. Polym. Sci*. **1981**, *28***,** 1637**.**
13. Shiho, H.; Desimone, J. M. *Macromolecules* **2001**, *34*, 1198-1203.
14. Fitch, R. M. *Polym. Reaction Engineering* **2003**, *11*, 911-953.

15. Fitch, R. M. In *Polymer Colloids – A Comprehensive Introduction*; Ottewill, R. H.; Rowell, R. L., Eds.; Academic Press, 1997, pp 1-4.

16. Daniels, E. S.; Sudol, E. D.; El-Aasser, M. S. In *Polymer Colloids*; Daniels, E. S.; Sudol, E. D.; El-Aasser, M. S., Eds.; ACS: Washington DC, 2001, pp 1-12.

17. Elaissari, A. *Macromol. Symp.* **2005**, *229*, 47–55.

18. Bernard, M.; Ford, W. T.; Taylor, T. W. *Macromolecules* **1984,** *17*, 1812-1814.

19. Lee, J. J.; Ford, W. T. *J. Org. Chem.* **1993**, *58*, 4070-4077.

20. Lee, J. J.; Ford, W. T. *J. Am. Chem. Soc.* **1994**, *116*, 3753-3159.

21. Miller, P. D.; Spivey, H. O.; Copeland, S. L.; Sanders, R.; Woodruff, A.; Gearhart, D.; Ford, W. T. *Langmuir* **2000**, *16*, 108-114.

22. Ford, W. T. *Reactive* & *Functional Polymers* **2001**, *48*, 3 –13.

23. Ford, W. T.; Tomoi, M. *Adv. Polym. Sci.* **1984**, *55*, 49.

24. Tomoi, M.; Ford, W. T. *Synthesis and Separations Using Functional Polymers*; Sherrington, D. C., Hodge, P., Eds.; Wiley: Chichester **1988**; pp 181-207.

25. Yamazaki, N. *Polym. J.* **1980**, *12*, 231.

26. Fife, W. K. *Trends Polym. Sci.* **1995**, *3*, 214.

27. Fendler, J. H.; Fendler, E. H. *Catalysis in Micellar and Macromolecular Systems*; Academic: New York, 1975.

28. Zheng, Y.; Knoesel, R.; Galin, J. *Polym.* **1987**, *28*, 2297.

29. Yang, Y.; Engberts, J. *J. Org. Chem.* **1991**, *56*, 4300.

30. Zhu, Yan; Ford, W. T. *Langmuir* **2009**, *25*, 3435-3439.

31. Pederson, C. *J. Am. Chem. Soc.* **1967**, *89*, 2495.

32. Dietrich, B.; Lehn, J. *Tetrahedron Lett.* **1973**, 1225.

33. Rabinovitz, M.; Cohen, Y.; Halpern, M. *Angew. Chem. Int. Ed. Engl.* **1986**, *25*, 960-970.

CHAPTER II

SYNTHESIS OF SEMI-FLUORINATED CORE-SHELL LATEXES BY EMULSION POLYMERIZATION AND DECONTAMINATION OF CHEMICAL WARFARE AGENTS

INTRODUCTION

The goal of this research project is the decontamination of chemical warfare agents and other toxic organic chemicals. Decontamination is a challenging and a required task in the battle field, in buildings, in chemical manufacturing and in pilot plants. The primary target for decontamination is a solid surface or any kind of equipment in a building.[1] The decontaminants must be non corrosive and should work under any ambient temperature condition. Another important parameter needed to design a decontaminant is the medium or solvent for the decontaminant. The medium must dissolve the chemical warfare agent and promote the desired reaction of decontamination. The medium could be organic or aqueous. An aqueous medium is preferred over organic medium owing to the large amount of organic waste produced by decontamination in organic media. Since, most of the chemical warfare agents are organic in nature and the decontaminating reactants are polar, emulsion polymers or phase transfer systems have been investigated as suitable media for a decontaminant.

The existing decontamination methods make use of the solutions DS2 and decon green.[2] Solution DS2 is a strongly basic mixture of 70% diethylenetriamine, 28% ethylene glycol monomethyl ether, and 2% sodium hydroxide. This is a reactive solution known for its high stability and broad operating temperature range between -15 to 125 ^{o}F. But it suffers from its corrosiveness, flammability, and destruction of human tissue. Decon green is a mixture of hydrogen peroxide, potassium carbonate, potassium molybdate, propylene carbonate, and a surfactant. This is a replacement for solution DS2 as it forms non-toxic products during reaction. But it is a costlier alternative, the H_2O_2 has a shelf life of only a few years, and the H_2O_2 must be mixed with other components right before use. The health hazards posed by the use of these decontaminants and their costs have intensified the need for the development of new aqueous decontaminants. A recent advance in this field is the use of fluorinated solvents that can extract the chemical warfare agents from the nooks and crannies of electronic equipment.[3,4]

Recently, many fluorinated acrylic polymer coatings having perfluoroalkyl groups have gained much attention due to their unique surface properties and promising applications.[5-8] The CF_3 end groups on perfluoroalkyl moiety provide low surface energy to the coatings and acrylic groups on the polymer provide good adhesion to the substrate.[9-13] Because of low surface energy, the surfaces containing perfluoroalkyl groups are repellant to contaminants and are easy to clean.[14] The repellency of the surfaces increases as the weight fraction of the perfluoroalkyl in the polymer increases. However, the factors such as high cost of fluorinated monomers and insolubility of highly fluorinated polymers in common solvents, limits the use of highly fluorinated polymers.

In order to achieve better repellency from less fluorinated (or semi-fluorinated) polymers, the core-shell latexes are a better alternative. By synthesizing a non-fluorinated core and a fluorinated shell, desirable surface repellency of fluoro-polymers can be preserved.[15-20] Semi-fluorinated core-shell latexes are synthesized by shot-growth emulsion polymerization or two-stage emulsion polymerization. In this kind of polymerization, a core of non-fluorinated latex particles is synthesized in the first stage followed by second addition of monomers along with fluorinated monomers in the second stage forming a fluorinated shell.

There are reports on the use of the cationic polymer colloids in decontamination (or hydrolysis) of simulants of chemical warfare agents *p*-nitrophenyl hexanoate (PNPH) and diethyl *p*-nitrophenyl phosphate (Paraoxon). In our research group, polymer colloids in fluorinated solvent were synthesized by dispersion polymerization.[3,21] The resulting polymer colloids were tested for hydrolysis of PNPH and Paraoxon. Cross-linked copolymer particles of 2-ethylhexyl methacrylate (EHMA) with quaternary ammonium ionic sites had the highest catalytic activities for the hydrolysis of PNPH in aqueous borate buffer solution.[22]. This is due to the branched 2-ethylhexyl chains in EHMA which help to absorb larger amounts of organic compounds than other alkyl methacrylates. In these dispersions, EHMA (solvent monomer) helps to absorb the toxic organic compounds and the OH^- ions at the quaternary ammonium ionic sites derived from vinylbenzyl chloride (VBC) hydrolyze PNPH and Paraoxon.

This research project aims to synthesize semi-fluorinated core-shell latexes in aqueous media by emulsion polymerization and test the resulting dispersions for the hydrolysis of PNPH and Paraoxon in basic media. Interestingly, there is no literature on

the use of semi-fluorinated core-shell latexes in aqueous media containing quaternary ammonium ionic sites for the decontamination of chemical warfare agents. We made colloidal dispersions that can be applied to surfaces as coatings with the objective of having resistant fluorous surface and catalytic sites underneath for the decontamination of toxic chemicals that penetrate the surface.

Shot-growth or two-stage emulsion polymerization was employed to synthesize semi-fluorinated core-shell latexes of EHMA, VBC, vinylbenzyl(trimethyl)ammonium chloride (VBTMACl) and fluoro monomers such as 2-(perfluorobutyl)ethyl methacrylate (PFBEMA), 1H,1H,2H,2H-perfluorooctyl methacrylate (PFOMA), and 2,2,2-trifluoroethyl methacrylate (TFEMA). This chapter presents the results of emulsion polymerization, functional group conversion of VBC repeat units to quaternary ammonium ionic sites in the presence of aqueous trimethylamine, and hydrolysis of PNPH and Paraoxon using colloidal particles and colloidal coatings.

Results

2.1 Emulsion Polymerization

Our aim was to synthesize semi-fluorinated core shell cationic polymer colloids as phase transfer catalysts to study the hydrolysis of PNPH and Paraoxon which are stimulants of chemical warfare agents. The phase transfer catalytic dispersions in water as well as on the coatings (or films) made from these dispersions were tested for the hydrolysis of PNPH and Paraoxon under basic conditions. We choose emulsion polymerization without emulsifiers to synthesize semi-fluorinated core shell latexes since

emulsifier-free emulsion polymerization provides stable coatings.[23] As nucleation finishes early in emulsifier-free emulsion polymerization, it leads to longer growth period giving exceptionally uniform particle size dispersions as compared to conventional emulsion polymerization.[24] Polymerizations were carried out in water at 60 ^{o}C in the presence of the ionic initiator 2,2'-azobis(2-methylpropionamidine) dihydrochloride using the ionic monomer VBTMACl and no emulsifier. The polymerization started in water. The rate of polymerization was slow in the beginning since EHMA and VBC were insoluble in water. As the polymerization progressed, the polymeric chain coiled up to form polymer particles. The polymer chain grew continuously by propagation as more and more EHMA and VBC are absorbed by polymer particles to form a core of non-fluorinated polymer. The fluorinated shell is created by the addition of fluoromonomers in the second stage. In order to study the effect of perfluoroalkyl side chain to lower surface energy of the coatings,[17] three different fluoromonomers, PFOMA, PFBEMA and TFEMA were used to synthesize polymer dispersions. Moreover, success in synthesizing semi-fluorinated core shell latexes depends upon number of factors such as relative solubility of the monomers in water and the degree of incompatibility between polymer particles of core and shell.[25-26] Owing to the solubility issues of fluorinated vs. non-fluorinated monomers, different amounts (2.5 wt% to 25 wt%) of fluorinated monomers were added to the reaction mixture in the second stage to get stable dispersions of semi-fluorinated core-shell latexes. Cationic polymer colloidal phase transfer catalysts were synthesized from the latexes by reacting VBC with aqueous trimethylamine at 60 ^{o}C in water. Cationic polymer colloids containing different compositions of fluoromonomers

and VBC were synthesized. The overall synthesis of semi-fluorinated core-shell cationic polymer colloids is shown in Scheme 1.

All of the polymerizations were carried out in water at 60 ^{o}C.[27] Tables 1 and 2 show the results of polymerization containing different amounts (2.5 wt%, 5 wt%, 10 wt%, and 25 wt%) of different fluoromonomers (PFBEMA, PFOMA, and TFEMA) and different amounts of VBC (10 wt% and 25 wt%).

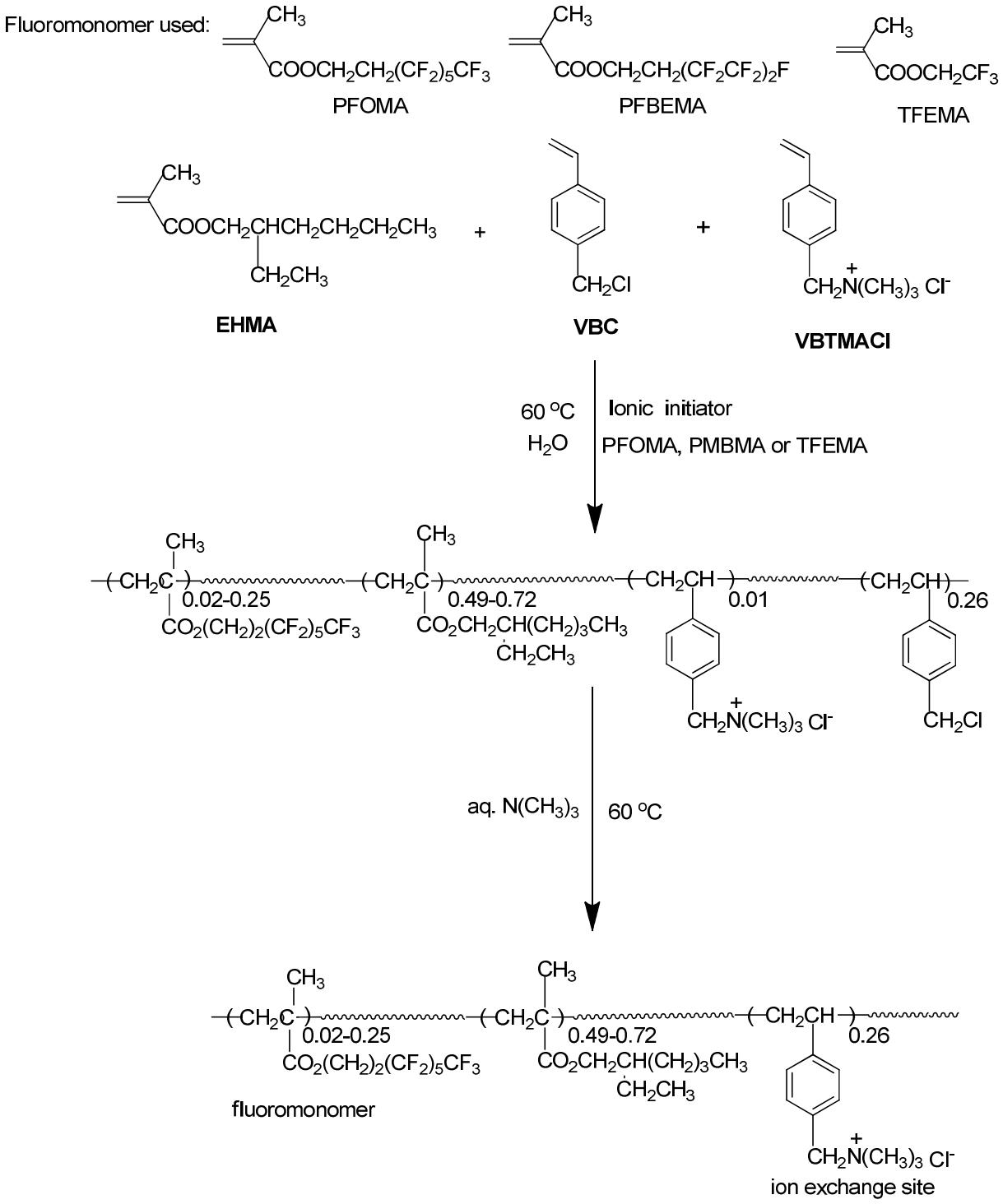

Scheme 1. Synthesis of cationic polymer colloids.

Table 1. Composition of Latexes with 25% VBC

product ID	fluoromonomer	Wt %	yield[a] (%)	diameter[b] (nm)
BK-1F	TFEMA	2.5	89	94
BK-2F	PFOMA	2.5	48	94
BK-3F	TFEMA	5.0	84	92
BK-4F	PFOMA	5.0	90	88
BK-5F	TFEMA	10.0	38	98
BK-6F	PFOMA	10.0	32	120
BK-10F	PFBEMA	10.0	34	142
BK-11F	PFOMA	25.0	97	105
BK-12F	PFBEMA	25.0	97	162
BK-13F	TFEMA	25.0	96	132

[a] Calculated from the weight of copolymer obtained and the weight of monomer mixture used for polymerization, [b] Hydrodynamic diameter from dynamic light scattering.

Polymerization of EHMA (74%), VBC (25%), and VBTACl (1%) in presence of each of the fluoromonomers with different compositions gave stable colloidal dispersions of BK-1F to BK-10F. All of the polymerization mixtures started clear and turned cloudy within 35-40 min due to nucleation of the particles. Dispersions were filtered by passing them through a cotton plug to remove traces of coagulum. The solid content of all latexes was determined by accurately weighing 1 mL of the latex and evaporating it to a constant weight at 110 ^{o}C. The percent yield was calculated as the ratio of the weight of copolymer obtained after evaporation to the weight of monomer mixture used for polymerization. Samples BK-5F to BK-10F had yields less than 50%. A possible reason for lower yield could be the inadequate mixing due to a different mechanical stirrer used

in synthesizing the above samples. Polymer colloids containing 10% VBC with each of the fluoromonomer were synthesized using a similar procedure.[27] The results of polymerization are shown in Table 2.

Table 2. Composition of Latexes with 10% VBC and 10% Fluoromonomer

product ID	fluoromonomer	yield[a] (%)	diameter[b] (nm)
BK-14F	TFEMA	16	107
BK-15F	PFOMA	51	157
BK-16F	PFBEMA	44	136

[a]Calculated from the weights of copolymer obtained to weight of monomer mixture used for polymerization, [b] Hydrodynamic diameter from dynamic light scattering

Diameters of the particles were measured by dynamic light scattering (DLS). The DLS study showed monodisperse distribution of particles and diameter of the particles in the range of 88-162 nm. The uniformity of the particle size in all the latexes was due to early completion of the nucleation stage.[24] The short nucleation stage allows a longer growth stage, leading to exceptionally uniform particle sizes The particles have hydrophilic surfaces due to a small amount of the cationic monomer in the copolymer and polymer end groups derived from a cationic initiator. The cores of the latex particles are hydrophobic due to fluorinated methacrylate, EHMA, and VBC.

Core shell morphology was introduced by the addition of varied composition of fluorinated monomers PFBEMA, PFOMA, and TFEMA in the second stage giving stable polymer colloids with good percent yield. The chemical structure of the core-shell latexes containing different fluoromonomers in the shell was confirmed by FTIR spectroscopy of dry powdered samples. The copolymers BK-5F to BK-10F were dried by evaporating

aqueous dispersions at 110 ^{o}C, and the solid particles were pulverized to fine powder to get FTIR spectra. All of the copolymers showed characteristic peaks corresponding to carbonyl stretch at 1720-1718 cm^{-1}, C-O-C stretch at 1200-1000 cm^{-1}, C-H stretch at 2980-2800 cm^{-1} and a wide region corresponding to CF_2 stretch at 1260-1150 cm^{-1} and CF_2 wagging and rocking at (710-660 cm^{-1}).[28] Figure 1 shows the IR spectra of fluoromoner TFEMA and the corresponding copolymer of BK-13F.

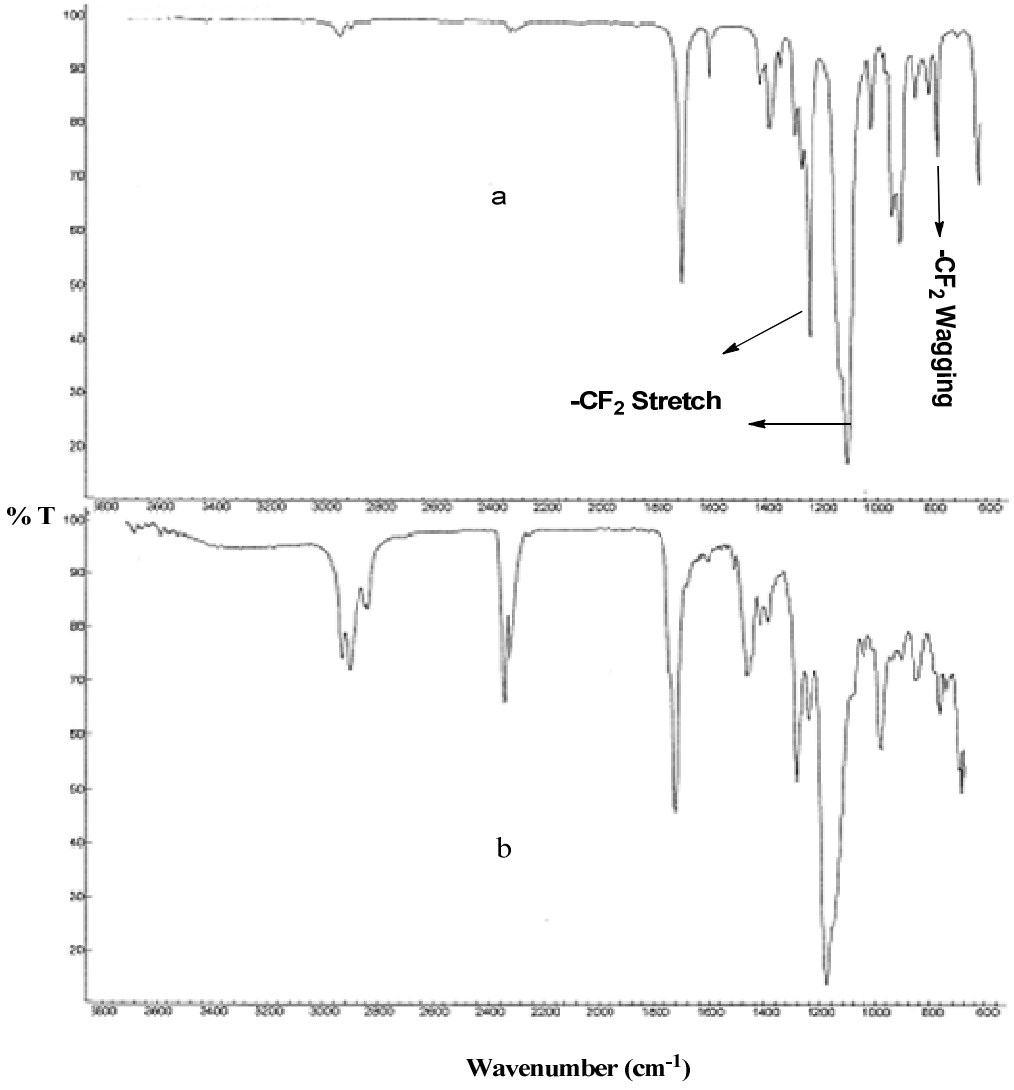

Figure 1. FTIR spectra of (a) fluoromonomer TFEMA; (b) copolymer BK-13F containing TFEMA.

2.2 Functional Group Conversion of VBC Units to Quaternary Ammonium Ions

All of the aqueous dispersions of copolymers BK-1F to BK-13F were reacted with an excess of a 25 wt% aqueous solution of trimethylamine at 60 ^{o}C.[27] Quaternary ammonium ion polymers were produced as shown below in Scheme 2.

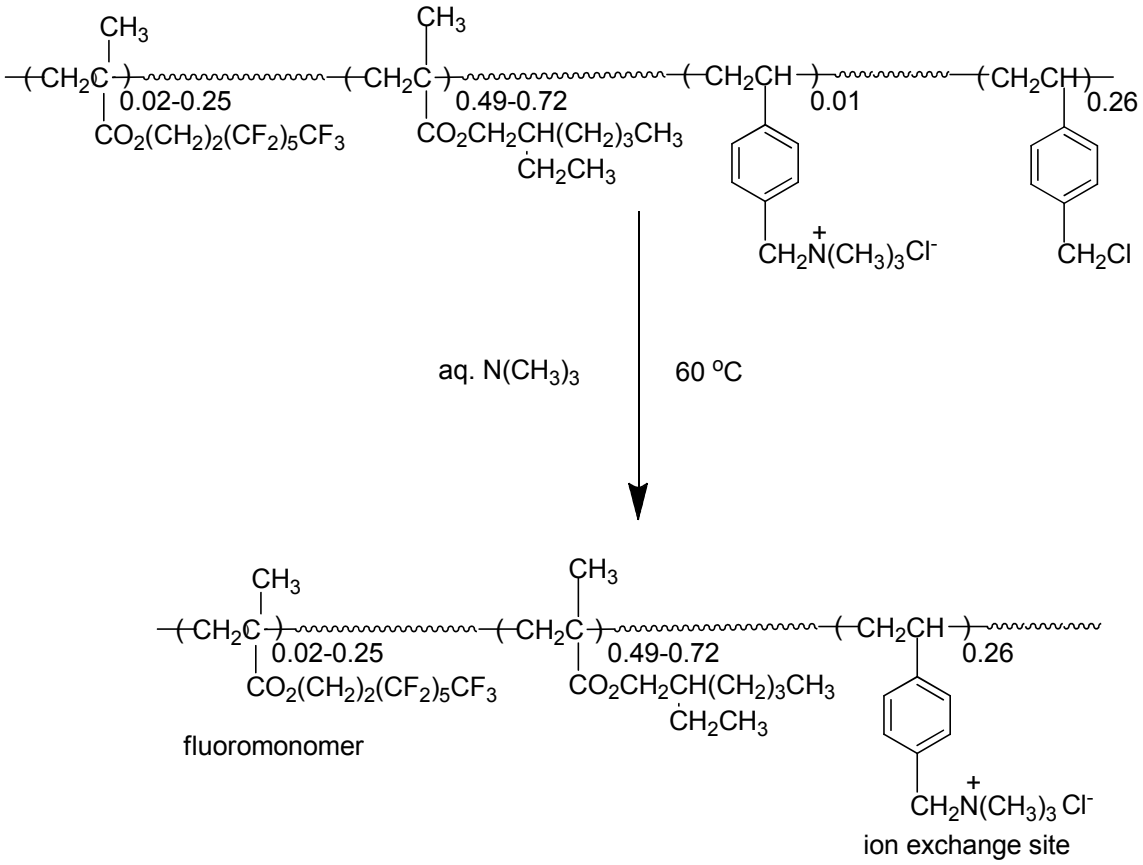

Scheme 2. Quaternization of polymer colloids.

The yield of the quaternization reactions was in the range of 43-68%. Evaporation of trimethylamine from the reaction mixture (stirred in a glass round-bottomed flask) at 60 ^{o}C is the probable reason for the lower yields of quaternization. The yield can be increased by doing the reaction in a stainless steel reactor (which can hold higher

pressure than a round-bottomed flask). The results of quaternization are shown in Tables 3 and 4. The diameters of the quaternary ammonium ion functionalized particles are larger than the diameters of their parent latex particles as calculated from DLS. The quaternary ammonium ion particles in aqueous dispersion are highly swollen by water because of the presence of large number of ionic functional groups in the core of the particles. The diameters are in the range of 113-280 nm.

Table 3. Composition of Quaternized Latexes Having 25% VBC Units

quaternized polymer	fluoromonomer, wt %	yield (%)	diameter (nm)[a]	volume ratio[b]	Cl^- (mmol/g)
BK-1QF	TFEMA, 2.5	43	140.	3.3	0.67
BK-2QF	PFOMA, 2.5	40	113	1.7	0.58
BK-3QF	TFEMA, 5.0	42	129	2.8	0.66
BK-4QF	PFOMA, 5.0	59	140	4.2	0.91
BK-5QF	TFEMA, 10.0	65	173	5.5	1.00
BK-6QF	PFOMA, 10.0	82	279	12.6	1.25
BK-10F	PFBEM, 10.0	69	279	3.8	1.06
BK-11QF	PFOMA, 25.0	53	207	7.6	0.63
BK-12QF	PFBEMA, 25.0	56	280	5.2	0.67
BK-13QF	TFEMA, 25.0	56	198	3.4	0.67

[a] Hydrodynamic diameter from dynamic light scattering, [b](Particle volume of quaternized polymer)/ (volume of precursor polymer)^3

Table 4. Composition of Quaternized Latexes Having 10% VBC Units and 10% Fluoromonomer

quaternized polymer	fluoromonomer	yield (%)	diameter[a] (nm)	Cl^- (mmol/g)
BK-14QF	TFEMA	45	138	0.30
BK-15QF	PFOMA	32	222	0.21
BK-16QF	PFBEMA	34	140	0.23

[a] Hydrodynamic diameter from dynamic light scattering

Quaternary ammonium chloride content of the latex or mmol/g of N^+ was measured by potentiometric titration with standard silver nitrate solution using a chloride selective electrode. A titration curve of milliliters of silver nitrate vs. millivolts (as shown in Figure 2) was constructed and the end point was taken as the point of maximum slope.

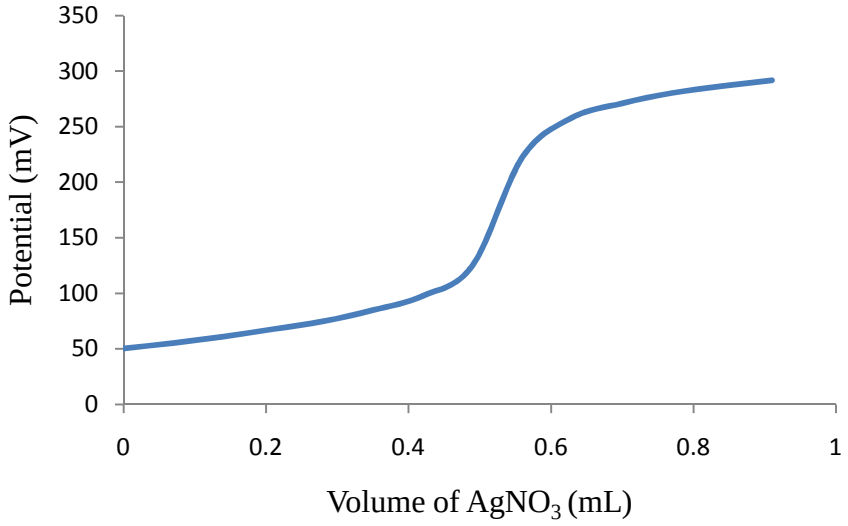

Figure 2. Potentiometric curve for BK-13QF vs. $AgNO_3$.

The chemical structure of quaternized polymers was confirmed by FTIR spectroscopy. FTIR spectra of the quaternized polymers showed no peak at 1262 cm^{-1} corresponding to – CH_2Cl. Figure 3 shows the IR spectrum of the VBC and corresponding quaternized polymer BK-12QF.

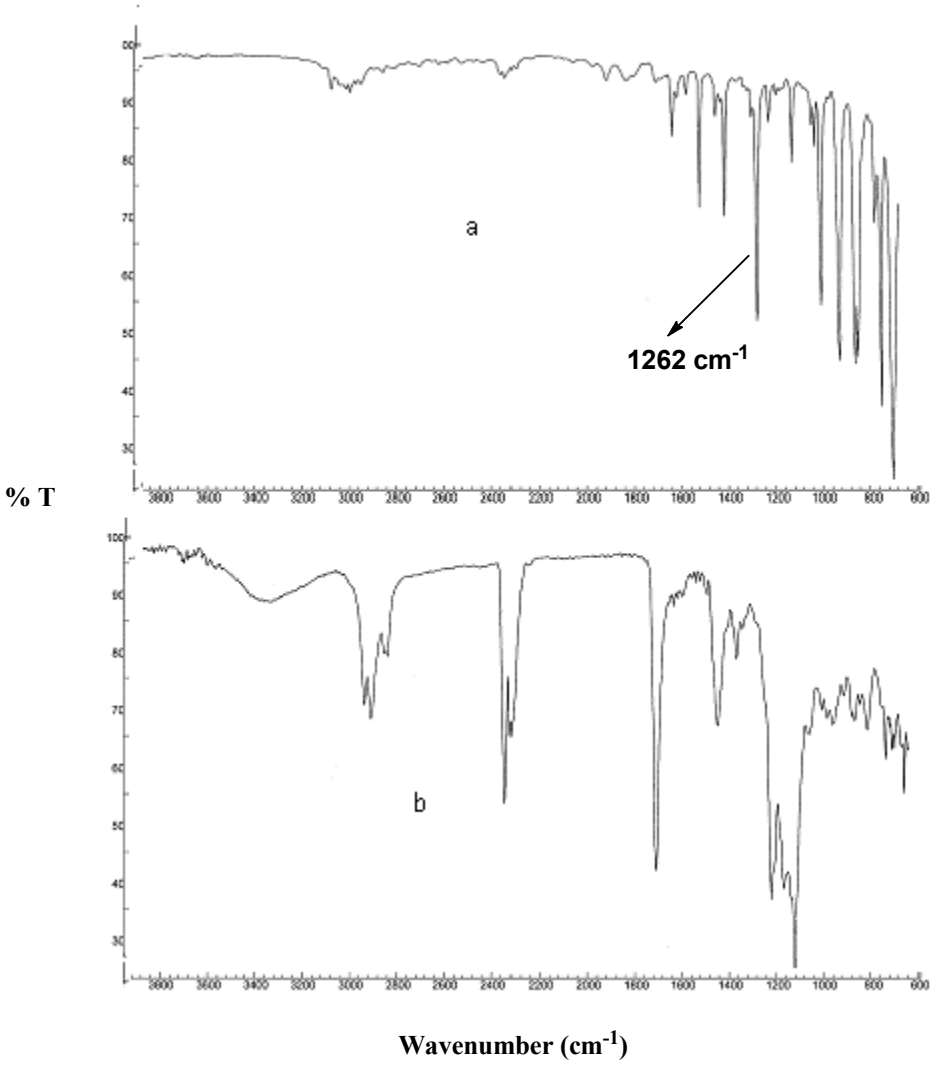

Figure 3. FTIR spectra (a) VBC; (b) Quaternized BK-12QF.

2.3 DSC Analysis of Copolymer and Quaternized Polymers

Glass transition temperatures (T_g) of the dried solid polymer colloids were measured by differential scanning calorimetry (DSC). An aqueous dispersion was dried at 110 ^oC to get solid polymer, and the solid particles were pulverized to fine powder before analysis. DSC analysis was conducted at temperature range of -100 ^oC to 150 ^oC with the ramp of 5 ^oC per minute. DSC analysis showed T_g of 38 ^oC for the BK-6F dried copolymer of EHMA, VBC and PFOMA and the result is shown in Figure 4.

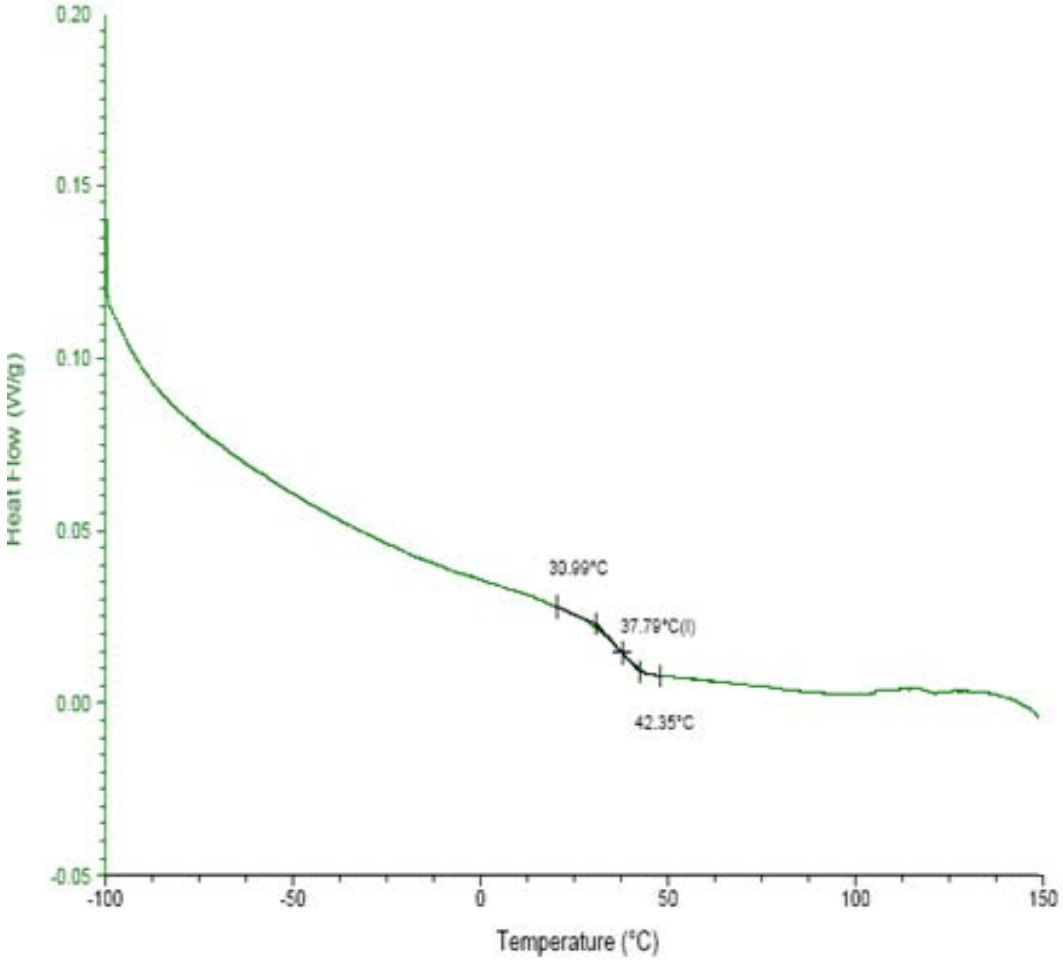

Figure 4. DSC of BK-6F.

DSC analysis of quaternized polymers for BK-5, 6, 8, 11, 12, 13QF showed T_g values in the range of 92 ^{o}-106 ^{o}C. Since the quaternized polymer contains a large number of ionic groups in the core, the T_g of quaternized polymer is higher than the T_g of unquaternized polymer. Table 5 below shows the T_g of the quaternized polymers BK-5, 6, 11 – 13QF and Figure 5 shows the DSC result of BK-6QF.

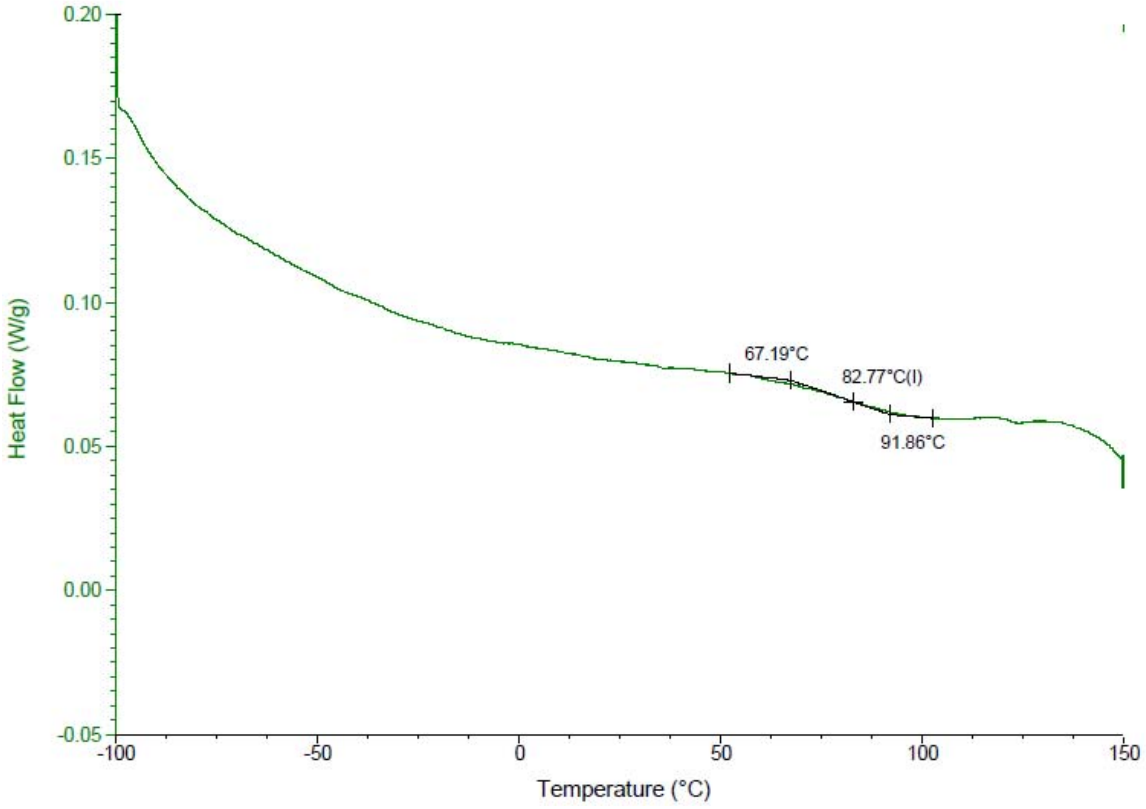

Figure 5. DSC of BK-6QF.

Table 5. DSC Results of BK-5, 6, 11, 12, 13QF Polymers

quaternized polymer	T_g (^oC)
BK-5QF	106
BK-6QF	83
BK-11QF	102
BK-12QF	94
BK-13QF	91

2.4 Atomic Force Microscopy (AFM) Analysis

The morphology of the polymer dispersions of BK-5, 6, 10, 11-13QF was studied by atomic force microscopy (AFM) at Oklahoma State University (OSU). The samples were prepared by spreading latex particles as thin films (drop cast method) on glass cover slips. The coatings were dried at room temperature for 18 h. The thicknesses of the films (calculated by the amount of polymer in the liquid spread to the surface area of the glass cover slip) were 2 µm. AFM images of the films showed surface contours of layers of particles about the same size as the parent particles measured by DLS. Since the polymer coating does not flow at room temperature and knowing the T_g of the polymer BK-6F (38 ^oC), the coatings were annealed at 60 ^oC for 18 h. AFM images of annealed samples showed that films with bumpy surfaces obtained at room temperature were converted to more robust films having smoother surfaces. Annealing flattens the films and promotes surface enrichment of fluorinated branches. Figure 6 shows the AFM images of BK-6F-drop-25 or before annealing, and BK-6F-drop-60 or after annealing.

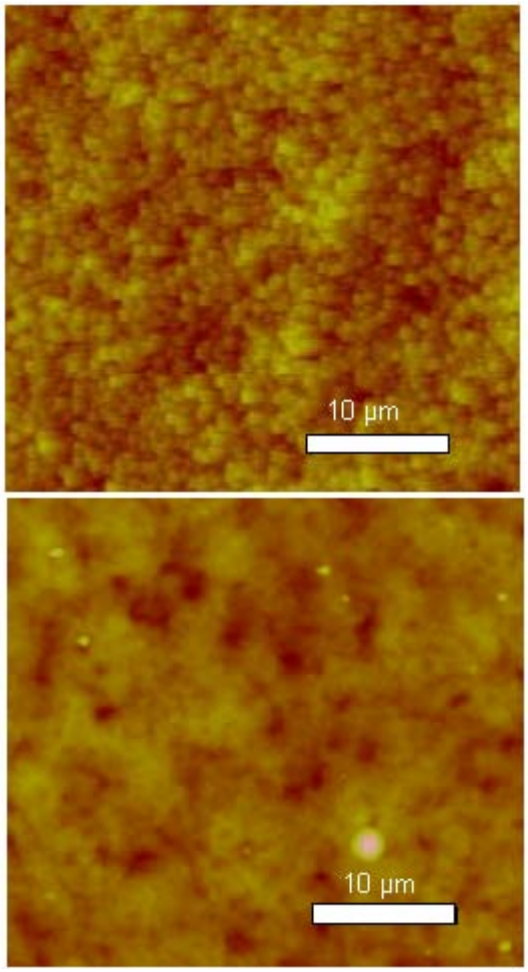

(a)

(b)

Figure 6. AFM images (a) BK-6F-drop-25 and (b) BK-6F-drop-60

Morphologies of the films of quaternized particles annealed at 120 ^{o}C and 165 ^{o}C were studied by AFM at Kansas State University. The coatings were prepared by drop casting and spin casting the aqueous dispersion. The drop cast films were prepared by spreading the latex particles on glass cover slips and were annealed at 120 ^{o}C. The spin cast films were prepared by applying quaternized dispersions (95 µL) to the glass cover slips treated with a mixture of potassium hydroxide and isopropyl alcohol for 1 h followed by washings with deionized water and coating at 1200 rpm on a spin coater. The

process was repeated several times. The final thicknesses of the coatings were in the range of 0.70-1.4 µm. The spin coated films were annealed at 165 ^{o}C for 18 h. The coatings of the quaternized particles annealed at 120 ^{o}C showed the presence of particles and the surfaces were rough. Figure 7 (a) shows the AFM image of BK-11QF-drop-120 after annealing. The AFM images of the spin coated samples annealed at 165 ^{o}C shows that latex particles are not coalesced to a continuous film even at high temperature. Figure 7 shows the AFM images of the quaternized polymer (a) BK-11QF-drop-120(coating of BK-11QF made by drop cast and annealed at 120 ^{o}C) and (b) BK-11QF-spin-165(coating of BK-11QF made by spin cast and annealed at 165 ^{o}C).

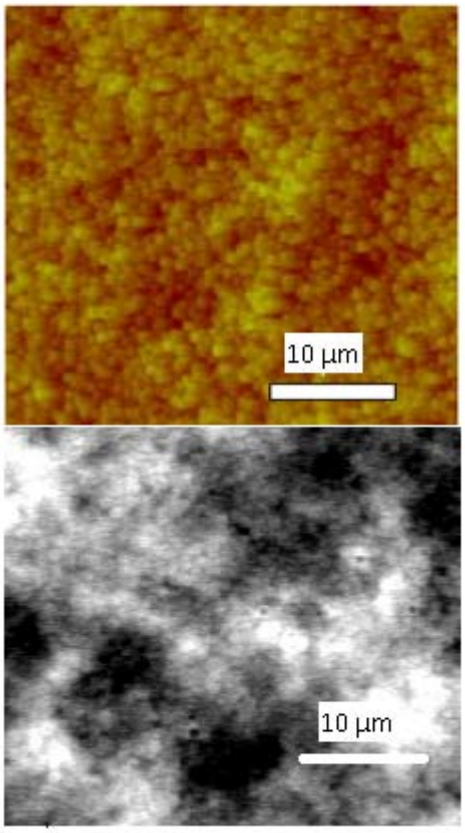

Figure 7. AFM images (a) BK-11QF-drop-120 and (b) BK-11QF-spin-165.

2.5 Contact Angle Measurements

Contact angle measurement determines surface energy of the material.[29] The lower the surface energy of the material, the higher is the contact angle of water. If the contact angle of a substance with water is more than 90^{o} then the surface of the substance is called hydrophobic. Oil spreads on water because the surface energy of oil is much less than the surface energy of water.[30] Static contact angles of the annealed coatings of BK-5F-drop-60 and BK-6F-drop-60 measured at OSU from photographs of a 0.05 mL drop of deionized water on coatings were in the range of 100^{o}-107^{o}. Dynamic contact angles of the copolymers (BK-5,6,10,11-13F-drop-90) measured by Sean McBride at Kansas State University were sometimes difficult to measure because of pinning of the contact line of the drop at the surface of the coating. Pinning of the drop means that the contact line did not move when the volume of the drop was increased or decreased. The pinning of water drop into the coating was due to roughness of the surface of the coatings.

In order to decrease the chances of pinning water drops to the coatings, the quaternized polymers were spin coated. The spin coated samples were annealed at 120 ^{o}C. Reliable contact angles were achieved due to the smooth surfaces obtained by spin coating the samples. The advancing contact angles were in the range of 95^{o}-100^{o}.

The contact angles of spin coated samples annealed at 165 ^{o}C were measured against hexadecane. The contact angles were higher for BK-11-13QF-spin-165 (having higher fluoromonomer content, 25 % by weight). Annealing at high temperature results in the replacement of surface hydrocarbon groups by surface fluoro groups as indicated by the higher contact angles against hexadecane for these samples. Tables 6 and 7 show the results of contact angle measurements against water and hexadecane.

Table 6. Contact Angles of Water on the Quaternized Polymer Films

polymer films	thickness of film (μm)	[a]θ_A (^{o})	[b]θ_R (^{o})
BK-5QF-spin-120	0.71	96.6	64.7
BK-6QF-spin-120	0.76	99.0	67.2
BK-10QF-spin-120	0.76	95.5	-
BK-11QF-spin-120	1.41	103	69.8
BK-12QF-spin-120	0.95	-	-
BK-13QF-spin-120	1.21	101	69.1

[a]Advancing contact angle; [b]Receding contact angle;

Table 7. Contact Angles of Hexadecane on the Quaternized Polymer Films

polymer films	thickness of film (μm)	[c]θ_H (^{o})
BK-5QF-spin-165	0.71	4.0
BK-6QF-spin-165	0.76	5.0
BK-10QF-spin-165	0.76	8.0
BK-11QF-spin-165	1.41	35
BK-12QF-spin-165	0.95	23
BK-13QF-spin-165	1.21	14

2.6 Kinetics of Hydrolysis of PNPH and Paraoxon

Cationic polymer colloids of BK-1QF - BK-13QF were tested as phase transfer catalyst for the hydrolysis of PNPH and Paraoxon as shown in Scheme 3. Quaternary ammonium ion functionalized polymers BK-1QF - BK-13QF differ by the type and composition of fluoromonomer in the shell (Table 3). All the quaternized polymers in aqueous solution were swollen as determined by dynamic light scattering (Table 3). Both the aqueous dispersions and the coatings made from the dispersions catalyzed the hydrolyses of PNPH and Paraoxon. The cationic polymer colloids BK-14QF - BK-16QF containing 10% VBC units were not tested for hydrolysis because the N^+ content was low (0.2-0.3).

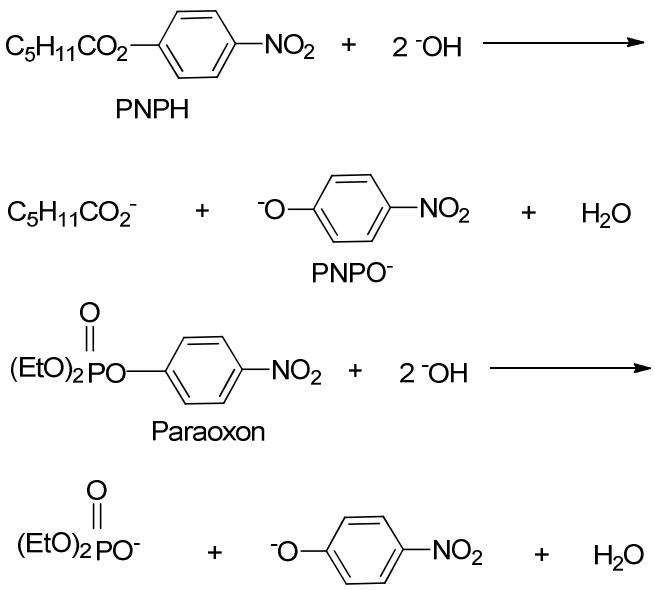

Scheme 3.

Results of the hydrolysis study such as pseudo-first order rate constants, second order rate constants, half lives ($t_{1/2}$), and conditions of hydrolysis along with mmols/g of N^+ used are discussed in detail in the following subsections.

2.6.1 Hydrolysis of PNPH using Colloidal Particles (BK-1QF - BK-13QF)

Aqueous dispersions of polymers BK-1QF - BK-13QF (see Table 3) were used to study the hydrolysis of PNPH at pH 9.4 in borate buffer solution at 30 ^oC. The hydrolysis reaction was fast and 80% of the conversion of PNPH to $PNPO^-$ occurred within 10 min. The values of k_{obs} were calculated using the integrated first-order rate equation $k_{obs}t = \ln[(A_\infty-A_o)/(A_\infty-A_t)]$ where t, A_∞, A_o, and A_t are time, absorbance at infinity, initial absorbance and absorbance at time t. The kinetic calculations were done by plotting the data over the first 60% conversion of PNPH. Concentration of PNPH (8.3×10^{-5} M) changes with time t, with no change of pH due to the borate buffer (taken in excess, 0.02 M). Therefore, the reaction should follow pseudo first-order kinetics. The data fit pseudo first-order kinetics for the hydrolysis of PNPH as shown below for BK-3QF in Figure 8.

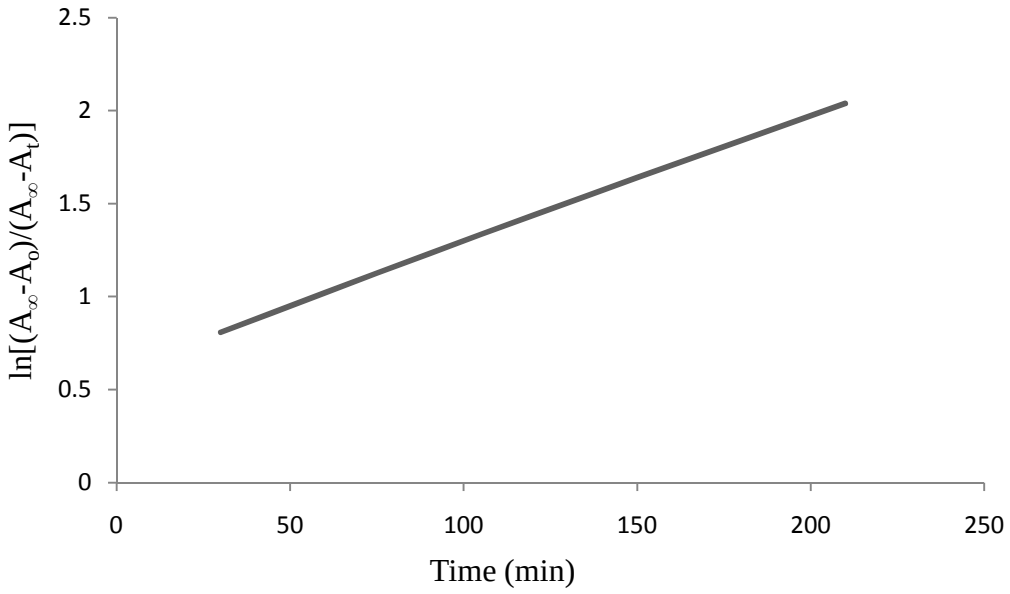

Figure 8. Pseudo first-order kinetics of PNPH hydrolysis using BK-5QF.

The first-order rate constant k_{obs} was calculated from the slope of the curve in Figure 8. The second-order rate constant k_2 and half life $t_{1/2}$ were calculated using the following equations:

$k_2 = k_1 / [N^+]$ where $k_1 = k_{obs}$

where, $[N^+]$ is the concentration of quaternary ammonium ion in the reaction mixture.

$t_{1/2} = 0.693/k_1$

where, k_1 is first-order rate constant,

The results for all the quaternized polymer dispersions for hydrolysis of PNPH such as the amount and concentration of quaternary ammonium ion latexes, the pseudo first-order rate constants (k_1), the second order rate constants (k_2), the half lives ($t_{1/2}$) and the change of absorbance at 400 nm of PNPH stock solution are shown in Table 8 and Figures 9 and 10.

Table 8. Kinetic Results of Particle Catalysis for Hydrolysis of PNPH at 30 ±1 ^{o}C

product ID	particles (mg)	$[N^+]$ (M)	k_1 (min^{-1})	k_2 (L mol^{-1} min^{-1})	$t_{1/2}$ (min)
BK-1QF	0.60	1.7×10^{-4}	0.173	1.01×10^{3}	4.0
BK-2QF	0.30	2.6×10^{-4}	0.099	3.80×10^{2}	7.0
BK-3QF	0.60	1.7×10^{-4}	0.277	1.62×10^{3}	2.5
BK-4QF	0.60	2.6×10^{-4}	0.198	7.61×10^{2}	3.5
BK-5QF	0.60	2.5×10^{-4}	0.277	1.10×10^{3}	2.5
BK-6QF	0.50	2.5×10^{-4}	0.346	1.38×10^{3}	2.0
BK-10QF	0.68	3.1×10^{-4}	0.198	6.34×10^{2}	3.5
BK-11QF	0.64	1.8×10^{-4}	0.198	1.10×10^{3}	3.5
BK-12QF	0.84	2.5×10^{-4}	0.231	9.24×10^{2}	3.0
BK-13QF	0.84	2.5×10^{-4}	0.154	6.16×10^{2}	4.5

All the quaternized aqueous dispersions derived from 25% VBC particles (BK-1QF - BK-13QF) were tested as phase transfer catalysts for the hydrolysis of PNPH and Paraoxon in basic solution. Hydrolysis was carried out in a polystyrene cuvette at 30 ^{o}C containing a mixture of colloidal dispersion or colloidal coating and borate buffer solution at pH 9.4 (for hydrolysis of PNPH) or 0.1 M NaOH (for hydrolysis of Paraoxon). In all of the experiments, the appearance of $PNPO^-$ was monitored by the increase in absorbance of the aqueous phase at 400 nm. There was rapid increase of absorbance for 5-7 minutes after the injection of a stock solution of PNPH followed by a slow increase or a constant absorbance up to 60 minutes. All of the experiments show a significant absorbance at time zero, which was due to the absorbance contributed by $PNPO^-$ that was already present and to scattering of the light by the latex particles. As the time delay

between the addition of the stock solution of PNPH to the reaction mixture and the first measurement was only a few seconds, there was not a significant absorbance at time = 0 due to the absorption of light by $PNPO^-$. It is clear from all the Figures that there was wide range of absorbance values (0.2-0.7) at t = 0. All the catalysts tested had different diameters and hence could scatter the light by different extent. This could be the reason for the wide range of absorbance values at t = 0. As shown in Figure 9, there was not a fast increase of absorbance over the first 5-7 minutes for the hydrolysis of PNPH in a control experiment (entry 'h' in Figure 9) performed with no colloidal particles in the reaction mixture. The data for the hydrolysis of PNPH in the presence of colloidal particles fit pseudo first order kinetics and all data extrapolate to a lesser amount of $PNPO^-$ than the quantitative amount of $PNPO^-$ after correction for the absorbance at t = 0 because of the turbidity.

Hydrolysis of Paraoxon was studied likewise using quaternary ammonium ion exchange colloidal particles as well as coatings made from aqueous colloidal dispersion in 0.1 M NaOH solution except that the concentration of Paraoxon was in the range of 8.3×10^{-5} - 1.7×10^{-4} M. The hydrolysis of the Paraoxon in colloidal particles as well as in the coatings is shown in Figures 14, 15, 16, 17, 18. All the experimental data fit pseudo first order kinetics. The hydrolysis of the Paraoxon was tested further on spin coated polymers of BK-18F - BK-23F. The thicknesses of the spin coated samples were 0.7-1.2 µm compared with 2-5 µm thicknesses of non-spin coated samples.

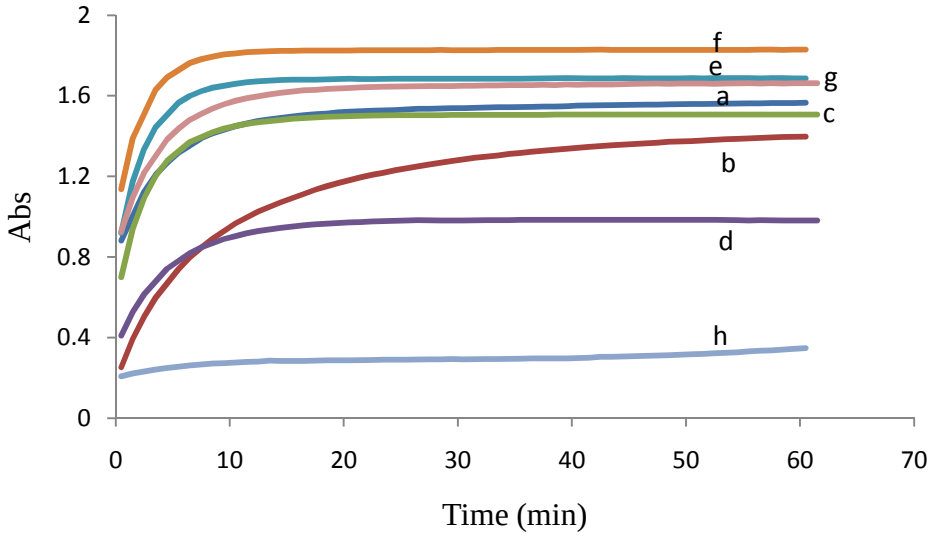

Figure 9. Change of absorbance at 400 nm due to hydrolysis of PNPH in pH 9.4 borate buffer solution at 30 ^{o}C using catalysts (a = BK-1QF; b = BK-2QF; c = BK-3QF; d = BK-4QF; e = BK-5QF; f = BK-6QF; g=BK-10QF; h = control experiment without particles).

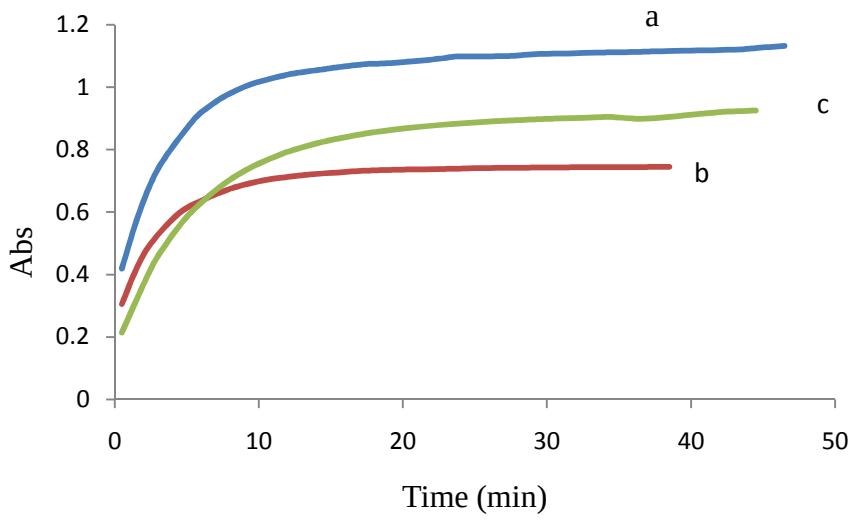

Figure 10. Change of absorbance at 400 nm due to hydrolysis of PNPH in borate buffer solution at 30 ^{o}C using catalysts (a = BK-11QF; b = BK-12QF; c = BK-13QF).

2.6.2 Hydrolysis of PNPH on Colloidal Coatings or Films Made from (BK-1QF - BK-13QF)

Colloidal dispersions were spread on to the clean glass cover slips. The resulting films were annealed at 75 ^{o}C (BK-1QF – 10QF) and 90 ^{o}C (BK-11QF - BK-13QF) for 18 h since colloidal particles peeled off the unannealed coatings during catalysis. The thicknesses of the coatings were calculated from the dimensions of the glass cover slips, the volume of aqueous dispersion spread on to the cover slips and the solids content of the dispersions. The coatings were inserted next to the opaque side of the polystyrene cuvettes to study the hydrolysis reaction of PNPH in contact with the colloidal particles on the coatings as shown in Figure 11.

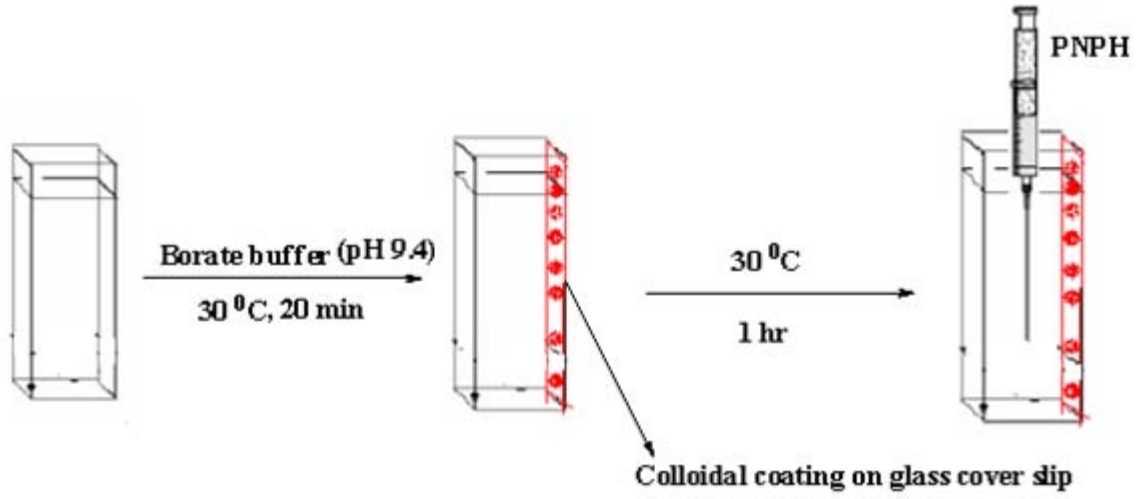

Figure 11. Hydrolysis of PNPH on colloidal coating.

The results of the hydrolyses (using coatings) such as rate constants, half lives ($t_{1/2}$), amount of N^{+}, thicknesses of the coatings, are shown in Tables 9 and 10, and Figures 12 and 13. The data in Figures 12 and 13 are noisier than in Figures 9, 10 because the instrumental setting that controls noise was set differently in these experiments and

the data for these experiments was recorded and plotted every second rather than every minute. The hydrolyses of PNPH with the coatings was slower than the hydrolyses with the aqueous colloidal particles. The data for runs a, b, and e in Figure 12 show deviation from first order kinetics. The probable cause of the deviation is air bubbles in the reaction mixture. But the slope of the curve calculated by using the linear least squares method shows that reactions nearly follow pseudo first order kinetics.

Table 9. Amounts of Particles and Thicknesses of Coatings[a]

product ID	particles (mg)	area of cover slip (cm^2)	thickness of film (μm)
BK-1QF-drop-75	0.85	3.2	2.1
BK-2QF-drop-75	0.38	3.2	0.9
BK-3QF-drop-75	0.75	3.6	2.0
BK-4QF-drop-75	0.83	3.2	2.3
BK-5QF-drop-75	0.68	3.6	2.1
BK-6QF-drop-75	0.54	3.6	1.5
BK-10QF-drop-75	0.77	3.6	2.1
BK-11QF-drop-90	1.28	3.2	3.5
BK-12QF-drop-90	1.68	3.6	5.2
BK-13QF-drop-90	1.68	3.6	4.6

Table 10. Kinetic Results of Coating Catalysis for Hydrolysis of PNPH[a]

product ID	$[N^+]$ (M)	$t_{1/2}$ (min)	k_1 (min^{-1})	k_2 ($L\ mol^{-1}\ min^{-1}$)
BK-1QF-drop-75	2.4×10^{-4}	41.0	0.016	6.60×10^{1}
BK-2QF-drop-75	3.4×10^{-4}	43.0	0.016	4.70×10^{1}
BK-3QF-drop-75	2.2×10^{-4}	14.0	0.049	2.26×10^{2}
BK-4QF-drop-75	3.3×10^{-4}	3.5	0.198	6.00×10^{2}
BK-5QF-drop-75	3.0×10^{-4}	23.0	0.030	1.02×10^{2}
BK-6QF-drop-75	3.0×10^{-4}	10.5	0.066	2.26×10^{2}
BK-10QF-drop-75	3.5×10^{-4}	12.0	0.057	1.62×10^{2}
BK-11QF-drop-90	3.5×10^{-4}	70.0	0.010	0.28×10^{2}
BK-12QF-drop-90	4.8×10^{-4}	85.0	0.008	0.17×10^{2}
BK-13QF-drop-90	4.8×10^{-4}	80.0	0.009	0.19×10^{2}

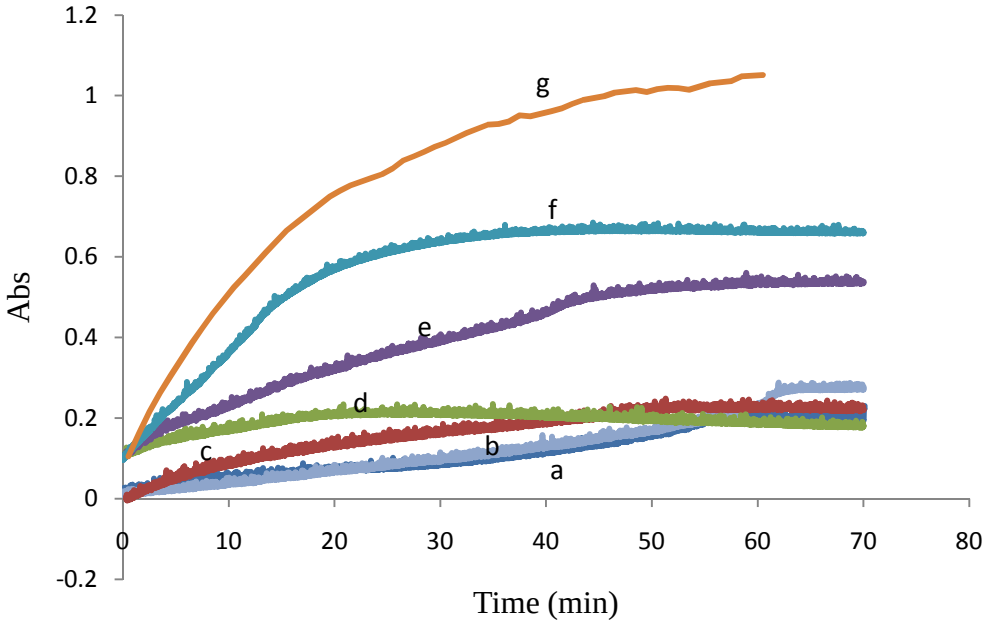

Figure 12. Change of absorbance at 400 nm due to hydrolysis of PNPH in pH 9.4 borate buffer solution at 30 ^{o}C using catalyst coatings (a = BK-1QF-drop-75; b = BK-2QF-drop-75; c = BK-3QF-drop-75; d = BK-4QF-drop-75; e = BK-5QF-drop-75; f = BK-6QF-drop-75; g=BK-10QF-drop-75).

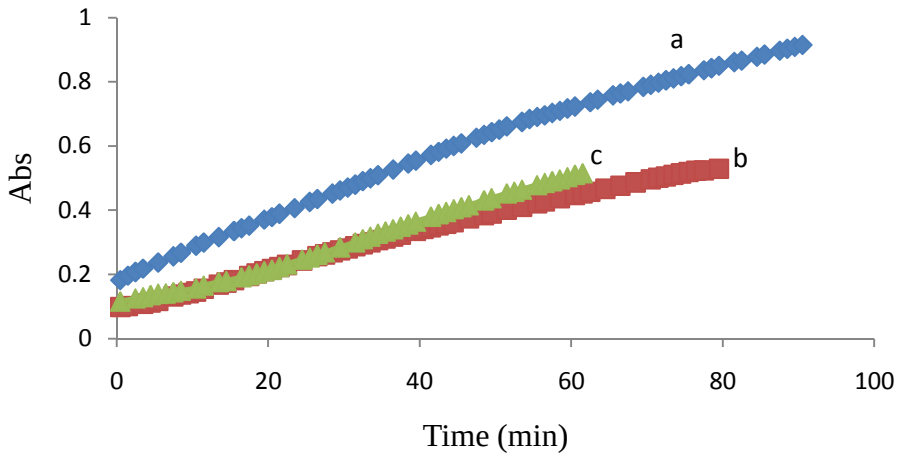

Figure 13. Change of absorbance at 400 nm due to hydrolysis of PNPH in pH 9.4 borate buffer solution at 30 ^{o}C using catalyst coatings (a = BK-11QF-drop-90; b = BK-12QF-drop-90; c = BK-13QF-drop-90).

2.6.3 Hydrolysis of Paraoxon using Colloidal Particles (BK-1QF - BK-13QF)

Aqueous dispersions of polymers BK-1QF - BK-13QF were used to study the hydrolysis of Paraoxon in 0.10 M sodium hydroxide solution at 30 ±1 ^{o}C. The hydrolysis reaction was fast, 80% conversion occurred within 10 min. The results for all the quaternized polymer dispersions for hydrolysis of Paraoxon such as concentrations of quaternary ammonium ion latexes, first-order rate constant, second order rate constants, half life period ($t_{1/2}$), and change of absorbance at 400 nm of Paraoxon are shown in Figures 14 and 15, and Table 11.

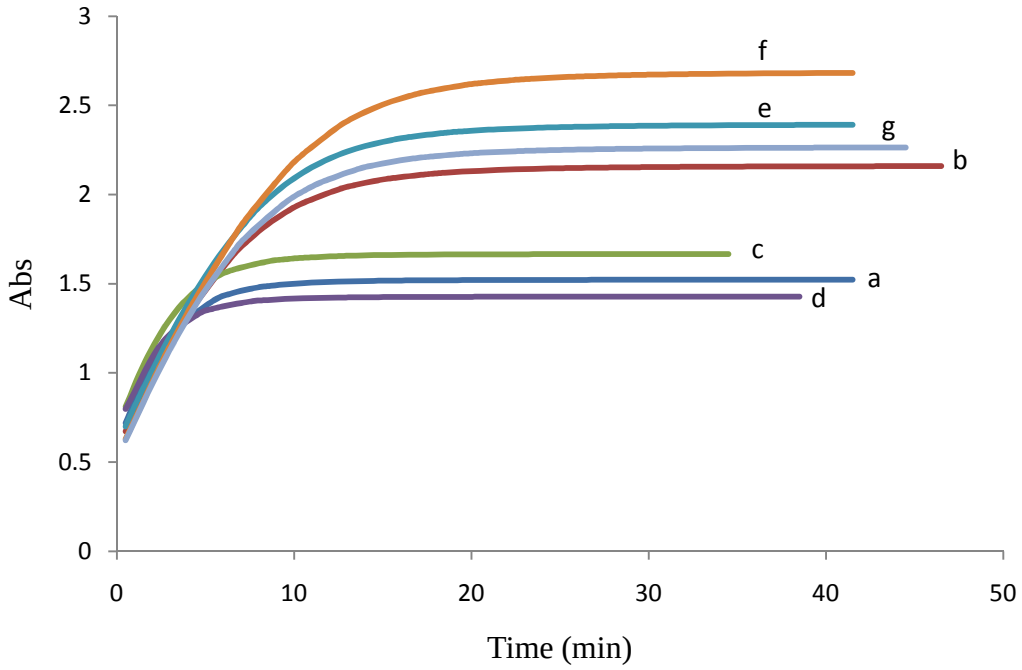

Figure 14. Change of absorbance at 400 nm due to hydrolysis of Paraoxon in 0.10 M NaOH using catalysts (a = BK-1QF; b = BK-2QF; c = BK-3QF; d = BK-4QF; e = BK-5QF; f = BK-6QF;g= BK-10QF).

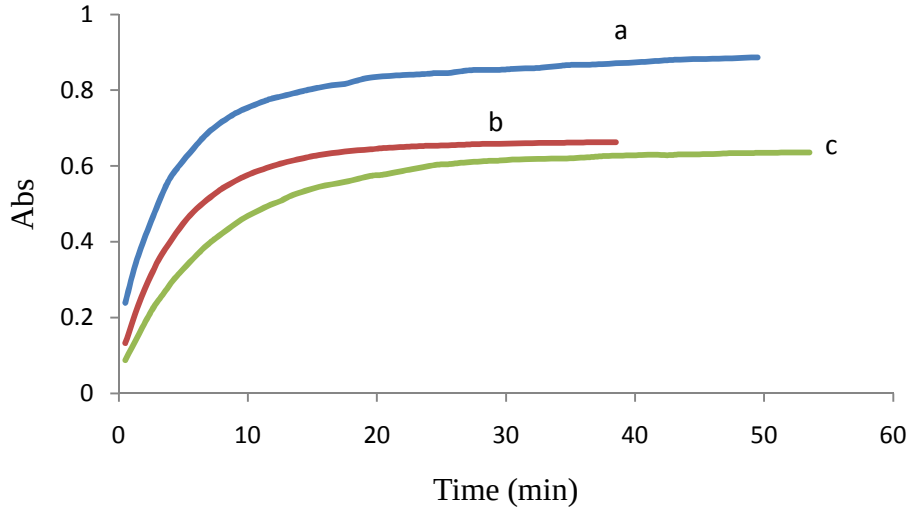

Figure 15. Change of absorbance at 400 nm due to hydrolysis of Paraoxon in 0.10 M NaOH using catalysts (a = BK-11QF; b = BK-12QF; c = BK-13QF).

Table 11. Kinetic Results of Particle Catalysis for Hydrolysis of Paraoxon

product ID	particles (mg)	$[N^+]$ (M)	k_1 (min^{-1})	k_2 ($L\ mol^{-1}\ min^{-1}$)	$t_{1/2}$ (min)
BK-1QF	0.60	1.7×10^{-4}	0.231	13.5×10^2	3.0
BK-2QF	0.30	2.6×10^{-4}	0.154	5.92×10^2	4.5
BK-3QF	0.60	1.7×10^{-4}	0.277	16.2×10^2	2.5
BK-4QF	0.60	2.6×10^{-4}	0.277	10.6×10^2	2.5
BK-5QF	0.60	2.5×10^{-4}	0.154	6.16×10^2	4.5
BK-6QF	0.50	2.5×10^{-4}	0.126	5.04×10^2	5.5
BK-10QF	0.68	3.1×10^{-4}	0.138	4.42×10^2	5.0
BK-11QF	0.64	1.8×10^{-4}	0.173	9.61×10^2	4.0
BK-12QF	0.84	2.5×10^{-4}	0.173	6.92×10^2	4.0
BK-13QF	0.84	2.5×10^{-4}	0.120	4.80×10^2	6.0

2.6.4 Hydrolysis of Paroxon on Colloidal Coatings or Films made from (BK-1QF-BK-13QF)

The coatings were made by drop casting. Colloidal dispersions were spread on to the clean glass cover slips. The resulting films were annealed at 90 ^oC for 18 h. The results of the hydrolysis of Paraoxon such as, rate constants, half life periods ($t_{1/2}$), concentration of N^+, thicknesses of the coatings, and change of absorbance vs. time are shown in Tables 12 and 13, and Figures 16-18.

Table 12. Kinetic Results of Coating Catalysis for Hydrolysis of Paraoxon[a]

product ID	$[N^+]$ (M)	$t_{1/2}$ (min)	k_1 (min^{-1})	k_2 ($L\ mol^{-1}\ min^{-1}$)
BK-1QF-drop-90	2.4×10^{-4}	5.5	0.126	5.25×10^2
BK-2QF-drop-90	3.4×10^{-4}	6.5	0.106	3.11×10^2
BK-3QF-drop-90	2.2×10^{-4}	5.5	0.126	58.3×10^2
BK-4QF-drop-90	3.3×10^{-4}	5.5	0.126	3.81×10^2
BK-5QF-drop-90	3.0×10^{-4}	10.0	0.069	2.34×10^2
BK-6QF-drop-90	3.0×10^{-4}	6.5	0.106	3.63×10^2
BK-10QF-drop-90	3.5×10^{-4}	6.0	0.115	3.27×10^2
BK-11QF-drop-90	3.5×10^{-4}	8.5	0.081	2.31×10^2
BK-12QF-drop-90	4.8×10^{-4}	8.5	0.081	1.68×10^2
BK-13QF-drop-90	4.8×10^{-4}	8.0	0.086	1.79×10^2

Table 13. Concentrations of Particles and Thicknesses of Coatings

product ID	particles (mg)	area of cover slip (cm^2)	thickness of film (µm)
BK-1QF-drop-90	0.85	3.2	2.60
BK-2QF-drop-90	0.38	3.2	1.19
BK-3QF-drop-90	0.75	3.6	2.08
BK-4QF-drop-90	0.83	3.2	2.59
BK-5QF-drop-90	0.68	3.6	1.90
BK-6QF-drop-90	0.54	3.6	1.50
BK-10QF-drop-90	0.77	3.6	2.10
BK-11QF-drop-90	1.28	3.2	4.00
BK-12QF-drop-90	1.68	3.6	4.60
BK-13QF-drop-90	1.68	3.6	4.60

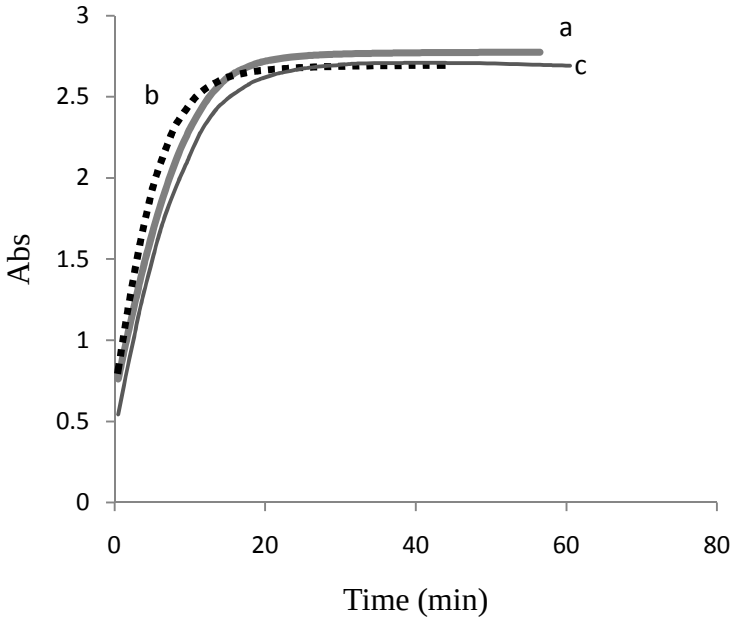

Figure 16. Change of absorbance at 400 nm due to hydrolysis of Paraoxon in 0.10 M NaOH using catalyst coatings (a = BK-1QF-drop-90; b = BK-2QF-drop-90; c = BK-3QF-drop-90).

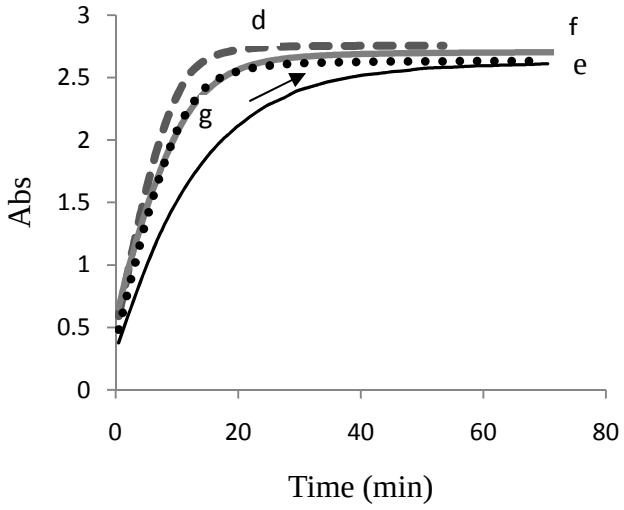

Figure 17. Change of absorbance at 400 nm due to hydrolysis a Paraoxon in 0.10 M NaOH using catalyst coatings (d = BK-4QF-drop-90; e = BK-5QF-drop-90; f = BK-6QF-drop-90; g = BK-10QF-drop-90).

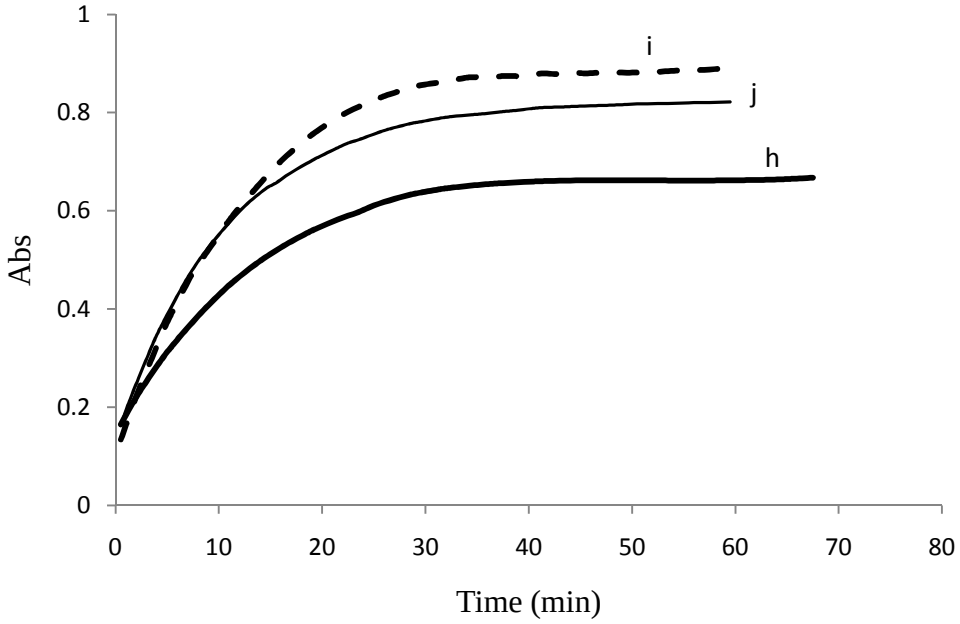

Figure 18. Change of absorbance at 400 nm due to hydrolysis of Paraoxon in 0.10 M NaOH using catalyst coatings (h = BK-11QF-drop-90; i = BK-12QF-drop-90; j = BK-13QF-drop-90).

2.6.5 Hydrolysis of Paraoxon on Spin Coated Films of BK-5, 6,10, 11-13QF

Hydrolysis of Paraoxon was further tested on the spin coated films of BK-5,6,10, 11-13QF. The spin coatings were made as described above for measuring the contact angles. Though the thicknesses of the spin coated samples were less (0.71-1.4 µm) than those of the drop coated samples (having thicknesses on the order of 2 µm), the rates of hydrolysis of Paraoxon were comparable. The above observation reveals that the diffusion of Paraoxon to the catalytic sites is not affected by the thickness of the films. The results of these catalysis studies are shown in Tables 14 and 15, and Figures 19 and 20.

Table 14. Concentrations of Particles and Thicknesses of Spin Coatings

product ID	particles (mg)	thickness of film[a,] (μm)
BK-5QF-spin-120	0.47	0.71
BK-6QF-spin-120	0.50	0.76
BK-10QF-spin-120	0.51	0.76
BK-11QF-spin-120	0.93	1.41
BK-12QF-spin-120	0.63	0.95
BK-13QF-spin-120	0.80	1.21

[a] Area of all the cover slips was 2.40 cm^2.

Table 15. Kinetic Results for Hydrolysis of Paraoxon on Spin Coatings

product ID	$[N^+]$ (M)	$t_{1/2}$ (min)	k_1 (min^{-1})	k_2 ($L\ mol^{-1}\ min^{-1}$)
BK-5QF-spin-120	2.0×10^{-4}	10.0	0.069	3.45×10^2
BK-6QF-spin-120	2.7×10^{-4}	9.5	0.072	2.66×10^2
BK-10QF-spin-120	2.4×10^{-4}	9.0	0.077	3.23×10^2
BK-11QF-spin-120	2.6×10^{-4}	9.0	0.077	2.98×10^2
BK-12QF-spin-120	1.9×10^{-4}	9.0	0.077	4.11×10^2
BK-13QF-spin-120	2.4×10^{-4}	14.0	0.049	2.07×10^2

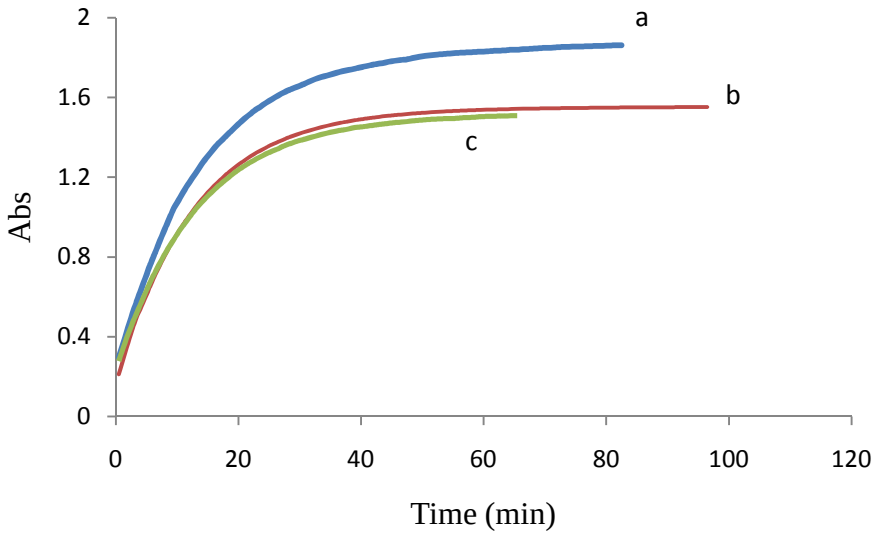

Figure 19. Change of absorbance at 400 nm due to hydrolysis of Paraoxon in 0.10 M NaOH using catalyst spin coatings (a = BK-5QF-spin-120;b = BK-6QF-spin-120; c = BK-10QF-spin-120).

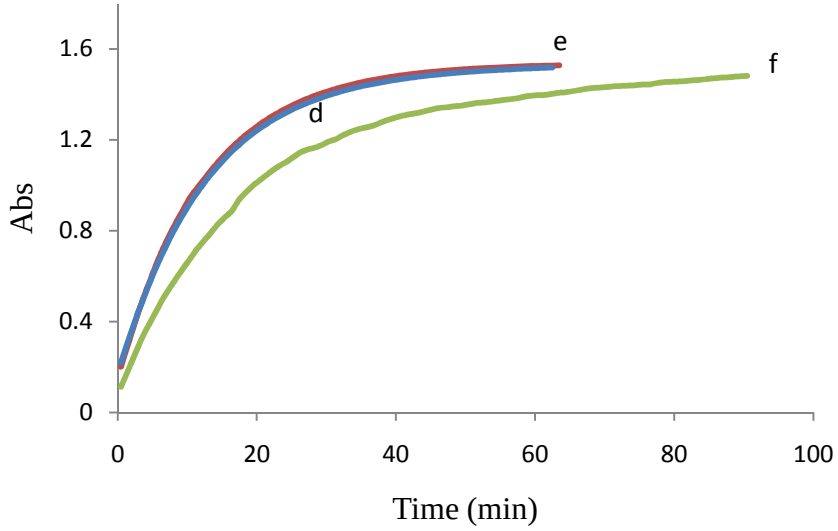

Figure 20. Change of absorbance at 400 nm due to hydrolysis of Paraoxon in 0.10 M NaOH using catalyst spin coatings (d = BK-11QF-spin-120; e = BK-12QF-spin-120; f = BK-13QF-spin-120).

2.7 Discussion

The contact angle measurements against water carried out on spin coated films of polymer colloids containing 10% and 25% fluoromonomers gave advancing contact angles in the range of 97^{o} -103^{o} and receding angles in the range of 65^{o}-75^{o}C. The contact angles indicate that the surface is not all fluoropolymer, because poly(tetrafluoroethylene)[31] (Teflon) has a contact angle of 115^{o}. However, it is known that after film formation the polymer chains of the original particles (core or shell) are rarely totally mixed homogeneously.[26] They, rather, form a heterogeneous material where the core and the shell polymer can be distributed in various fashions.[26] For instance, this occurs when the T_g of the core and shell are different. Hence, the polymer originally comprising the shell can form a uniform matrix in which the core stays intact and is uniformally distributed in the matrix along the shell. This can lower the contact angle expected from a fluorous shell. Polymer colloids synthesized in this study have polymer particles in the core and the shell with different T_g. This may be the reason for getting lower dynamic contact angles. The contact angles against hexadecane for samples 11QF, 12QF and 13QF are large, which is consistent with a higher fluorine content on or at the surface. Those samples were made with 25 wt% of the fluoro monomer, whereas the 5QF, 6QF and 10QF samples were made with 10 wt% of the fluouro monomer. Moreover the hexadecane contact angles increase with an increasing number of fluorine atoms in the fluoromonomer (BK-11QF, perfluorooctyl methacrylate (13 F atoms), contact angle=35^{o} 12QF, perfluorobutyl ethyl methacrylate (9 F atoms) contact angle = 23^{o} and BK-13QF trifluoroethyl methacrylate (3 F atoms) contact angle = 14^{o}

Theoretical A_∞ was calculated manually using $A_\infty = \varepsilon bc$ where, ε is the molar extinction coefficient (ε = 18000 M^{-1} cm^{-1}),[32] b = path length (1 cm), and c is the concentration of PNPH used and theoretical A_∞ = 1.5. The data for the hydrolysis of PNPH in the presence of colloidal particles extrapolate to lesser amount of $PNPO^-$ than the quantitative amount of $PNPO^-$ after correction for the absorbance at t = 0 because of the turbidity. This is probably due to presence of some $PNPO^-$ at t = 0 or due to slow mass transfer of PNPH to the ion exchange particles in the latex or the retention of more hydrophobic $PNPO^-$ ion over more hydrophilic hydroxide ion or borate ions.[33] Hence, retention of $PNPO^-$ in the ion exchange sites reduces the concentration of hydroxide ion or borate ion and thus the rate of reaction. For example, a slow increase of absorbance after 10 min in some of the entries, such as entry 'b' in Figure 9 and entry 'c' in Figure 10 is observed.

The hydrolysis of PNPH using quaternary ammonium ion exchange latexes in the form of coatings was slower than the hydrolysis of PNPH using colloidal particles as shown in Figures 12 and 13. The possible reason could be the slow diffusion of PNPH from the solution to the quaternary ammonium ion catalytic sites in the coatings.

The hydrolysis of the Paraoxon was studied on spin coated polymers of BK-5QF - BK-13QF. There was only a small difference in the rate of hydrolysis of Paraoxon using spin coated samples vs. non-spin coated samples as shown in Table 15. Possible reasons are (1) only the top 0.7-1.2 μm of the coating is catalytically active because reaction occurs before Paraoxon can diffuse deeper into the drop-cast films or spin-coated films, or (2) annealing of spin-coated films was carried out at higher temperature (120 ^oC). Annealing increases the concentration of N^+ sites near the surface of the coatings.

In order to achieve our goal of decontaminating simulants of chemical warfare agents from army buildings or equipment on the battlefield, the polymer colloids should be made on a large scale so that we can paint a wall of an army building to test the efficiency of quaternary ammonium ion colloidal catalyst for the hydrolysis of chemical warfare agents. To achieve stable coatings in catalysis and to avoid annealing of the coatings at high temperature before catalysis, the polymerization should be carried out in the presence of a suitable monomer having a T_g that can flow the dispersion properly at low temperature.

2.8 Conclusion

Our research on the semi-fluorinated core-shell latexes has proved that emulsifier-free emulsion polymerization in aqueous solution gave stable dispersions of EHMA, VBC, VBTACl, PFBEMA, PFOMA, and TFEMA. The polymerizations were fast and simple. Quaternary ammonium ion exchange phase transfer colloidal catalysts were synthesized from the copolymer by reacting the chloromethyl group of VBC with aqueous trimethylamine. The copolymers and the quaternized polymers were characterized by DLS, AFM, FTIR, and DSC analysis. Quaternized polymers of BK-1QF - BK-13QF were tested successfully as phase transfer catalysts for the hydrolysis of PNPH and Paraoxon at 30 ^{o}C in basic solution. The higher rate of reaction in polymer colloidal ion exchange catalysts are due to the high local concentration of the reactants.

2.9 Experimental

Materials. Vinylbenzyl chloride (VBC, 96%, m/p isomeric mixture) was purchased from Scientific Polymer Products, Inc. 2-Ethylhexyl methacrylate (EHMA, 98%) and vinylbenzyl(trimethyl)ammonium chloride (VBTMACl) were purchased from Aldrich Co, Inc.. Fluoromonomers 1H,1H,2H,2H-perfluorooctyl methacrylate (PFOMA) and 1H,1H,2H,2H-perfluorobutyl ethyl methacrylate (PFBEMA) were purchased from Top Fluorochem Inc.. Trifluoroethyl methacrylate (TFEMA) was from Aldrich Chemical Co. The initiator, 2,2-azobis(*2*-methylpropionamidine*)* dihydrochloride (Aldrich) and trimethylamine (Aldrich) 25% (w/w) solution in water were used as received. Diethyl *p*-nitrophenyl phosphate (Paraoxon) was purchased from Aldrich and *p*-nitrophenyl hexanoate was purchased from TCI Chemicals. Aluminum oxide (Al_2O_3, activated, basic, ~ 150 mesh, 58 Å) and acetonitrile from Aldrich were used as received. All the organic monomers were purified before use by passing through basic aluminium oxide. Triply deionized water was used in all the experiments. Borate buffer solution at pH 9.4 was prepared from aqueous boric acid solution by titration with sodium hydroxide.

Instrumentation. FTIR spectra were taken usinga Varian 800 FTIR Scimiter Series spectrophotometer. Potentiometric titrations were carried out with an Orion combination chloride selective electrode (model 9617B). Kinetic measurements were made using a Varian Cary 5000 spectrophotometer. DSC analysis of the copolymers and the quaternized polymers was performed on TA Instruments DSC Q2000. Morphologies of the precursor latex particles were studied by atomic force microscopy at OSU (Veeco Multimode SPM with conductive AFM module and heating/cooling stages) and of

quaternized latex were studied at Kansas State University. The particle size distributions of the latexes were studied dynamic light scattering (Malvern HPPS 3.1 instrument equipped with He-Ne, 3.0 mW, 633 nm laser). The samples for DLS measurement were prepared diluting a drop of aqueous dispersion of copolymer with 3 mL of deionized water. The particle size and size distribution were measured at 25 ^{o}C. Glass cover slips (1 cm^2) were cleaned with deionized water and acetone. The samples for AFM images were prepared by spreading 45 µL of the dispersion on a cover slip and annealing at 60 ^{o}C for 18 h.

2.9.1 Synthesis of Aqueous Polymer Colloids (BK-1F-BK-16F)

All the copolymers were made by shot growth emulsion polymerization of EHMA, VBC (10% and 25%), VBTMACl and PFBMA, PFOMA, and TFEMA (2.5% - 25%). A 50 mL three-necked round-bottomed flask fitted with an addition funnel, a mechanical stirrer fitted with a Teflon blade, and a reflux condenser equipped with a nitrogen inlet was purged with nitrogen for 10 min. Deionized water (20 mL) was charged to the flask and flushed with nitrogen for 30 min at 60 ^{o}C under continuous stirring. Nitrogen purged solid VBTMACl (10 mg) was added and the solution was stirred for 5 min. Purified and nitrogen-purged EHMA (0.740 g) and VBC (0.250 g) were added and stirred for 10 min. Initiator 2,2-azobis(*2*-methylpropionamidine*)* dihydrochloride (10 mg) dissolved in 1.0 mL of water was added to the reaction mixture. The reaction mixture was kept at 60 ^{o}C for 1.0 h. The mixture turned cloudy due to nucleation of the particles within 35-40 min. After 1.0 h a mixture of EHMA (0.215 g), VBC (0.073 g), VBTMACl (9 mg), and TFEMA (0.033 g) followed by initiator (3 mg)

was added. The reaction mixture was stirred for 4 h at 60 ^{o}C. The reaction mixture was cooled and filtered through a cotton plug to remove traces of coagulum to give a stable dispersion of BK-1F. The same procedure was repeated using different wt% of PFBMA, PFOMA, or TFEMA and of VBC to give the stable polymer colloids of BK-2F - BK-16F in Tables 1 and 2.

2.9.2 Quaternizations of Copolymers BK-1F-BK-16F

A mixture of 10 mL of polymer colloid BK-1F (0.550 g of solid, 0.9 mmol of VBC groups) diluted with 7 mL of deionized water and 25 wt% aqueous trimethylamine (0.160 g, 2.7 mmol) was transferred to a 50 mL round bottom flask. The reaction mixture was stirred magnetically for 48 h at 60 ^{o}C. Since trimethylamine evaporates quickly at 60 ^{o}C, repeated additions (twice a day) of trimethylamine (0.160 g, 2.7 mmol) were carried out for samples BK-5QF-BK-13QF. The excess trimethylamine at the end of reaction was removed by purging nitrogen through the latex for 2 h to give stable cationic dispersions.

Solid Content of Precursor and Quaternized Latexes. The solid content of all the precursor and quaternized polymer colloids was measured by weighing 1.0 mL of the latex accurately and drying to constant weight in an oven at 110 ^{o}C. Determinations performed in triplicate were reproducible within 3% of the mean.

2.9.3 Determination of Chloride Content of Quaternized Polymer BK-1QF-BK-13QF

Quaternary ammonium chloride contents of the latexes were measured by potentiometric titration with an Orion 9617 chloride-selective electrode. To a 50 mL beaker were added 1.0 mL of the aqueous latex of accurately measured solid content, 0.5 mL of 5 M $NaNO_3$, and 20 mL of water to cover the tip of the electrode. The pH of the solution was adjusted to 2.0 with 1 M HNO_3, and the mixture was titrated with standard 0.05 M $AgNO_3$. A titration curve of millivolts vs. milliliters of titrant was constructed, and the end point was taken as the point of maximum slope as shown in Figure 2.

Kinetic Measurements. Stock solutions of 2.5 mM *p*-nitrophenyl hexanoate and 2.5 mM Paraoxon were prepared in acetonitrile on the day of use. Sodium hydroxide solution 0.10 M was prepared in nitrogen purged deionized water and was stored in an air tight container.

2.9.4 Hydrolysis of PNPH using Colloidal Particles

Colloidal particles as a dispersion of BK-1QF (0.60 mg, $[N^+]$ =1.7 $x10^{-4}$) and helium purged borate buffer solution (2.2 mL, pH 9.40, 0.02M) were added in sequence to a polystyrene cuvette. The solution was equilibrated at 30 ± 1 ^oC for 20 min with magnetic stirring in the thermostated cell compartment of a Varian Cary 5000 spectrophotometer. PNPH stock solution in acetonitrile (74 µL, 2.5 mM) was added to the reaction mixture by syringe. The absorbance of the solution at 400 nm was recorded. Hydrolysis of PNPH using colloidal particles of BK-2QF - BK-13QF was carried out by

the same procedure. The amounts and concentrations of quaternary ammonium ion exchange catalysts are shown in Table 7.

2.9.5 Preparation of Coatings by Drop Casting

To a glass cover slip having area of 3.2 cm^2, 25μL of BK-1QF (0.85 mg of particles, $[N^+]$ was 2.4 x 10^{-4} M in the whole mixture) polymer particles were applied at room temperature and the dispersion was spread by using a syringe plunger. The coating was annealed at 75 ^oC for 18 h. To the naked eye, the coatings look clear and colorless but it is hard to say anything about the uniformity. The average thickness of the final film was calculated as follows:

Thickness = Volume of particles applied/ Surface area of the glass slide.

25 μL of BK-1QF = 0.85 mg of particles with assumed density of 1.0 g cm^{-3} corresponds to a volume of particles = 0.85 x 1.0 $cm^3/10^3$mg = 8.5 x 10^{-4} cm^3.

Area of the glass cover slip = 4.0 cm x 0.80 cm = 3.2 cm^2.

Therefore, thickness = 8.5 x $10^{-4}cm^3$/ 3.2 cm^2 = 2.65 x 10^{-4} cm = 2.65 μm.

Hydrolysis of PNPH using Latex Coatings

The cover slip was inserted against the opaque side of the polystyrene cuvette. The cover slip was not in the light path of the spectrophotometer. Helium-purged borate buffer solution (2.2 mL, pH 9.4) was added to the cuvette. Helium was used to degas or to remove oxygen from the borate buffer solution before addition to the cuvette. The solution was equilibrated at 30 ^oC for 20 min with magnetic stirring in the thermostated cell compartment of a Varian Cary 5000 spectrophotometer. The magnetic stirring was

continued during absorbance measurements. PNPH stock solution in acetonitrile (74 μL, 2.5 mM) was added, and the absorbance of the solution at 400 nm was recorded every 0.9 s. Hydrolysis of PNPH using colloidal coatings of BK-2QF - BK-13QF was performed by the same procedure. The amounts and concentrations of quaternary ammonium ion exchange catalyst and thicknesses of the final films are shown in Table 8.

2.9.6 Hydrolysis of Paraoxon using Colloidal Particles

Colloidal particles of BK-1QF (0.60 mg, $[N^+]$ =1.7 x10^{-4} M) and nitrogen-purged sodium hydroxide solution (2.2 mL, 0.10 M) were added in sequence to a polystyrene cuvette. The solution was equilibrated at 30 ± 1 ^oC for 20 min with magnetic stirring in the thermostated cell compartment of a Varian Cary 5000 Spectrophotometer. After that, a Paraoxon stock solution in acetonitrile (74 μL, 2.5 mM) was added to the reaction mixture by syringe. The absorbance of the solution at 400 nm was recorded every 0.9 s. Hydrolysis of Paraoxon using colloidal particles of BK-2QF - BK-13QF was performed by the same procedure. The amounts and concentrations of quaternary ammonium ion exchange catalyst are shown in Table 10.

2.9.7 Hydrolysis of Paraoxon using Colloidal Coatings or Films

All the steps were same as for the hydrolysis of PNPH using colloidal coatings prepared by the spread drop method except nitrogen-purged sodium hydroxide solution (2.2 mL, 0.10 M) was added and the coatings were annealed at 90 ^oC. The solution was equilibrated at 30 ± 1 ^oC for 20 min with magnetic stirring in the thermostated cell compartment of a Varian Cary 5000 spectrophotometer. Paraoxon stock solution in

acetonitrile (74 μL, 2.5 mM) was then added and the absorbance of the solution at 400 nm was recorded every 0.9 s. Hydrolysis of Paraoxon using colloidal coatings of BK-2QF - BK-13QF was performed by the same procedure. The amounts and concentrations of quaternary ammonium ion exchange catalysts and thicknesses of the final films are shown in Table 12.

2.9.8 Preparations of Colloidal Spin Coatings

The glass cover slips were treated with a mixture of potassium hydroxide and isopropyl alcohol for 1.0 h and were washed with DI water before applying samples in a spin coater. Polymer dispersions (90 μL) were applied and spun at 1200 rpm in a spin coater. The process was repeated several times. The thickness was measured for BK-5QF sample as follows:

Weight of uncoated cover slip = 250.759 mg

Weight of cover slip after spin coating = 251.230 mg

Net weight of particles applied = 0.471 mg

Surface area of cover slip (3 cm x 2.2 cm) = 6.6 cm^2

The thickness was calculated using the same formula as used for calculating the thicknesses of colloidal coatings for the hydrolysis of PNPH.

Hydrolysis of Paraoxon using Colloidal Spin Coatings

The spin coatings used for the hydrolysis of Paraoxon were annealed at 120 ^{o}C. All the steps were same as for the hydrolysis of Paraoxon using drop cast colloidal

coatings. The amounts and concentrations of quaternary ammonium ion exchange catalysts and thicknesses of the final films are shown in Tables 13 and 14.

2.9.9 Calculation of k_{obs} for BK-3QF from Absorbance vs. Time Data

The k_{obs} values were calculated from equation:

$$k_{obs}t = \ln[(A_\infty - A_o)/(A_\infty - A_t)]$$

where,

A_o = absorbance at time = 0, A_∞ = is absorbance at 98% conversion and the calculations were done by plotting the data over the first 60% conversions.

The slope of the curve (Figure 8) was calculated by using the linear least squares method and it gave $k_{obs} = 0.099$.

If we take a different value of A_o (e.g. $A_o = 0.2$, actual absorbance observed at t = 0), there is only a change in the intercept of the line but the slope remains the same.

References

1. Yang, Y.C.; Baker, J. A.; Ward, J. R. *Chem. Rev.* **1992**, *92*, 1729-1743.
2. Talmage, S. S.; Watson, A. P.; Hauschild, V.; Munro, N. B.; King, J. *Current Organic Chemistry* **2007**, *11*, 285-298.
3. Zhu, Y.; Ford, W. T. *Macromolecules* **2008**, *41*, 6089-6093.
4. Zhu, Y.; Ford, W. T. *Langmuir* **2009**, *25*, 3435-3439.
5. Sacher, E. *Prog. Surf. Sci*. **1994**, *47*, 273-300.
6. Pu, F. R.; Williams, R. L.; Markkula, T. K.; Hunt, J. A. *Biomaterials* **2002**, *23*, 2411-2428.

7. Lazzari, M.; Chiantore, O; Castelvetro, V. *Polym. Int.* **2001**, *50*, 863-868.
8. Cui, X.; Zhang, S.; Wang, H. *Polymer* **2007**, *48*, 7241-7248.
9. Park, I. J.; Lee, S. B.; Choi, C. K. *Polymer* **1997**, *38*, 2523-2527.
10. Ameduri, B.; Bongiovanni, R.; Pollicino, A.; Priola, A. *J. Polym. Sci. Part A Polym. Chem.* **1999**, *37*, 77-87.
11. Pomes, V.; Fernandez, A.; Costarramone, N.; Grano, B.; Houi, D. *Colloid Surf. A* **1999**, *159(2-3)*, 481-490.
12. Yang, S; Wang, J.; Ogino, K.; Valiyaveettil, S.; Ober, C. K. *Chem. Mater* **2000**, *12*, 33-40.
13. Lee, J. R.; Jin, F. L.; Park, S. J.; Park, J. M. *Surf. Coat Technol.* **2004**, *650-654*.
14. Anton, D. *Adv. Materials* **1998**, *10*, 1197-1205.
15. Landfester, K.; Rothe, R.; Antoniette, M. *Macromolecules* **2002**, *35*, 1658-1662.
16. Cheng, S. Y.; Chen, Y. J.; Chen, Z. G. *J. Appl. Polym. Sci.* **2002**, *85*, 1147-1153.
17. Ha, J. W.; Park, I. J.; Lee, S. B.; Kim, D. K. *Macromolecules* **2002**, *35*, 6811-6818.
18. Marion, P.; Beinert, G.; Juhue, D.; Lang, J. *Macromolecules* **1997**, *30*, 123-129.
19. Marion, P.; Beinert, G.; Juhue, D.; Lang, J. *J. Appl. Polym. Sci.* **1997**, *64*, 2409-2419.
20. Zhang, C. C.; Chen, Y. J. *Polym. Int.* **2005**, *54*, 1027-1033.
21. Karnati, R.; Ford, W. T. *J. Polym Sci. Part A Polym Chem.* **2008**, *46*, 3813-3819.
22. Miller, P. D.; Ford, W. T. *Langmuir* **2000**, *16*, 592-596.
23. Ceska, G. W. *J. Appl. Polym. Sci.* **1974**, *18*, 427.
24. Juang, M. S.; Krieger, I. M. *J. Polym. Sci.* **1976**, *14*, 2089-2107.
25. Sundberg, D. C.; Casassa, A. P.; Pantazopoulos, J.; Muscato, M. R.; Kronberg, B.; Berg, J. *J. Appl. Polym. Sci.* **1990**, *41*, 1425.

26. Sundberg, E. J.; Sundberg, D. C. *J. Appl. Polym. Sci.* **1993**, *47*, 1277.

27. Miller, P. D.; Spivey, H. O.; Copeland, S. L.; Sanders, R.; Woodruff, A.; Gearhart, D.; Ford, W. T. *Langmuir* **2000**, *16*, 108-114.

28.Tingting, Y.; Hui, P.; Cheng, S.; Park, I. J. *J. Appl. Polym. Sci.* **2007**, *104*, 3277-3284.

29. Gao, J.; Wang, X.; Wei, Y.; Yang, W. *J. Fluorine Chem.* **2006**, *127*, 282-286.

30. Yoshio, H.; Naohiro, T.; Eiji, H.; Takashi, A. *Polymer* **1998**, *39*, 4151-4154.

31. Good, R.; M. Koo. *J. of Colloid and Interface Science* **1979**, *71(2)*, 283-292.

32. Ghosh, K. K.; Verma, S. K. *Indian J. Biochemistry & Biophysics* **2008**, *45*, 350-353.

33. Helfferich, F. *Ion Exchange;* McGraw: New York, **1962**, p175.

CHAPTER III

POLYAMPHOLYTES

INTRODUCTION

The charged polymers are among the most important classes of macromolecules. They have attracted much attention due to their unique properties and their technological importance as rheology modifiers, dispersing aids, stabilizers, gelling agents and binders.[1,2] They range from naturally occurring biopolymers such as proteins and nucleotides to synthetic viscosifiers and soaps.[1] They are divided into two groups – polyelectrolytes[3-6] and polyzwitterions.[7] Polyelectrolytes are polymers that contain either negatively charged functional group (polyanions) or positively charged functional group (polycations). On the other hand, polyzwitterions contain both anionic and cationic functional groups, and the charges may be located on the pendant side chains of monomer units or they may be located along the polymer backbone. Polyzwitterions are subdivided into two major families – polyampholytes and polybetaines.[8] Polyampholytes are the polymers having charged groups, specifically, on different monomer repeat units and polybetaines are the polymers with anionic and cationic groups on same monomer unit.

The characteristic difference between polyelectrolytes and polyampholytes is the chain extension or higher hydrodynamic volume of polyelectrolytes in water at low

concentration. The extension of the polymer chain in polyelectrolytes is due to the coulombic repulsion between like charged groups along the polymer chain forcing the polymer into an extended rod conformation. Addition of low molecular weight electrolytes, such as sodium chloride, screens the repulsive electrostatic forces, forcing the polymer coil to shrink. The change of polymer chains on addition of electrolytes from a more extended form to compact conformation is called the polyelectrolyte effect.[9] On the other hand, polyampholytes in water exhibit compact conformations because of attraction between unlike charges, which tend to collapse the polymer chain into a globule. Addition of electrolyte to polyampholyte screens the attractive interactions, thereby forcing the chains to adopt extended conformation. This is called the polyampholyte effect.[9] The behavior of polyelectrolytes and polyampholytes to added electrolyte is shown in Figures 1 and 2.

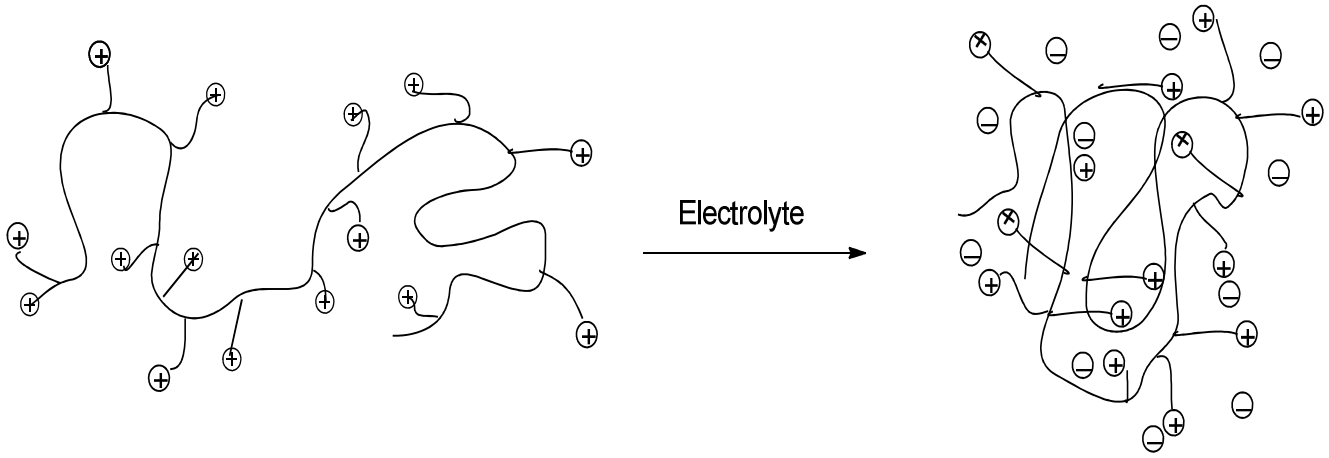

Figure 1. Representation of polyelectrolyte response to added electrolyte.

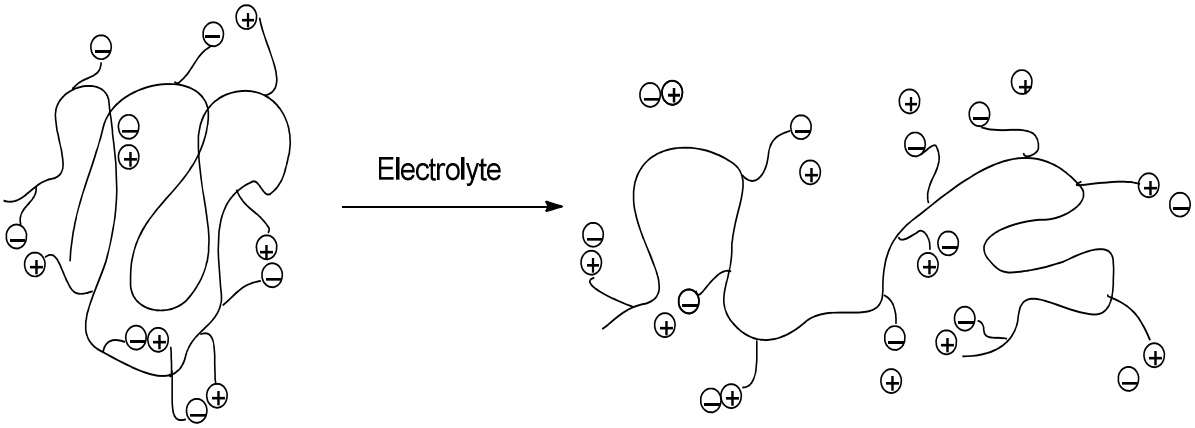

Figure 2. Representation of polyampholyte response to added electrolyte.

The most common example of a naturally occurring polyelectrolyte is DNA dissolved in water.[10] The phosphate groups of DNA are ionized at neutral pH. The repulsions between like charges help to stretch the molecule and contribute to the overall length of the polyanion (DNA).[11,12] On the other hand, proteins are examples of naturally occurring polyampholytes. Depending upon the molar ratio of anionic and cationic monomers, polyampholytes may be neutral (charge balanced) or can have a net charge of one sign (charge unbalanced). Synthetic polyampholytes can be subdivided into four different types[7] – **(1)** strong cation-strong anion polyampholytes in which both anionic and cationic residues are insensitive to pH changes, such as quaternary ammonium sulfonates; **(2)** strong cation-weak anion polyampholytes in which the anionic residue can be neutralized but the cationic residue is insensitive to pH changes, such as quaternary ammonium carboxylate; **(3)** weak cation-strong anion polyampholytes in which the cationic residue can be neutralized but the anionic residue is insensitive to pH changes, such as tertiary ammonium sulfonates; and **(4)** weak cation-weak anion polyampholytes

in which both cationic and anionic residues can be neutralized. Figure 3 shows the examples of four different polyampholytes. Proteins are type **(4)**.

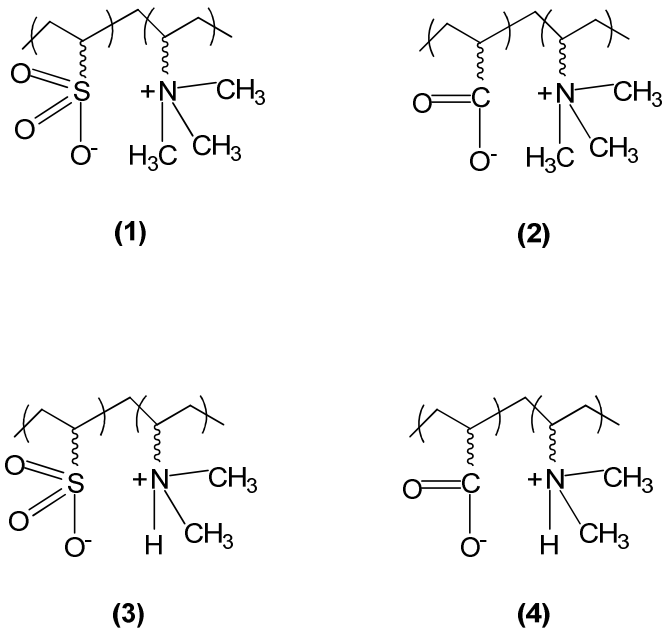

Figure 3. Structures of four different types of polyampholytes.

Polyampholytes have wide range of applications. Statistical polyampholytes made of 2-vinylpyridine and acrylic acid have been used in desalination membranes.[7] Synthetic and natural polyampholytes have been used in sewage treatment, flocculation, drag-reduction, enhanced oil recovery, and in personal care products. Polyampholytes can make complexes with proteins, making them useful for protein separations. Block polyampholytes of methacrylic acid, (dimethylamino)ethyl methacrylate and methyl methacrylate have been utilized successfully as protein displacers for the resolution of a crude mixture of β-lactoglobulin proteins.[13]

3.1 History of Synthesis of Polyampholytes

Polyampholytes were synthesized via conventional free radical copolymerization of cationic and anionic monomers in the early 1950s.[14-19] Examples of early reports of statistical polyampholytes include methacrylic acid-stat-2(dimethylamino)ethyl methacrylate copolymers,[17] acrylic acid-stat-2(diethylamino)ethyl methacrylate copolymers,[16] and acrylic acid-stat-2-vinylpyridine copolymers.[14] Since then numerous works have reported the synthesis and properties of a wide range of statistical polyampholytes.[20-25]

In early 1970s, the synthesis of first block polyampholyte was reported.[26,27] Block copolymers of 2-vinylpyridine (2VP) with trimethylsilyl methacrylate (TMSMA) were synthesized by anionic polymerization. The polymer precursor was converted to AB diblock polyampholyte by hydrolysis of TMSMA to poly(methacrylic acid) (PMAA). Since then many other block polyampholytes had been synthesized using anionic polymerization.[28-32] As monomers having a labile proton could not be directly polymerized by classical anionic polymerization, the protected acid monomers such as TMSMA, 2-tetrahydropyranyl methacrylate (THPMA), and *tert*-butyl methacrylate (tBMA) were used to synthesize polyampholytes.[28-32] Later in 1994 syntheses of diblock, triblock, and statistical methacrylic polyampholytes were reported via group transfer polymerization (GTP).[33,34]

Though anionic polymerization and GTP techniques do offer the ability to synthesize block polyampholytes, both are limited with respect to the monomer choice. Both techniques cannot be applied with unprotected methacrylic acid monomers having labile protons. Recent developments in controlled or living radical polymerization such as

nitroxide-mediated polymerization (NMP),[35,36] atom transfer radical polymerization (ATRP),[37-39] and reversible addition-fragmentation chain transfer polymerization (RAFT)[40-42] allow the direct synthesis of many polyampholyte block copolymers without the need for protecting group chemistry.

3.2 Solution Properties of Polyampholytes[43]

The aqueous solution behavior of polyampholytes is governed by the coulombic interaction between anionic and cationic residues located on different monomer units. Polyampholytes have the ability to exhibit both polyelectrolyte as well as polyampholyte behavior in aqueous media depending upon solution pH, copolymer composition, the absence/presence of low molecular weight electrolyte, and strength of acidic and basic residues. The first experimental study of a synthetic polyampholyte was reported in the 1950s where polyampholytes were described as "synthetic electrical analogs of proteins".[13] Since then, the experimental studies of dilute aqueous solutions of synthetic polyampholytes have reached five basic findings listed below. (1) Weakly hydrophobic polyampholytes at its isoelectric pH show minima in viscosity, electrical conductivity, and coil size because of collapse of polymer coil due to intramolecular electrostatic attraction between acidic and basic repeat units. (2) A hydrophobic polyampholyte precipitates near or in the vicinity of isoelectric pH (isoelectric point is defined as the pH at which polyampholyte is electrically neutral). (3) The addition of salt such as sodium chloride to a nearly charge-balanced polyampholyte causes the random coil of a polyampholyte chain to expand and the viscosity of the solution to increase. (4) Polyampholytes with a large net charge behave as polyelectrolytes. The viscosity and coil

size decrease with the addition of salt. (5) The viscosity and coil size of a polyampholyte in pure water shows a strong minimum as a function of copolymer composition, where the positive and negative charges are balanced. Swelling of a polyampholyte gel varies likewise.[44,45] Swelling increases with the addition of salt to a nearly charge-balanced polyampholyte gel and decreases strongly with addition of salt to a charge-imbalanced gel.

The influence of oppositely charged groups on the dissociation of polyampholyte in aqueous solution was further studied by Katchalsky and Miller in 1954.[18] They found that a larger fraction of the basic monomers dissociated at a given pH as the acid content of their copolymer increased. This is due to the screening of electrostatic interaction of the polyampholyte with added salt, which reduces the inductive influence of the neighboring groups. This experimental observation was further studied by Salamone *et al.*[46-50] The results of their study were very similar to the results from the 1950s described above. Later, McCormick and Johnson confirmed that size of a polyampholyte decreases as more charged groups are added.[51] Polyampholytes used in these studies are copolymers of sodium 2-(acrylamido)-2-methylpropanesulfonate (NaAMPS) and [2-(acrylamido)-2-methylpropyl]trimethylammonium chloride (AMPTAC) and (2-acrylamido-2-methylpropyl)dimethylammonium chloride (AMPDAC) .

In addition to the classical findings for dilute polyampholyte solutions discussed above, McCormick and co-workers found that for charge-imbalanced polyampholytes (polyelectrolyte limit) the viscosity first decreases with the addition of salt and then it increases as more salt is added (polyampholyte limit). A more recent or modern theory of polyampholytes explains this observation. The addition of salt first screens the charge

repulsion on large scale causing the polymer coil to adapt compact conformation. Later, at higher salt concentration, the charge attraction is screened causing the chain to swell. A polyampholyte gel behaves similarly.[52]

The compositional distribution of randomly prepared polyampholytes strongly affects the properties of polyampholyte solution. Candau and co-workers found that strongly hydrophobic polyampholytes with an average balanced charge stoichiometry are soluble in water in the presence of excess salts, and the truly charge-balanced polyampholytes precipitate from the solution leaving only the highly extended charge-imbalanced chains in the solution.[53-55] Thus, salt can provide a means of fractionation. Wittmer *et al.* studied the effect of charge distribution in polyampholytes having the same overall compositions. They conclude that alternating polyampholytes are more soluble in water than random polyampholytes because of a lack of charge fluctuations.[56]

3.3 Theory of Polyampholyte Solution[43]

The theory and computational modeling of polyampholyte solutions have been reported by numerous researchers.[43,57,58] The properties of charge-balanced polyampholyte chains in dilute aqueous solutions depend upon the average composition (fraction of positively charged and negatively charged monomers) as well as the distribution of the charged monomers along the polymer backbone. The distribution of the charged monomer is fixed by polymer synthesis and is known as a quenched charge distribution. But even in cases of charge-balanced polyampholytes, there are different charge sequences along the polymer backbone. The theoretical models along with the computer simulations consider ensemble average properties (property of the most

probable member). This may not always be true. Moreover, one can only have control over the composition of an initial monomeric mixture for synthetic polyampholytes prepared by copolymerization. Even for a symmetric mixture with equal concentration of positively and negatively charged monomers in the reaction mixture, the individual polymer chains will have an excess of negatively charged groups, positively charged groups, or be neutral. These reasons intensify the need for the synthesis of model random polyampholytes having narrow distributions of compositions and molecular weights to test the theory of polyampholyte solutions. The conformations of polyampholytes, such as overall size and shape, in dilute aqueous solutions depend upon the following parameters – (1) the net charge on the polymer chain; (2) the sequence distribution of charged units; (3) degree of polymerization; and (4) the ratio of Bjerrum length to the size of the monomer. Bjerrum length is the distance at which electrostatic energy of two like charges is equal to the thermal energy (k_BT). The intrachain electrostatic attraction in nearly charge balanced polyampholytes causes the chains to collapse into a globule. With an increase in net charge, the globule disappears and forms a necklace of charge-balanced beads. At this stage polyampholytes behave as polyelectrolytes. Thus, the above four key parameters control the charges and conformations of polyampholytes in dilute solution.

3.4 Model Random Polyampholytes

As described above, the dependence of polyampholyte solution properties on copolymer composition and sequence distribution intensifies the need for the synthesis of random charge-balanced polyampholytes of controlled molecular weight and narrow molecular weight distributions. Theoretical models of random polyampholytes cannot be

tested with polyampholytes that are synthesized from charged or ionic monomers in water because of microstructures with alternating positive and negative units, having no random sequences of repeat units. A statistical copolymer is defined as the copolymer in which the sequential distribution of the monomeric units obeys known statistical laws. A random copolymer is a special case of statistical copolymer in which the probability of finding a given monomeric unit at any given site in the polymer chain is independent of the nature of the neighboring units at that position. An alternating copolymer is comprised of two species of monomeric units distributed in an alternating sequence.

Using conventional radical polymerization, the composition drift with conversion produces polyampholytes which are polydispersed and have contents of positively and negatively charged residues that are heterogeneous. To prepare well defined polymers with narrow molecular weight distribution using free radical polymerizations, it is necessary to minimize the termination reactions occurring in conventional radical polymerization. Termination reactions can only be reduced by employing very low radical concentrations. Controlled radical polymerizations, on the other hand, are carried out under conditions of low polymer radical concentrations and, as a result, the rate of termination is suppressed to a greater degree. All the macromolecules in the reaction mixture grow at the same time giving the same composition gradient in every polymer.[59,60] Using controlled radical polymerization various copolymer architectures such as alternating, statistical/random, AB diblock, ABA triblock, graft and star copolymers can be achieved as shown below in Figure 4.

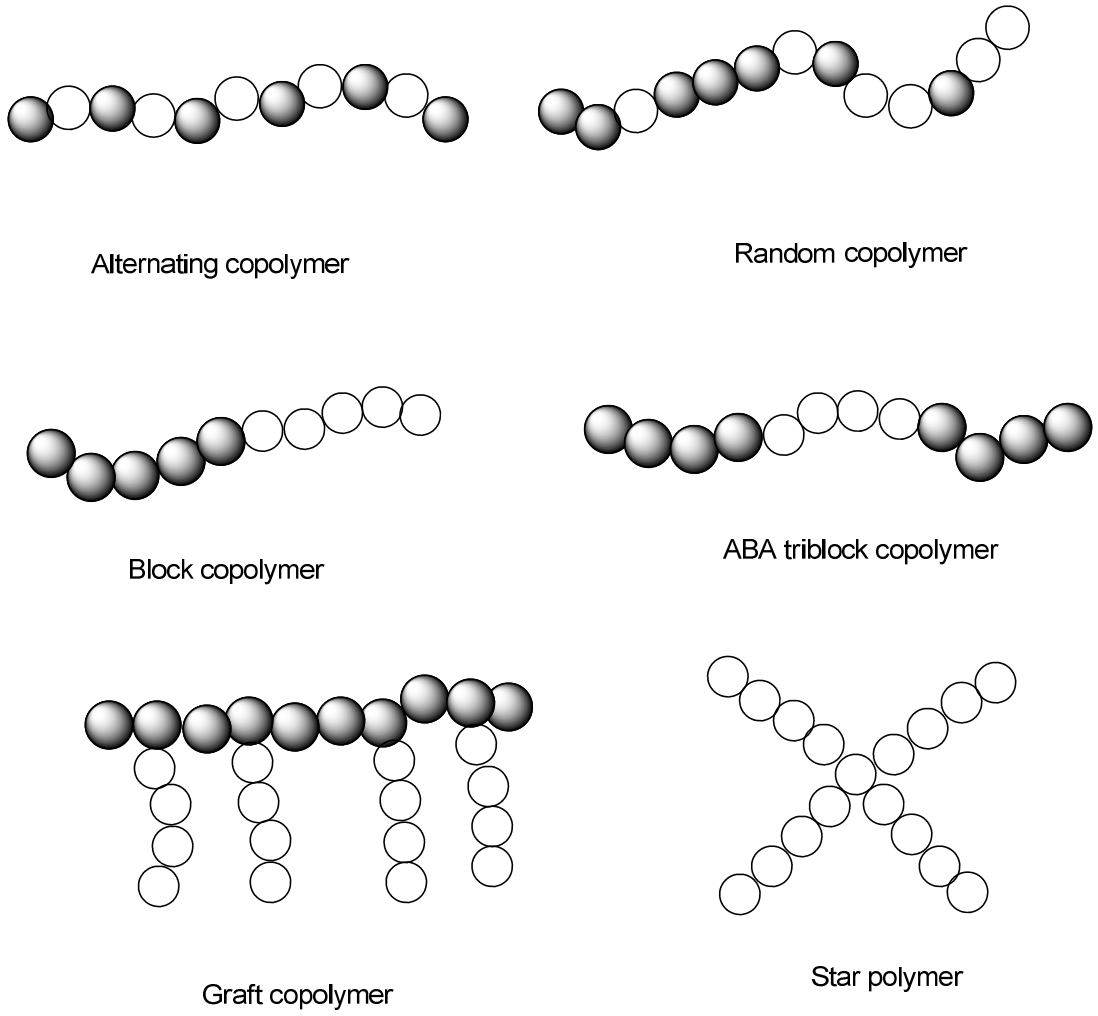

Figure 4. Copolymer architectures via controlled radical polymerization.

Out of different living radical polymerizations (such as NMP, ATRP, and RAFT), RAFT is the most versatile for controlled radical polymerization of acrylate and methacrylate monomers. We have synthesized random polyampholytes using RAFT polymerization.

3.5 Reversible Addition-Fragmentation Chain Transfer (RAFT) Polymerization

RAFT polymerization is a new, more convenient, and robust method to synthesize

polymers with predetermined molecular weight, narrow polydispersity, and tailored architecture.[61-63] It was first introduced in 1998 by the CSIRO group.[40] The process involves the polymerization in the presence of a chain transfer agent (CTA), a dithiocarbonylthio or trithiocarbonylthio compound, which reacts by reversible addition-fragmentation chain transfer. RAFT polymerizations can be conducted by adding an appropriate RAFT CTA to a conventional free radical polymerization. The advantage of RAFT polymerization over other types of living radical polymerizations is its compatibility with a wide range of monomers. It can be applied for the polymerization of monomers containing functional groups such as acid,[64] amine,[65] hydroxyl,[66] epoxy,[67] and amide.[68] Also, it can be applied in aqueous environment at low temperatures.

Ideally, in a living radical polymerization all chains initiate at the same rate in the beginning and get an equal chance for propagation. To confer living character in RAFT polymerizations, the chain transfer agent reacts with propagating radicals by reversible chain transfer making sure that a majority of the chains are maintained in dormant form. Rapid equilibrium between active and dormant species ensures that all chains posses equal chance for growth and survive polymerization.[69] Under these conditions the molecular weight increases linearly with conversion and molecular weight distributions are very narrow. The mechanism of RAFT polymerization is shown in Scheme 1.

The key feature of the mechanism is a sequence of addition-fragmentation equilibria. As with conventional free radical polymerization the process starts with the initiation.[69]

Initiation. Azo compound or peroxide can act as initiator in RAFT polymerization. Initiator I_2 splits homolytically to produce two free radicals ($I^{\bullet}$). Initiator radical adds to monomers to form monomer-derived radical ($M^{\bullet}$).

Propagation. Monomer-derived radicals add to more monomers to form propagating macroradical ($P^{\bullet}_n$). The process of propagation is indentical to the propagation in conventional free radical polymerization.

Chain transfer. In this step addition of propagating radical ($P^{\bullet}_n$) to C=S bond of thiocarbonylthio group of CTA **(1)** occurs with a rate constant (k_{add}) to form a carbon center intermediate radical species **(2)**. The resulting radical **(2)** fragments into a macro CTA **(3)** and a reinitiating radical ($R^{\bullet}$) with a rate constant (k_{β}), or the radical **(2)** may fragment into the original reactant with a rate constant (k_{-add}). The new radical species formed ($R^{\bullet}$) reacts with macro CTA **(3)** with a rate constant ($k_{-\beta}$) or it may add to the monomers to reinitiate the polymerization forming radical species ($P^{\bullet}_m$) with a rate constant (k_i). The propagating radical $P^{\bullet}_m$ adds to macro CTA **(3)** once initial CTA **(1)** is consumed. In the main equilibrium, a rapid exchange of dithioester end-groups occurs between the dormant radical species **(5)** and the propagating radical ($P^{\bullet}_n$), imparting living character to the polymerization.

I. Initiation

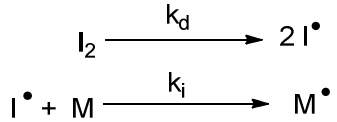

II. Propagation

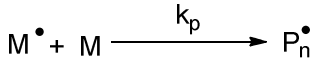

III. Reversible Chain Transfer

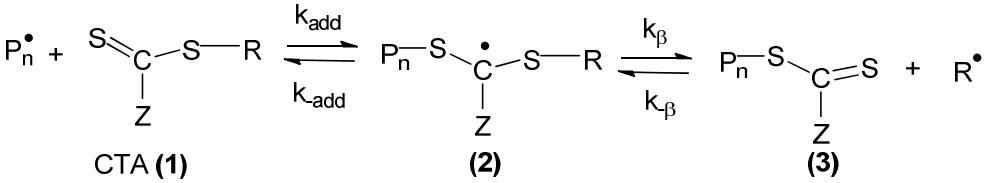

CTA **(1)** **(2)** **(3)**

IV. Reinitiation

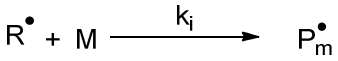

V. Chain Equilibration

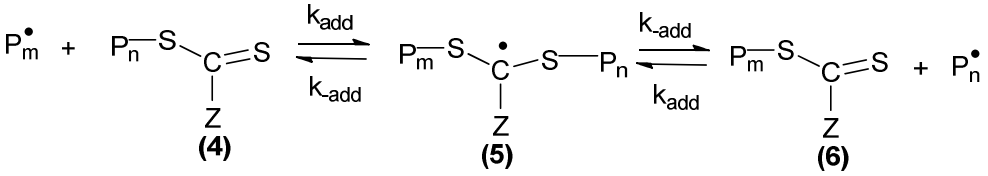

(4) **(5)** **(6)**

VI. Chain Termination

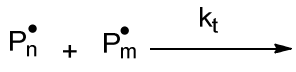

I= initiator

M= monomer

$P_n^{\bullet}$, $P_m^{\bullet}$ = active propagating radicals

(3), (4), (6)= dormant polymeric species

k_d = rate constant of decomposition

k_i = rate constant of initiation

k_p = rate constant of propagation

k_{add}= rate constant of addition of $P_n^{\bullet}$ to CTA

k_{-add}= rate constant of fragmentation of radical **(2)** to reactant

k_{β}= rate constant of fragmentation of radical **(2)** to radical $R^{\bullet}$

$k_{-\beta}$ = rate constant of addition of $R^{\bullet}$ macro CTA **(3)**

k_t = rate constant of termination

Scheme 1. Mechanism of RAFT polymerization.

Chain termination. Since RAFT polymerization does involve free radical intermediates, radical-radical termination cannot be avoided. Termination can occur either by coupling of the polymer radicals or by disproportionation. The number of dead chains is equal to half the initiator-derived chains when termination is due to radical coupling. The number of dead chains is equal to number of initiator derived chains when termination is by disproportionation.[40]

The effectiveness of a CTA in RAFT polymerization depends upon the monomer used in polymerization and the properties of free-radical leaving group (R) and the group (Z). Therefore, it is crucial to select the suitable CTA to synthesize well-defined polymers. The general structure of RAFT CTA is shown in Figure 5.

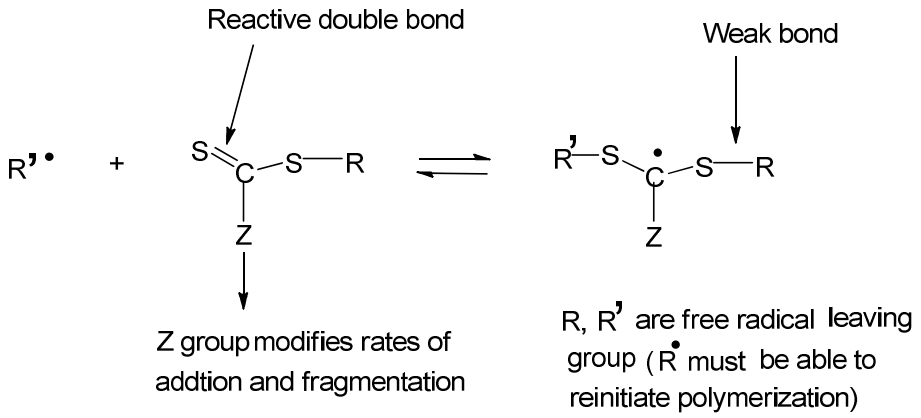

Figure 5. General structure of RAFT CTA.

The R group must be a good leaving group and the Z group must activate the addition of radicals to C=S bond. Following are the structural requirements for an effective RAFT polymerization:[69]

(1) A reactive C=S bond in the CTA **(1)** and macro-CTA **(3)** to facilitate the radical addition, i.e., high k_{add}.

(2) Rapid fragmentation of the intermediate radical species (**2** and **5**) with no side reactions, i.e., high k_{β} and weak S – R bond in CTA.

(3) Partitioning of intermediate radical species **(2)** in favor of products, i.e., $k_{\beta} \geq k_{-add}$.

(4) Efficient re-initiation of polymerization by expelled radicals ($R^{\bullet}$).

3.6 Objective of Research

The overall objective of the proposed research is to synthesize model random polyampholytes having high molecular weight and narrow molecular weight distributions in our lab, to measure aqueous solution properties of synthesized polyampholytes in the lab of Ralph Colby at Pennsylvania State University, and to compare experimental results with the theory of model random polyampholytes in the lab of Michael Rubinstein at the University of North Carolina. Molecular weight distributions of the polyampholytes were determined in the lab of Thomas Mourey at Eastman Kodak Company.

Terpolymers of uncharged methacrylate monomers, such as solketal methacrylate (2,2–dimethyl-1,3-dioxolan-4-yl)methyl methacrylate (SMA), 2-(*N*,*N*-dimethylamino)ethyl methacrylate (DMAEMA), and *tert*-butyl methacrylate (tBMA), were synthesized using living radical polymerization. The RAFT method was employed to afford terpolymers with a controlled molecular weight (M_n) and a narrow molecular weight distribution ($1 < (M_w / M_n) < 1.5$). Three different CTAs were used, namely, cumyl dithiobenzoate (CDB), 2-methyl-2-(dodecylsulfanylthiocarbonyl) sulfanylpropanoic acid,

and 4-cyano-4-(dodecylsulfanylthiocarbonyl)sulfanylpentanoic acid. Structures of the monomers and CTAs are shown in Figure 6 below.

We chose DMAEMA as the precursor of the positively charged unit of the polyampholyte because it is already known to polymerize by both RAFT[41,70,71] and ATRP.[72-74] tBMA was chosen as the precursor of the negatively charged unit of the polyampholyte and is well polymerized in both RAFT[70,75] and ATRP.[76,77] SMA was chosen as the precursor of hydrophilic neutral unit of polyampholyte.

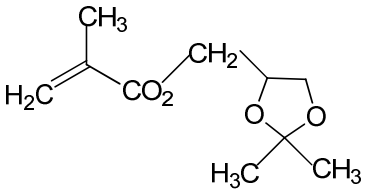

Solketal methacrylate)
(SMA)

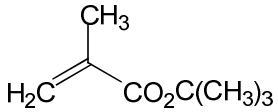

tert-butyl methacrylate
(tBMA)

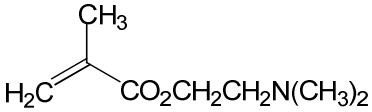

2-(N,N-dimethylamino)ethyl methacrylate
(DMAEMA)

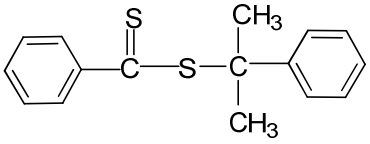

Cumyl dithiobenzoate
CDB

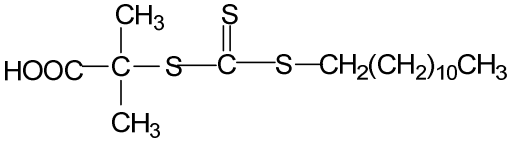

2-methyl-2-(dodecylsulfanylthiocarbonyl)sulfanylpropanoic acid

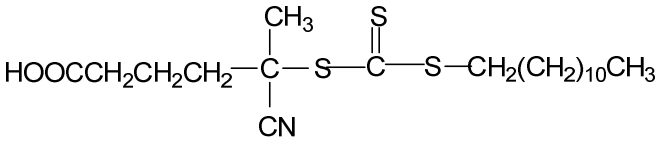

4-cyano-4-(dodecylsulfanylthiocarbonyl)sulfanylpentanoic acid

Figure 6. Structures of monomers and CTAs.

The terpolymer was converted into polyampholyte by functional group conversions of DMAEMA to quaternary ammonium ions at room temperature, deprotection of tBMA to methacrylic acid units and of SMA to glycidyl methacrylate units in the presence of concentrated HCl at room temperature. Polyampholytes can be synthesized by an aqueous route using ionic monomers, such as methacrylic acid (MAA), glyceryl monomethacrylate (GMA), and 2-(*N*,*N*-dimethylamino)ethyl methacrylate (DMAEMA) or by an organic route using protected monomers, such as *tert*-butyl methacrylate (tBMA), solketal methacrylate (SMA), and 2-(*N*,*N*-dimethylamino)ethyl methacrylate (DMAEMA). We choose the organic route since the aqueous route are known to form alternating polyampholytes.[20,78] The compositions of the polyampholytes made in this study have a mole ratios of 80:10:10 and 60:20:20 of SMA:DMAEMA:tBMA. SMA was chosen as the major component to ensure that the polyampholytes made are water soluble at room temperature and at all pH values. The compositions of polyampholyte made were analyzed by ^{1}H NMR spectroscopy. Dynamic light scattering (DLS) was applied to test the possible aggregation of polyampholytes in water.

References

1. Hara, M. *Polyelectrolytes*; Dekker, New York, 1993.
2. Tanford, C. *Physical Chemistry of Macromolecules*; Wiley, New York, 1961.
3. Dubin, P.; Bock, J.; Davies, R. M.; Schulz, D. N.; Thies, C. *Macromolecular Complexes in Chemistry and Biology*, Springer-Verlag: Berlin, 1994.
4. Mortimer, D. A. *Polym. Int.* **1991**, *25*, 29.

5. Bromberg, L. In *Handbook of Surfaces and Interfaces of Materials*, Nalwa, H. S., Ed.; Academic Press; New York, 2001; Vol. 4, Chapter 7.
6. Oosawa, F. *Polyelectrolytes*; Marcel-Dekker; New York, 1971.
7. McCormick, C. L.; Ayres, N.; Lowe, A. B. In *Water Soluble Polymers*; Encyclopedia of Polymer Science & Technology, *12(3)*, Wiley; New York, 2004, 452-521.
8. Lowe, A. B.; McCormick, C. L. *Chem. Rev.* **2002**, *102*, 4177-4189.
9. Munk, P. *Introduction to Macromolecular Science*; Wiley-Interscience; New York, 1989, 89.
10. Manning, G. S. *J. Chem. Phys.* **1969**, *51*, 924.
11. Fixman, M. *J. Chem. Phys.* **1979**, *70*, 4995.
12. Odjik, T. *Macromolecules* **1979**, *12*, 688.
13. Patrickios, C. S.; Gadam, S. D.; Cramer, S. M.; Hertler, W. R.; Hatton, T. A. *Biotechnol. Prog.* **1995**, *11*, 33-38.
14. Alfrey, T.; Morawetz, H. *J. Am. Chem. Soc.* **1952**, *74*, 436.
15. Alfrey, T.; Fuoss, R.; Morawetz, H.; Pinner, S. H. *J. Am. Chem. Soc.* **1952**, *74*, 438.
16. Alfrey, T.; Pinner, S. H. *J. Polym. Sci.* **1957**, *23*, 533.
17. Ehrlich, G.; Doty, P. *J. Am. Chem. Soc.* **1954**, *76*, 3764.
18. Katchalsky, A.; Miller, I. R. *J. Polym. Sci.* **1954**, *14*, 57.
19. Mazur, J.; Silberberg, A.; Katchalsky, A. *J. Polym. Sci.* **1959**, *35*, 43.
20. McCormick, C. L.; Johnson, C. B. *Macromolecules* **1988**, *21*, 686.
21. McCormick, C. L.; Johnson, C. B. *Macromolecules* **1988**, *21*, 694.
22. Park, J. S.; Lim, Y. B.; Kwon, Y. M.; Jeong, B.; Choi, Y. H.; Kim, S. W. *J. Polym. Sci., Polym. Chem.* **1999**, *37*, 2305.

23. Bekturov, E. A.; Kudaibergenov, S. E.; Rafikov, S. R. *Macromol. Sci. Rev., Macromol. Chem. Phys.* **1990**, *C30(2)*, 233.

24. Kudaibergenov, S. E.; Sigitov, V. B. *Langmuir* **1999**, *15*, 4230.

25. Salamone, J. C.; Tsai, C. C.; Watterson, A. C. *J. Macromol. Sci., Chem.* **1979**, *A13(5)*, 665.

26. Kamachi, M.; Kurihara, M.; Stille, J. K. *Macromolecules* **1972**, *5*, 161.

27. Kurihara, M.; Kamachi, M.; Stille, J. K. *J. Polym. Sci., Chem. Ed.* **1973**, *11*, 587.

28. Varoqui, R.; Tran, Q.; Pefferkorn, E. *Macromolecules* **1979**, *12*, 831.

29. Morishima, Y.; Hashimoto, T.; Itoh, Y.; Kamachi, M.; Nozakura, S. *J. Polym. Sci., Polym. Chem.* **1982**, *20*, 299.

30. Bekturov, E. A.; Frolova, V. A.; Kudaibergenov, S. E.; Schulz, R. C.; Zoller, J. *Makromol. Chem.* **1990**, *191*, 457.

31. Bekturov, E. A.; Kudaibergenov, S. E.; Khamzamulina, R. E.; Frolova, V. A.; Nurgalieva, D. E.; Schulz, R. C.; Zoller, J. *Makromol. Chem., Rapid Commum.* **1992**, *13*, 225.

32. Creutz, S.; Teyssié, P.; Jérome, R. *Macromolecules* **1997**, *30*, 6.

33. Chen, W. I.; Alexandridis, P.; Su, C. K.; Patrickios, C. S.; Hertler, W. R.; Hatton, T. A. *Macromolecules* **1995**, *28*, 8604.

34. Webster, O. W.; Hertler, W. R.; Sogah, D. Y.; Farnham, W. B.; Rajanbabu, T. V. *J. Am. Chem. Soc.* **1983**, *105*, 5706.

35. Soloman, D. H.; Rizzardo, E.; Cacioli, P. U.S. Patent 4,581,429.

36. Georges, M. K.; Veregin, R. P. N.; Kazmaier, P. M.; Hamer, G. K. *Trends Polym. Sci.* **1994**, *2*, 66.

37. Wang, J. S.; Matyjaszewski, K. *J. Am. Chem. Soc.* **1995**, *117*, 5614.

38. Wang, J. S.; Matyjaszewski, K. *Macromolecules* **1995**, *28*, 7901.

39. Kato, M.; Kamigaito, M.; Sawamoto, M.; Higashimura, T. *Macromolecules* **1995**, *28*, 1721.

40. Chiefari, J.; Chong, Y. K.; Ercole, F.; Krstina, J.; Jeffery, J.; Le, T. P. T.; Mayadunne, R. T. A.; Meijs, G. F.; Moad, C. L.; Moad, G.; Rizzardo, E.; Thang, S. H. *Macromolecules* **1998**, *31*, 5559.

41. Chong, Y. K.; Le, T. P. T.; Moad, G.; Rizzardo, E.; Thang, S. H. *Macromolecules* **1999**, *32*, 2071.

42. Mayadunne, R. T. A.; Rizzardo, E.; Chiefari, J.; Krstina, J.; Moad, G.; Postma, A.; Thang, S. H. *Macromolecules* **2000**, *33*, 243.

43. Dobrynin, A. V.; Colby, R. H.; Rubinstein, M. *J. Polym. Sci. Part B, Polym. Phys.* **2004**, *42*, 3513.

44. Baker, J. P.; Stephens, D. R.; Blanch, H. W.; Prausnitz, J. M. *Macromolecules* **1992**, *25*, 1955.

45. Baker, J. P.; Blanch, H. W.; Prausnitz, J. M. *Polymer* **1995**, *36*, 1061.

46. Salamone, J. C.; Amhed, I.; Rodriguez, E. L.; Quach, L.; Watterson, A. C. *J. Macromol. Sci.* **1988**, *A25*, 811.

47. Salamone, J. C.; Quach, L.; Watterson, A. C.; Krauser, S.; Mahmud, M. U. *J. Macromol. Sci.* **1985**, *A22*, 653.

48. Salamone, J. C.; Amhed, I.; Raheja, M. K.; Elayaperumal, P.; Watterson, A. C.; Olson, A. P. In *Water-Soluble Polymers for Petroleum Recovery*; Stahl, G. A.; Schulz, D. N., Eds.; Plenum: New York, 1988; 181.

49. Salamone, J. C.; Tsai, C. C.; Olson, A. P.; Watterson, A. C. In *Ions in Polymers*; Eisenberg, A., Ed.; American Chemical Society: Washington, DC, 1980; 337.

50. Salamone, J. C.; Tsai, C. C.; Olson, A. P.; Watterson, A. C. *Polym. Preprints* **1978**, *19*, 261.

51. McCormick, C. L.; Johnson, C. B. *Polymer* **1990**, *31*, 1100.

52. English, A. E.; Mafe, S.; Manzanares, J. A.; Yu, X.; Grosberg, A. Y.; Tanaka, T. *J. Chem. Phys.* **1996**, *104*, 8713.

53. Skouri, M.; Munch, J. P.; Candau, S. J.; Neyret, S.; Candau, F. *Macromolecules* **1994**, *27*, 69.

54. Ohlemacher, A.; Candau, F.; Munch, J. P.; Candau, S. J. *J. Polym. Sci. Part B, Polym. Phys.* **1996**, *34*, 2747.

55. Candau, F.; Ohlemacher, A.; Munch, J. P.; Candau, S. J. *J. Rev. Instit. Francais Petrole.* **1997**, *52*, 133.

56. Wittmer, J.; Johner, A.; Joanny, J. F. *Macromolecules* **1997**, *24*, 263.

57. Higgs, P. G.; Joanny, J. F. *J. Chem. Phys.* **1991**, *94(2)*, 1543.

58. Edwards, S. F.; King, P. R.; Pincus, P. *Ferroelectrics (GB)* **1980**, *30*, 3.

59. Matyjaszewski, K.; Xia, J. *Chem. Rev.* **2001**, *101*, 2921.

60. Davis, K. A.; Matyjaszewski, K. *Adv. Polym. Sci.* **2002**, *159*, 2.

61. Rizzardo, E.; Chiefari, J.; Chong, Y. K.; Ercole, F.; Krstina, J.; Jeffery, J.; Le, T. P. T.; Mayadunne, R. T. A.; Meijs, G. F.; Moad, C. L.; Moad, G.; Thang, S. H. *Macromol. Symp.* **1999**, *143*, 291.

62. Rizzardo, E.; Chiefari, J.; Mayadunne, R. T. A.; Moad, G.; Thang, S. H. *ACS Symp. Ser.* **2000**, *768*, 278.

63. Chiefari, J.; Rizzardo, E. In *Handbook of Radical Polymerization*; Davis, T. P.; Matyjaszewski, K., Eds.; Wiley & sons: New York, 2002, 263.

64. Ladaviere, C.; Dorr, N.; Claverie, J. P. *Macromolecules* **2001**, *34*, 5370.

65. Sumerlin, B. S.; Donovan, M. S.; Mitsukami, Y.; Lowe, A. B.; McCormick, C. L. *Macromolecules* **2001**, *34*, 6561.

66. Ganachaud, F.; Monteiro, M. J.; Gilbert, R. G.; Dourges, M. A.; Thang, S. H.; Rizzardo, E. *Macromolecules* **2000**, *33*, 6378.

67. Zhu, J.; Zhou, D.; Zhu, X.; Chen, G. *J. Polym. Sci. Part A, Polym. Chem.* **2004**, *42*, 2558.

68. Thomas, D. B.; Sumerlin, B. S.; Lowe, A. B.; McCormick, C. L. *Macromolecules* **2003**, *36*, 1436.

69. Moad, G.; Rizzardo, E.; Thang, S. H. *Aust. J. Chem.* **2005**, *58*, 379.

70. Gan, L. H.; Ravi, P.; Mao, B. W.; Tam, K. C. *J. Polym. Sci. Part A, Polym. Chem.* **2003**, *41*, 2688.

71. Xiong, Q.; Ni, P.; Zhang, F.; Yu, Z. *Polym. Bull.* **2004**, *53*, 1.

72. Wager, C. M.; Haddleton, D. M.; Bon, S. A. F. *Eur. Polym. J.* **2004**, *40*, 641.

73. Zhang, X.; Matyjaszewski, K. *Macromolecules* **1999**, *32*, 1763.

74. Narrainen, A. P.; Pascual, S.; Haddleton, D. M. *J. Polym. Sci. Part A, Polym Chem.* **2002**, *40*, 439.

75. Nuopponen, M.; Ojala, J.; Tenhu, H. *Polymer* **2004**, *45*, 3643.

76. Qin, S.; Saget, J.; Pyun, J.; Jia, S.; Kowalewski, T.; Matyjaszewski, K. *Macromolecules* **2003**, *36*, 8969.

77. Krishnan, R.; Srinivasan, K. S. V. *Eur. Polym. J.* **2004**, *40*, 2269.

78. Corpart, J. M.; Candau, F. *Macromolecules* **1993**, *26*, 1333.

CHAPTER IV

SYNTHESIS OF MODEL RANDOM POLYAMPHOLYTES

INTRODUCTION

The main objective of this research is to synthesize model random polyampholytes in order to test the modern theory of polyampholytes. Control radical polymerization, namely, reversible addition fragmentation chain transfer (RAFT), was employed to synthesize precursor terpolymers of uncharged methacrylate monomers. The terpolymers with compositions 80:10:10 and 60:20:20 of solketal methacrylate (SMA), 2-(*N*,*N*-dimethylamino)ethyl methacrylate (DMAEMA), and *tert*-butyl methacrylate (tBMA) were converted into water soluble polyampholytes by functional group conversions. Scheme 1 shows the overall synthesis of polyampholytes using uncharged alkyl methacrylate monomers.

The transformation of precursor terpolymers to water soluble polyampholytes involves three functional group conversions, alkylation of the tertiary amine group of DMAEMA to a quaternary ammonium ion, removal of the *ter*t-butyl group of tBMA, and deprotection of the ketal ring of SMA. Quaternization of *N*-methyl group in DMAEMA is reported successfully in literature[1]. The acid catalyzed hydrolyses of *ter*t-butyl esters, and cyclic ketals such as SMA are well studied.[1,2] There are reports for the simultaneous deprotection of copolymer of tBMA and acetal under mild acidic conditions.[3,4]

Hence, our precursor terpolymers can be simultaneously deprotected under acidic conditions.

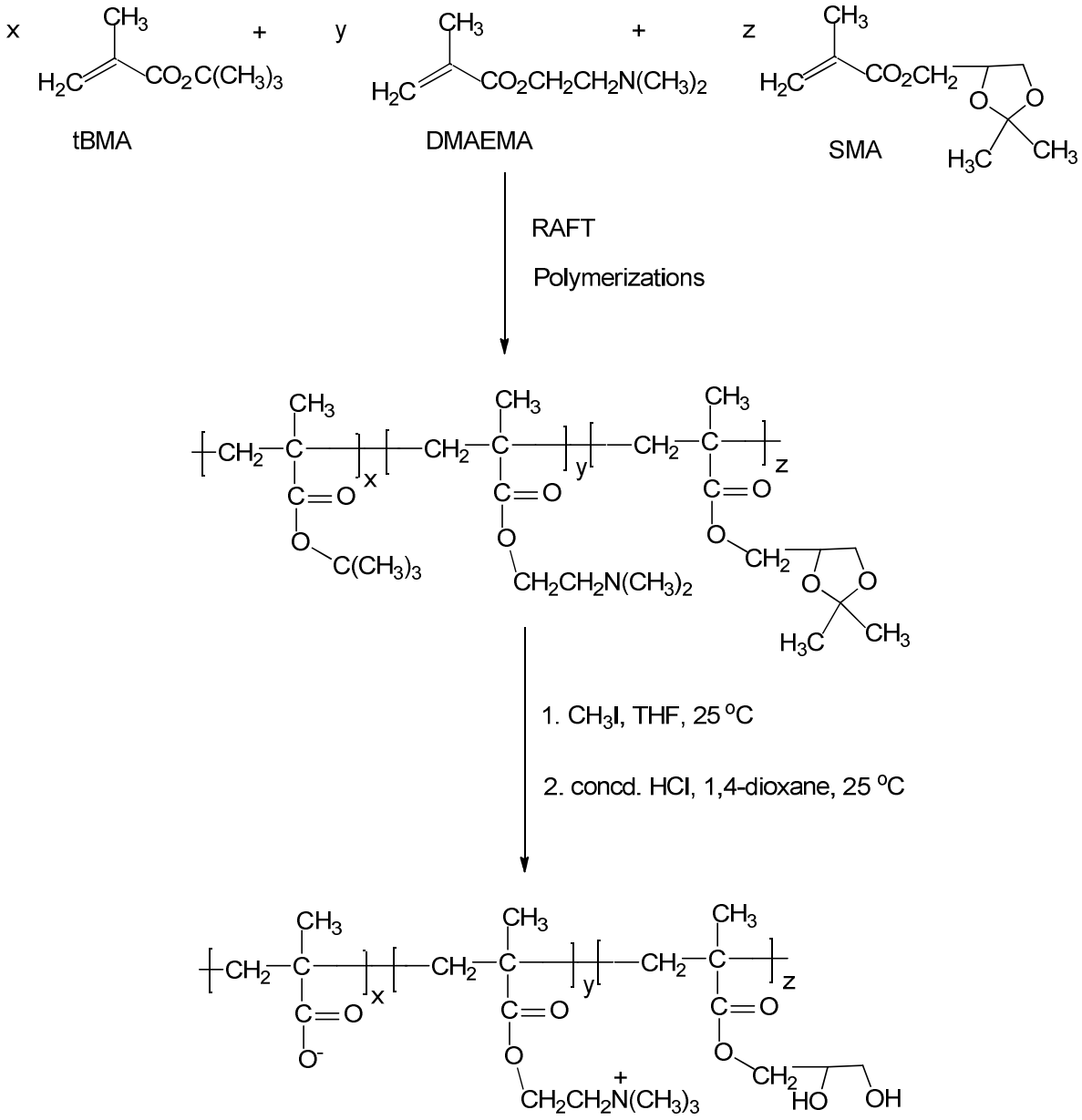

Scheme 1. Synthesis of model random polyampholytes.

The reason for choosing the uncharged monomers is their ability to produce copolymers with reactivity ratios close to 1.0, which corresponds to perfectly random copolymers. Binary copolymer reactivity ratios were determined previously in our lab for all the combinations of SMA, DMAEMA and tBMA by conventional radical polymerization.[5] The results are shown in Table 1.

Table 1. Binary Copolymer Reactivity Ratios of Monomers

M_1, M_2	r_1	r_2	r_1r_2
tBMA, SMA	1.40	0.79	1.10
tBMA, DMAEMA	1.26	0.97	1.22
DMAEMA, SMA	1.40	0.67	0.91

The expected desirable properties of the resulting polyampholytes are (1) solubility in water at room temperature; (2) charge-balanced structure of positively charged monomer and negatively charged monomer in the polyampholytes; (3) variation of charge with pH; (4) narrow molecular weight distributions; and (5) molecular weight high enough to measure the aqueous properties of semi-dilute solution of polyampholytes. In this research project seven polyampholytes were designed as models for investigation of solution properties as a function of the four key parameters described in Chapter III: net charge, sequence distribution, degree of polymerization, and the ratio of Bjeirum length to the size of monomer. The proposed compositions and degrees of polymerization of seven design polyampholytes are listed in Table 2.

Table 2. Compositions and Degree of Polymerization of Proposed Polyampholytes.

DP[a]	N_+[b]	N_-[c]	N_n[d]	% (N_++ N_-)	balanced
300	60	60	180	40	Yes
300	30	30	240	20	Yes
300	15	15	270	10	Yes
100	10	10	80	20	Yes
1000	100	100	800	20	Yes
300	30	60	210	30	No
300	15	30	355	15	No

[a]DP = degree of polymerization, [b]N_+ = number of (+) units, [c]N_- = number of (-) units,[d]N_n = number of uncharged units.

RAFT polymerizations were performed using three different chain transfer agents (CTA), cumyl dithiobenzoate (CDB) synthesized in our laboratory,[6] 2-methyl-2-(dodecylsulfanylthiocarbonyl)sulfanyl propanoic acid (MDSP) and 4-cyano-4-(dodecylsulfanylthiocarbonyl)sulfanyl pentanoic acid (CDSP). SMA (major component of the precursor terpolymers) is not commercially available. Therefore, SMA was synthesized on a large scale (100 g scale) in our laboratory.[2] This chapter details the synthesis of polyampholytes, their characterization, and aqueous solution properties

Although, there are reports of RAFT polymerization of tBMA and DMAEMA in the literature,[7-9] SMA was polymerized for the first time in our laboratory. The target composition of first large scale model random polyampholytes synthesized[1] using CDB as CTA in our laboratory was entry 2 in Table 2. Two new chain transfer agents MDSP and CDSP were used to synthesize polyampholytes with composition (80:10:10 and 60:20:20) and degrees of polymerization of 300 and 1000.

Terpolymers were synthesized previously in our laboratory on a 0.1 g and 2.0 g scale using CDB as RAFT CTA. The copolymer compositions calculated from ^{1}H NMR

spectroscopy, and from binary copolymer reactivity ratios shows that there is no drift in compositions of terpolymer at higher conversion. The size exclusion chromatography (SEC) analyses of terpolymers show that the molecular weight increases linearly with conversions and the molecular weight distributions were narrow. The conversion of terpolymer to water soluble polyampholytes under aqueous acidic condition resulted in partial deprotection.

Based on the previous results of syntheses of terpolymers on small scale, new terpolymers were synthesized on a 5.0 g scale using three different CTAs in 1,4-dioxane. Terpolymers with degrees of polymerization of 300 and 1000 were synthesized successfully using RAFT polymerization. There are reports on RAFT polymerization with a degree of polymerization of 300,[10,11,12] but very few with a degree of polymerization of 1000.

Results and Discussion

4.1 Purification of CDB

The effect of impurities in cumyl dithiobenzoate was studied by Ronda *et al*.[13] The impurities retarded the polymerization of styrene and methacrylate monomers. Major impurities in CDB solution were dithiobenzoic acid and α-methyl styrene.[14] The ^{1}H NMR spectrum of cumyl dithiobenzoate solution synthesized in our laboratory showed tiny peaks corresponding to aliphatic impurities in the region between 3-5 ppm. Figure 1 in the Appendix shows the ^{1}H NMR spectrum of impure CDB. CDB was

purified using basic alumina before using it in a RAFT polymerization. The ^{1}H NMR spectrum of pure CDB is shown in Figure 2 in the Appendix.

4.2 Synthesis of Terpolymers

Terpolymers were synthesized on a large scale by RAFT polymerization. Table 3 shows the compositions of all the terpolymers made.

4.2.1 Synthesis of Terpolymers using CDB as RAFT CTA

Terpolymers of SMA, tBMA and DMAEMA were synthesized in 1,4-dioxane at 75 ^{o}C. Polymerization was carried out in dioxane solvent due to good separation of vinyl protons of SMA and DMAEMA which is required to do accurate NMR integrations, which are used to determined compositions of unreacted monomers during the polymerizations. Five terpolymers B1-B5 were synthesized on scale greater than 2 g by RAFT polymerization. Degrees of polymerization (DP) of 368, 225, and 1950 with 80:10:10 composition and DP of 263 and 2125 with composition of 60:20:20 were obtained in good yields. DP is defined as the number average of repeat units in terpolymers.[15] Synthesis of terpolymers is shown below in Scheme 2 and structures of CTAs and initiator are shown in Scheme 3.

Table 3. Terpolymers made by RAFT Polymerization

sample	composition	[a]DP_{calc}
B1	80:10:10	368
B2	80:10:10	225
B3	80:10:10	1950
B4	60:20:20	263
B5	60:20:20	2125
B6	80:10:10	270
B7	80:10:10	240
B8	80:10:10	2150
B9	80:10:10	2000
B10	80:10:10	1825
B11	60:20:20	1075

[a] DP_{calc} = ([monomer]/ [CDB]) x (fractional conversion)

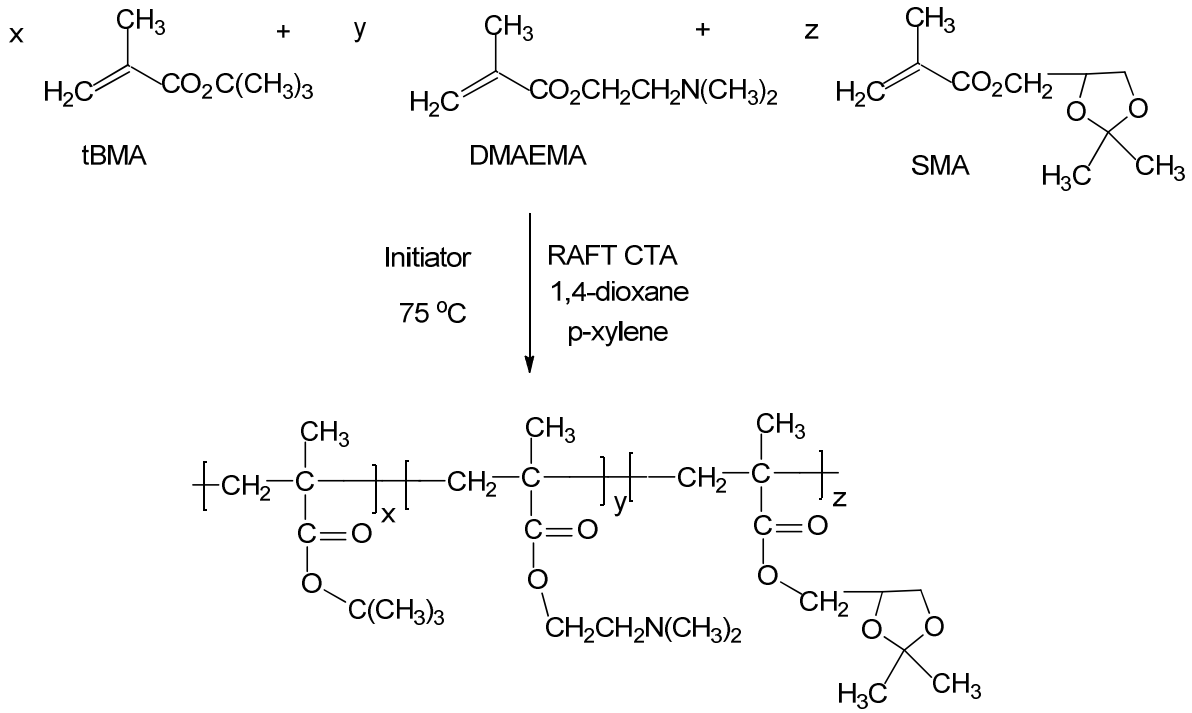

Scheme 2. Synthesis of RAFT terpolymers.

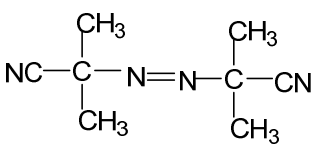

2,2-Azobisisobutyronitrile

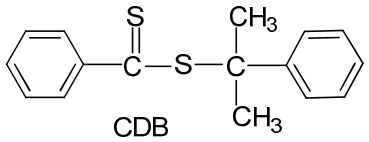

CDB

Cumyl dithiobenzoate

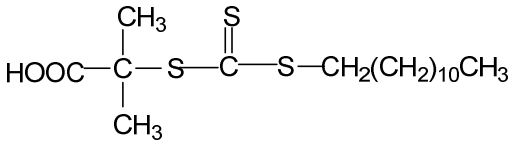

2-methyl-2-(dodecylsulfanylthiocarbonyl)sulfanylpropanoic acid

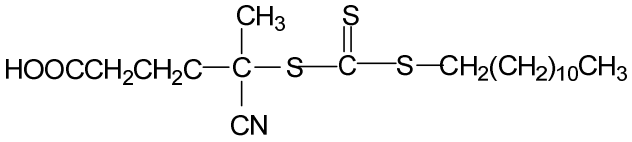

4-cyano-4-(dodecylsulfanylthiocarbonyl)sulfanylpentanoic acid

Scheme 3. Structure of RAFT CTAs and initiator.

In order to avoid drift in composition, all the polymerizations were carried out only to 40 % conversion. Therefore, we started with much higher ratios of [M]/ [CTA]. As an example, to get a DP of 300 and 1000, we started at [M]/ [CTA] of 750 and 2500, respectively. The terpolymers were characterized by ^{1}H NMR spectroscopy.

The ^{1}H NMR spectrum of sample B1 is shown in Figure 3 in the Appendix. Percent conversions of monomers in the terpolymers were determined from ^{1}H NMR spectra of the unreacted monomers at room temperature, and after partial conversions at 75 ^{o}C by integrating the vinyl resonances from 5-6 ppm, and the singlet for aromatic protons of p-xylene (added as an internal standard) at 6.98 ppm. Figure 4 in the Appendix

shows the ^{1}H NMR spectrum used to determine monomer conversions in dioxane-d_8. The DP was calculated using the formula:

DP (theoretical) = (Total moles of monomers/ moles of RAFT CTA) x weighted average % conversion of the three monomers after partial conversions.

DP (SEC) = Weighted average % conversion of the three monomers x theoretical DP

4.2.2 Determination of Percent Conversions and Compositions of Monomers in Solution from ^{1}H NMR Spectroscopy. The integration of areas under the vinyl hydrogen signals of SMA, DMAEMA, and tBMA in the ternary monomer mixtures was done at room temperature (Figure 4 in the Appendix). The area under the vinyl protons of SMA, DMAEMA, tBMA, and aromatic protons of *p*-xylene are denoted as *a* & *b* (SMA), *c* & *d* (DMAEMA), *e* & *f* (tBMA) and *x* (p-xylene). *p*-Xylene was added to the reaction mixture as an internal standard. The ratios of SMA, DMAEMA, and tBMA were calculated as shown below:

SMA ratio (M) = $(a+b)/ x$

DMAEMA ratio (N) = $(c+d)/ x$

tBMA ratio (O) = $(e+f)/ x$

The mole fraction feed composition f_1, f_2, and f_3 for SMA, DMAEMA, and tBMA was calculated as follows:

$$f_1 = M/ (M + N + O)$$

$$f_2 = N/ (M + N + O)$$

$$f_3 = O/ (M + N + O)$$

The ^{1}H NMR spectrum of the ternary mixture was integrated in a similar manner after partial conversion to get the ratios of three monomers denoted as *P* (SMA), *Q* (DMAEMA), and *R* (tBMA). The ratios obtained at room temperature and after partial conversions were used to calculate percent conversions of each monomer as shown below:

% SMA left (*A*) = (*P/M*) x 100

% SMA consumed (*B*) = 100 – *A*

% DMAEMA left (*C*) = (*Q/N*) x 100

% DMAEMA consumed (*D*) = 100 – *C*

% tBMA left (*E*) = (*R/O*) x 100

%tBMA consumed (*F*) = 100 – *E*

The final compositions of the three co-monomers incorporated into the terpolymers are calculated as follows:

Amount of SMA consumed (*S*) = f_1 *(B/100)*

Amount of DMAEMA consumed (*T*) = f_2 *(D/100)*

Amount of tBMA consumed (*U*) = f_3 *(F/100)*

Hence,

$f_1 = S/(S+T+U)$

$f_2 = T/(S+T+U)$

$f_3 = 1 - (f_1 + f_2)$

The terpolymers were isolated by precipitation with *n*-hexane. It is clear from ^{1}H NMR spectra of terpolymers that precipitation using *n*-hexane was unable to remove residual SMA monomer and p-xylene. The supernatant liquid after precipitation was

colorless indicating that the terpolymers are not soluble in *n*-hexane. The terpolymers precipitated from *n*-hexane have a pink color. Experimental data for the synthesis of five terpolymers using CDB as CTA are shown below in Table 4.

Table 4. Experimental Data of Terpolymers made using CDB as RAFT CTA

Sample	monomers (mmol)	CDB (µmol)	AIBN (µmol)	1,4-dioxane (mL)	*p*-xylene (mmol)	temp. (^{o}C)	time (h)
B1	52.8	70.40	23.400	4.40	3.81	75	1.05
B2	132.0	176.00	58.700	8.80	7.54	75	1.05
B3	13.2	5.28	0.528	1.10	0.94	60	48.00
B4	56.8	0.75	25.200	4.40	3.76	75	1.05
B5	13.2	5.28	0.528	1.10	0.94	60	24.00

4.2.3 Small Scale Synthesis of Terpolymers using MDSP and CDSP. Two small scale terpolymers B6 and B7 with composition of 80:10:10 were synthesized in NMR tubes using the new RAFT CTAs (MDSP and CDSP). The resulting terpolymers were characterized by ^{1}H NMR spectroscopy and SEC. Monomer conversions and feed compositions of three monomers in the ternary mixture at room temperature as well as the composition of the three monomers incorporated into the terpolymers was calculated from ^{1}H NMR as explained earlier. The experimental data for small scale terpolymer syntheses are shown in Table 5.

Table 5. Experimental Data of Terpolymers made on a 0.1 g Scale[a]

Sample	monomers (mmol)	CTA used	time (h)
B6	1.05	MDSP	2.45
B7	1.05	CDSP	2.0

[a] CTA = 1.4 µmol, AIBN = 0.46 µmol, 1,4-dioxane = 0.18 mL, *p*-xylene = 0.47 mmol, temp.= 85 ^{o}C

4.2.4 Bulk Polymerization using MDSP on a Large Scale Aiming at DP = 1000. Bulk polymerization was chosen in order to keep the reaction mixture free from traces of oxygen, since dioxane is known to form peroxides on exposure to air. Two terpolymers B8 and B9 with composition of 80:10:10 were synthesized by RAFT polymerization on a scale greater than 2 g using MDSP as the RAFT CTA. Though the ternary mixture of B8 and B9 was soluble in dioxane-d_8 after partial conversion to calculate % conversion and DP from ^{1}H NMR, the isolated terpolymers were insoluble in any of the common organic solvents such as 1,4-dioxane, tertrahydrofuran and chloroform. This could be due to the cross linking of terpolymers.

4.2.5 Solution Polymerization using MDSP on a Large Scale Aiming a DP = 1000. Since bulk polymerization led to cross linked terpolymer, solution polymerization was carried out for the synthesis of two terpolymers B10 with 80:10:10 composition and B11 with 60:20:20 composition. Terpolymers were characterized by ^{1}H NMR and SEC. Figures 5 and 6 in the Appendix show the ^{1}H NMR spectra of B10 and B11. The experimental data for the synthesis of B10 and B11 are shown in Table 6 below.

Table 6. Experimental Data of Terpolymers made on a 2.5 g Scale by Solution Polymerization using MDSP[a]

Sample	monomers (mmol)	MDSP (μmol)	time (h)
B10	13.2	1.4	4.0
B11	13.2	1.4	1.5

[a] AIBN = 5.28 μmol, 1,4-dioxane = 1.10 mL, *p*-xylene = 0.94 mmol, temp.= 85 °C

4.3 Calculation of Copolymer Compositions from Binary Copolymer Reactivity.[16,17]

The program ProCop[16-17] was used to calculate copolymer compositions in terpolymers. The calculations were done by inputting the reactivity ratios of the binary monomer mixture, feed composition, and the weighted average percent conversion of monomers. This program is based on the assumption that the random errors in the copolymer composition are normally distributed and statistically independent from run to run and the comonomers feed composition is considered to be errorless. The reactivity ratios were determined for the binary monomer mixture of SMA, tBMA, and DMAEMA via conventional radical polymerization in our lab.[5] The feed composition was calculated by ^{1}H NMR spectroscopy. The feed compositions and compositions after partial conversions of the large scale terpolymers are shown in Table 7. The results show that feed composition of starting reaction mixture and composition after partial conversion do not differ much from the target copolymer compositions of 80:10:10 and 60:20:20 respectively of SMA, tBMA, and DMAEMA. Therefore, there was a very little drift in copolymer composition over the course of polymerizations.

Table 7. ^{1}H NMR Data for Compositions of Terpolymers made by RAFT Polymerization

sample	DP[a]	feed composition[b] (NMR)			composition after partial conversion[b]			% conv.[c]
		SMA	tBMA	DMAEMA	SMA	tBMA	DMAEMA	
B1	368	0.798	0.102	0.099	0.793	0.104	0.103	49
B2	225	0.804	0.094	0.101	0.806	0.098	0.095	30
B3	1950	0.804	0.097	0.098	0.802	0.0.91	0.090	78
B4	263	0.541	0.234	0.223	0.536	0.231	0.232	35
B5	2125	0.813	0.092	0.094	0.839	0.080	0.080	85
B6	270	0.828	0.084	0.087	0.841	0.080	0.080	36
B7	240	0.910	0.053	0.050	0.922	0.048	0.050	33
B8	2125	0.838	0.078	0.082	0.799	0.102	0.110	86
B9	2000	0.807	0.092	0.099	0.804	0.097	0.095	80
B10	1825	0.866	0.070	0.065	0.720	0.140	0.140	73
B11	1075	0.544	0.234	0.229	0.543	0.236	0.228	43

[a] Calculated from % conversion. [b]Calculated from integrated ^{1}H NMR spectra at room temperature and after partial conversion. [c]Weighted average percent conversion from ^{1}H NMR.

The instantaneous and global copolymer compositions were calculated using the ProCop Software. Instantaneous copolymer composition is defined as the composition of the copolymer at a given instant in time whereas the global copolymer composition refers to the overall composition of the copolymer. Table 8 shows the instantaneous and global copolymer compositions calculated by ProCop. The global compositions of the ternary

mixtures estimated by ProCop and the compositions calculated from NMR analysis of unreacted monomers do not differ significantly.

Table 8. Procop Data for Compositions of Terpolymers made by RAFT Polymerization

sample	DP	instantaneous copolymer composition after partial conversion[a]			global copolymer composition after partial conversion[a]			% conv.[b]
		SMA	tBMA	DMAEMA	SMA	tBMA	DMAEMA	
B1	368	0.784	0.107	0.107	0.760	0.116	0.123	49
B2	225	0.771	0.106	0.123	0.760	0.110	0.131	30
B3	1950	0.819	0.089	0.900	0.809	0.097	0.101	78
B4	263	0.559	0.250	0.251	0.509	0.263	0.260	35
B5	2125	0.860	0.074	0.069	0.798	0.097	0.104	85
B6	270	0.794	0.093	0.112	0.780	0.098	0.123	36
B7	240	0.900	0.043	0.053	0.908	0.043	0.050	33
B8	2125	0.838	0.078	0.082	0.799	0.102	0.110	86
B9	2000	0.780	0.092	0.099	0.800	0.097	0.095	80
B10	1825	0.884	0.063	0.055	0.848	0.053	0.074	73
B11	1075	0.510	0.243	0.246	0.486	0.255	0.258	43

[a]Calculated from reactivity ratios. [b]Weighted average percent conversion from ^{1}H NMR.

The confirmation of the cumulative polymer composition by NMR analysis of the isolated terpolymers is a challenge. There is only one characteristic peak for the tert-butyl group of tBMA at 1.40 ppm. But this peak overlaps with two peaks corresponding to the two methyl groups of SMA and the methyl signals of the polymer backbone. This overlap led to poor baseline resolution to do accurate NMR integrations. However, compositions of DMAEMA and SMA repeat units in the terpolymers were determined from integrated ^{1}H NMR spectrum. Five protons of SMA (CH_2-CH-CH_2) and two protons of DMAEMA

($O\text{-}CH_2$) correspond to the signals from 3.70-4.40 ppm. The peak corresponding to $N(CH_3)_2$ of DMAEMA is well resolved at 2-2.5 ppm. Hence, deduction of two protons of DMAEMA from collective area under the curve at 3.70-4.40 ppm, gives the relative amount of SMA and DMAEMA in the terpolymer.

4.4 Size Exclusion Chromatography (SEC) Analysis of RAFT Terpolymers

In RAFT polymerization the theoretical number average molecular weight ($M_{n,th}$) of the polymers is calculated from the equation:

$$(M_{n,th}) = \{([M]_o\, M_M\, C)/\, [CTA]\} + M_{CTA}$$

where,

$[M]_o$, M_M, C, [CTA], and M_{CTA} are the initial monomer concentrations, the average molecular weight of the monomers, the mole fraction conversion, the initial concentration of CTA, and molecular weight of the RAFT CTA, respectively.

The relative molecular weights of the terpolymers B6 and B7 made on a small scale were measured in our laboratory by SEC using poly(methyl methacrylate) standards. Table 9 shows the results of the SEC analysis. There was a significant difference in ($M_{n,th}$) and ($M_{n,SEC}$). This could be due to the smaller coil expansion of the terpolymers than of poly(methyl methacrylate) standards causing smaller hydrodynamic volume and longer retention time (lower relative molecular weights). The absolute molecular weights of terpolymers were measured by light scattering detection in the laboratory of Thomas Mourey at Eastman Kodak Company.

Table 9. SEC Data for Terpolymers Absolute Molecular Weight Determined at the Eastman Kodak Company.

Sample	DP	% aonv.[a]	$M_{n,th}$[b]	$M_{n,SEC}$[c]	M_w/M_n[c]
B1	368	48	58000	43000	1.50
B2	225	30	38000	44000	1.30
B3[d]	1950	78	324000	61000	2.00
B4	263	35	44000	51000	1.33
B5	2125	85	380000	-	-
B6	270	36	45000	31000[d]	1.20
B7	240	33	41000	29000[d]	1.45
B10	1825	73	300000	93000	3.00
B11	1075	43	180000	200000	2.50

[a]Weighted average percent conversion from ^{1}H NMR. [b]Theoratical number average molecular weight. [c]Absolute molecular weights measured by light scattering detection, [d]Relative molecular weight determined in our lab for B3.

All the RAFT terpolymers made, aiming at a DP of 300, show a narrow molecular weight distribution ($M_w/M_n < 1.5$), which is evidence for the controlled or living nature of RAFT polymerizations. The terpolymers intended to have a DP of 1000 show broad molecular weight distribution. The reason could be the synthesis of higher DP polymers under ordinary lab conditions. There are reports for the synthesis of RAFT polymers having a DP of 1000 under high pressure. But at ordinary lab conditions, the chain terminations are probable cause for the broad molecular weight distributions.

Functional Group Conversions of Terpolymers to Polyampholytes

4.5 Quaternization of DMAEMA in Terpolymers[1]

The quaternization of DMAEMA was carried out in methyl iodide and tertrahydrofuran at room temperature. The quaternized polymer is shown in Scheme 4. The results of quaternization of terpolymers are shown in Table 10. The complete conversion of DMAEMA in terpolymers to quaternized polymer was confirmed by ^{1}H NMR spectroscopy. The presence of a new peak at 3.60 ppm corresponding to the $-N^+(CH_3)_3$ group of quaternized DMAEMA and the absence of a peak at 2.35 ppm corresponding to the $-N(CH_3)_2$ group of DMAEMA of the terpolymers confirms the complete quaternization of terpolymers. Figure 7 in the Appendix shows the ^{1}H NMR spectrum of quaternized terpolymer.

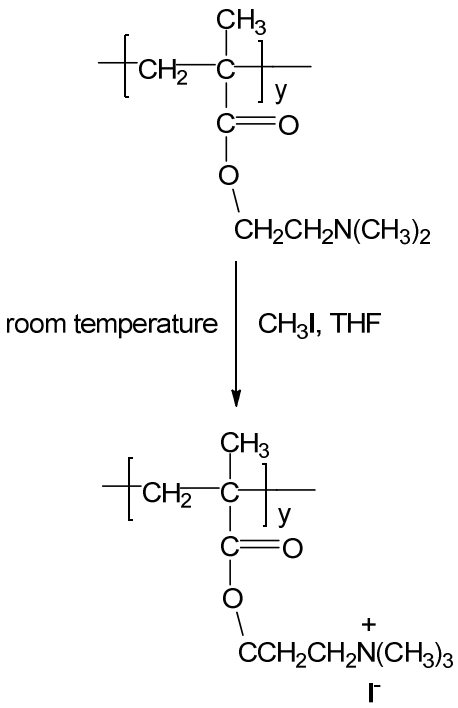

Scheme 4. Quaternized polymer.

The modification in the literature procedure[6] was carried out by doing quaternization with a lesser amount of methyl iodide. DMAEMA and methyl iodide (in 1:2 mol ratio instead of 1:130)[1] were added to the reaction mixture as shown in Samples (B4-2, B10, and B11) in Table 10. The complete quaternization of the three samples was confirmed by ^{1}H NMR spectroscopy.

Table 10. Experimental Data for Quaternizations of Terpolymers.

Sample	DP[a]	terpolymer (g)	THF (mL)	CH_3I (mmol)	DMAEMA[b] (mmol)	yield[c] (%)
B1	368	1.00	15.0	0.32×10^3	2.45	94
B1-2	368	1.76	15.0	0.32×10^3	2.45	95
B2	225	3.00	10.0	0.58×10^3	4.42	97
B2-2	225	2.36	10.0	0.58×10^3	4.42	94
B3	1950	0.09	15.0	0.13×10^3	1.0	88
B4	263	2.40	10.0	0.50×10^3	3.88	96
B4-2	263	0.01	2.0	0.08×10^2	3.88	90
B5	2125	1.47	15.0	0.14×10^3	1.09	87
B10	1825	1.15	10.0	0.02×10^2	1.04	85
B11	1075	0.08	10.0	0.02×10^2	1.24	88

[a] Calculated from % conversion in Table 3. [b]Caculated from % conversion of DMAEMA in terpolymer after partial conversion and moles of DMAEMA in the feed mixture. [c] Isolated quaternized polymer including weight gain due to methyl iodide.

4.6 Deprotection of Quaternized Polymers under Acidic Conditions[3]

The deprotection of the quaternized polymers was carried out in a 1:1 mixture of concentrated HCl and 1,4-dioxane at room temperature by modification of a literature procedure[3] as shown in Scheme 5.

Deprotection of quaternized polymers has been studied on large scale in the past in our lab[6] using aqueous 1M HCl and 1,4-dioxane[6], trifluoroacetic acid and chloroform,[6] and Amberlyst 15/methanol.[6] The results showed the incomplete deprotection of quaternized polymers. Complete deprotection was achieved using a 1:1 mixture of concentrated HCl and 1,4-dioxane at room temperature. The results of the complete acid-catalyzed deprotection of quaternized polymers are shown in Table 11.

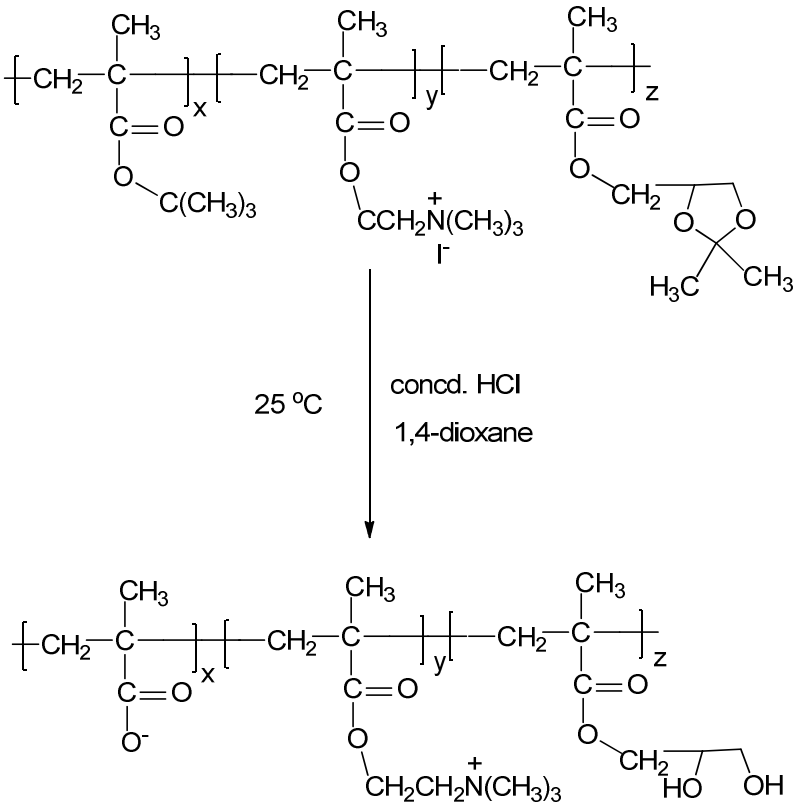

Scheme 5. Deprotection of quaternized polymers.

Table 11. Acid-Catalyzed Deprotection of Quaternized Polymers

quaternized sample	amount (g)	concentrated HCl (mL)	1,4-dioxane (mL)
B1-a	1.0	5	5
B1-b	1.76	7	7
B2-a	3.01	12	12
B2-b	2.50	7	7
B3[a]	1.03	3.5	3.5
B4	2.74	8	8
B10	1.49	5	5
B11	1.01	3	3

[a] Forms water-insoluble gel after deprotection

The ^{1}H NMR spectra of purified water-soluble polyampholytes in D_2O are shown in Figures 8, 9, 10, and 11 in the Appendix. It is clear qualitatively from all the ^{1}H NMR spectra of isolated polyampholytes that the *tert*-butyl peak at 1.4 ppm, and the peaks at 1.34 ppm and 1.38 ppm corresponding to two methyl groups of the ketal ring of SMA are completely absent.

Deprotected sample B3 (DP = 1950) resulted in a water-insoluble gel. The probable reason could be the acid-catalyzed transesterification reaction between the alcohol group of deprotected SMA or glyceryl monomethacrylate (GMA) and the ester units in polyampholytes.

The overall summary of isolated water-soluble polyampholytes is shown in Table 12. Water-soluble polyampholytes were characterized by SEC analysis in the laboratory of Thomas Mourey at Eastman Kodak Company. Table 13 shows the results of SEC analysis.

Table 12. Isolated Water-Soluble Polyampholytes

quaternized sample	amount (g)	Polyampholyte (g)	yield[a] (%)
B1-a	1.00	0.50	50.0
B1-b	1.76	0.89	50.0
B2-a	3.01	1.50	49.0
B2-b	2.50	1.53	61.0
B4	2.74	2.30	83.0
B10	1.49	1.05	70.0
B11	1.01	0.48	48.0

[a]Calculated including the weight loss due to acetone and tert-butyl alcohol.

Table 13. SEC Data for Absolute Molecular Weight Determined at Eastman Kodak Company

sample	DP	% conv.[a]	$M_{n,th}$[b]	$M_{n,SEC}$[c]	M_w/M_n[c]
B1-a	368	48	49000	51000	1.6
B1-b	368	48	49000	65000	1.5
B2-a	225	30	31000	36000	1.6
B2-b	225	30	31000	47000	1.7
B4	263	35	37000	71000	1.9
B10	1825	73	200000	370000	2.9
B11	1075	43	110000	230000	3.2

[a]Weighted average percent conversion from ^{1}H NMR. [b]Theoratical number average molecular weight. [c]Absolute molecular weights measured by light scattering detection.

We have not been able to measure the complete compositions of isolated polyampholytes by NMR analysis. However, the relative amounts of glyceryl monomethacrylate (GMA) and quaternized DMAEMA repeat units were calculated from integrated ^{1}H NMR spectra. The signals corresponding to the five protons of SMA are at 4.5 ppm and the signals corresponding to the thirteen protons of quaternized DMAEMA at 3.2-4.6 ppm were used to calculate the composition of DMAEMA and GMA in the polyampholytes. However, determination of composition of methacrylic acid in the polyampholyte is a challenge because the only signal corresponding to methacrylic acid is the backbone CH_3 and CH_2 groups which overlap with backbone CH_3 and CH_2 signals of of SMA and DMAEMA.

4.7 Dynamic light scattering (DLS) study of polyampholytes

DLS study of aqueous solutions of polyampholytes showed that polyampholyte molecules are partially aggregated at higher concentrations and the aggregation decreases with dilution. The DLS results for sample B4 (DP = 263) at a concentration of 1 mg/mL and at a concentration 0.1 mg/mL are shown in Figure 1 below. There were major peaks in the distribution of particle diameters at about 20 nm, about 300 nm, and about 4000 nm in the sample having a higher concentration (1 mg/mL). After dilution to 0.1 mg/mL the 20 nm peak accounted for more than 90% of the sample on volume basis. The probable reason for the aggregation of the polyampholyte molecules is the hydrophobic interaction of the methacrylate polymer backbone.

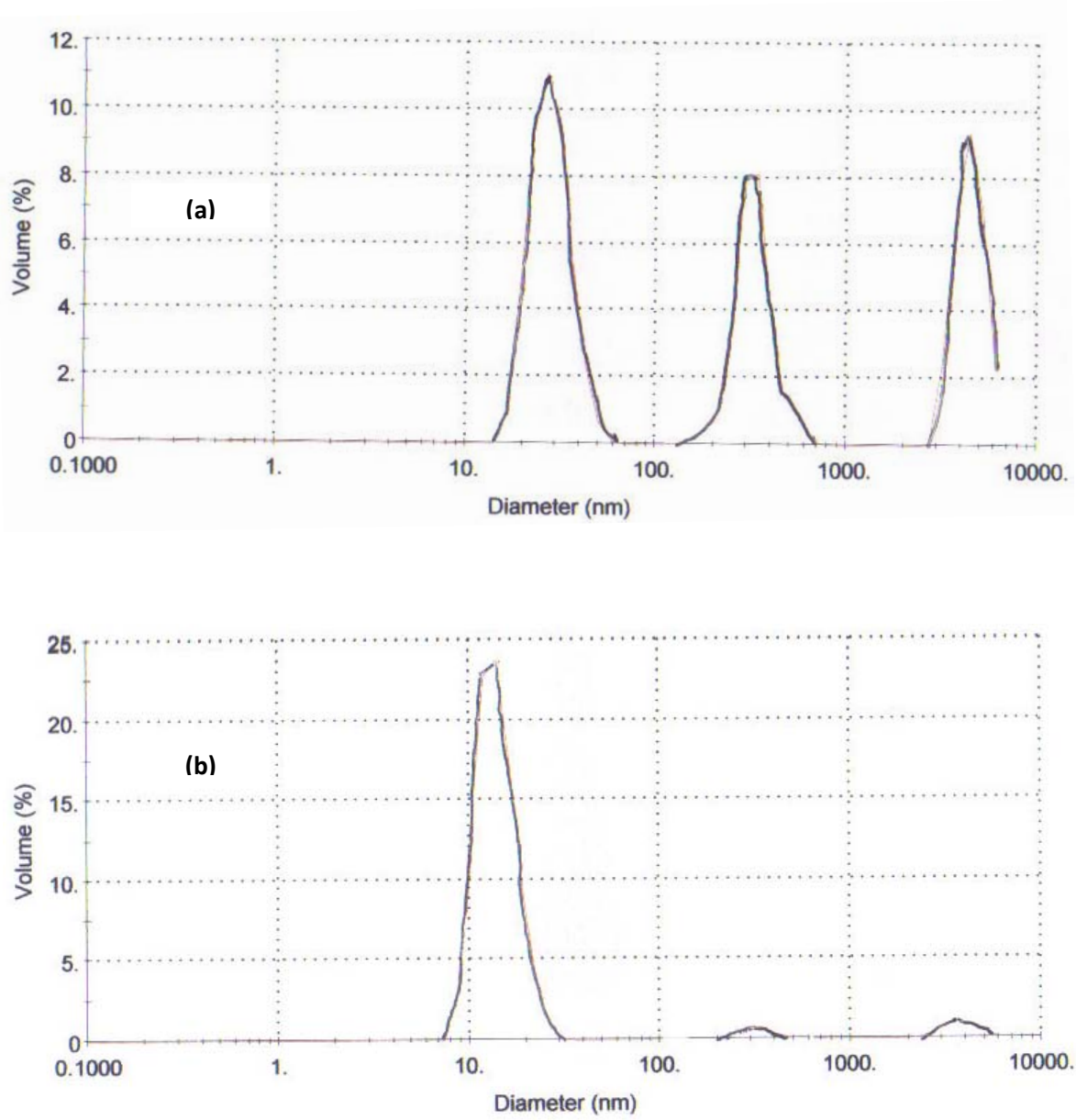

Figure 1. Sample B6 size distribution by volume at (a) 1 mg/ml; (b) 0.1 mg/ml.

4.8 Titration Curves and Viscosities Measurement of Polyampholyte Solutions

A characteristic feature of a polyampholyte is the presence of isoelectric point (IEP). The IEP is defined as the pH at which the polyampholyte is electrically neutral. IEP can be determined experimentally by titration or by measuring the reduced viscosity.

The pH to study the rheology of sample B1-b of polyampholyte was determined by titration curve of pH vs. volume of HCl added in Ralph Colby's laboratory at Pennsylvania State University. To construct the titration curve, 0.03 g of polyampholyte (B1-b) was dissolved in 1.5 mL of deionized water and the resulting solution was titrated first with aqueous HCl to a pH value below 4 and then with aqueous KOH solution to a pH value over 11. Similarly, the titration was repeated by titrating polymer solution with aqueous KOH solution to a pH value over 11 and then with aqueous HCl solution to a pH value lower than 4. The results of the titrations are shown in Figures 2 and 3. IEP of polyampholyte is 8.2 (Figure 2) and 8.5 (Figure 3).

The derivatives of the acidic to basic state curve in Figure 2 vs. volume show a peak at around a volume of KOH or HCl solution of 195 µL which corresponds to pH 8.14 (curve on right hand side of Figure 4) and the derivative of the basic to acidic state curve in Figure 3 vs. volume shows a peak at around volume of 12.5 µL which corresponds to pH 8.5 (curve on left hand side of Figure 4). Both peaks represent the transition between carboxylic acid and fully neutralized carboxylic sodium salt. The peaks nearly agree with each other and end point of the titration should be in the range from 8.14 to 8.5. The range is quite wide.

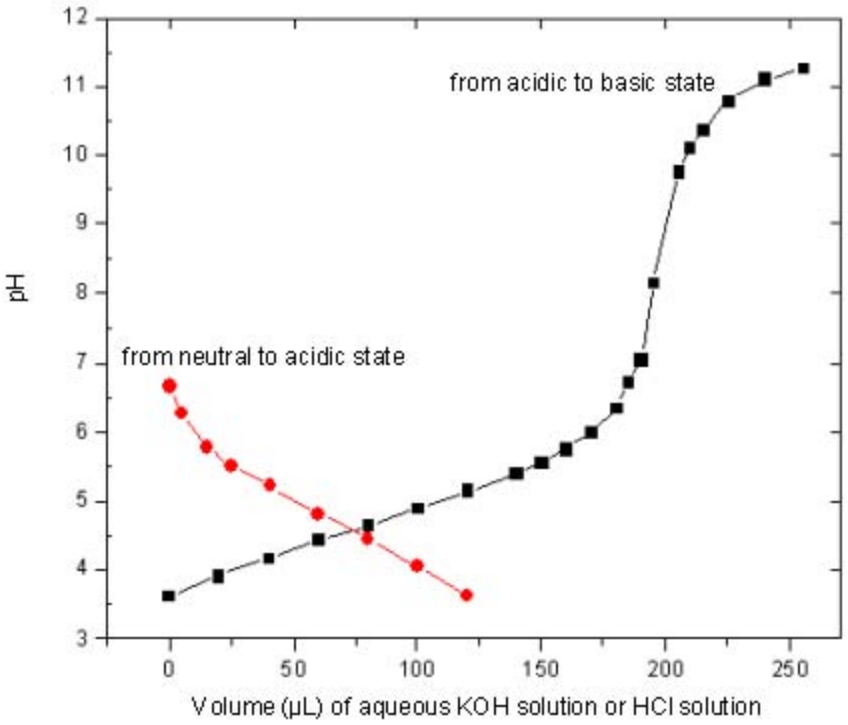

Figure 2. Titration curves of polyampholyte sample B1-b

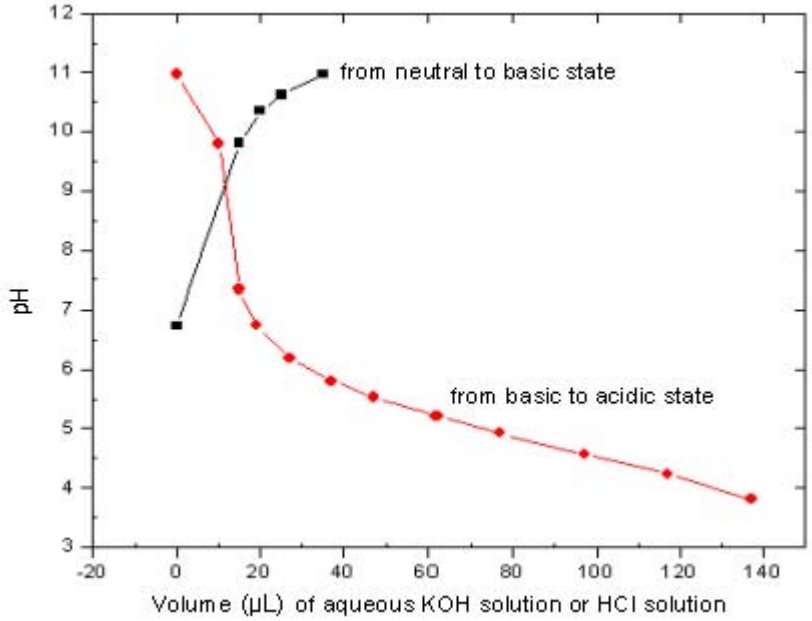

Figure 3. Titration curve of polyampholyte sample B1-b.

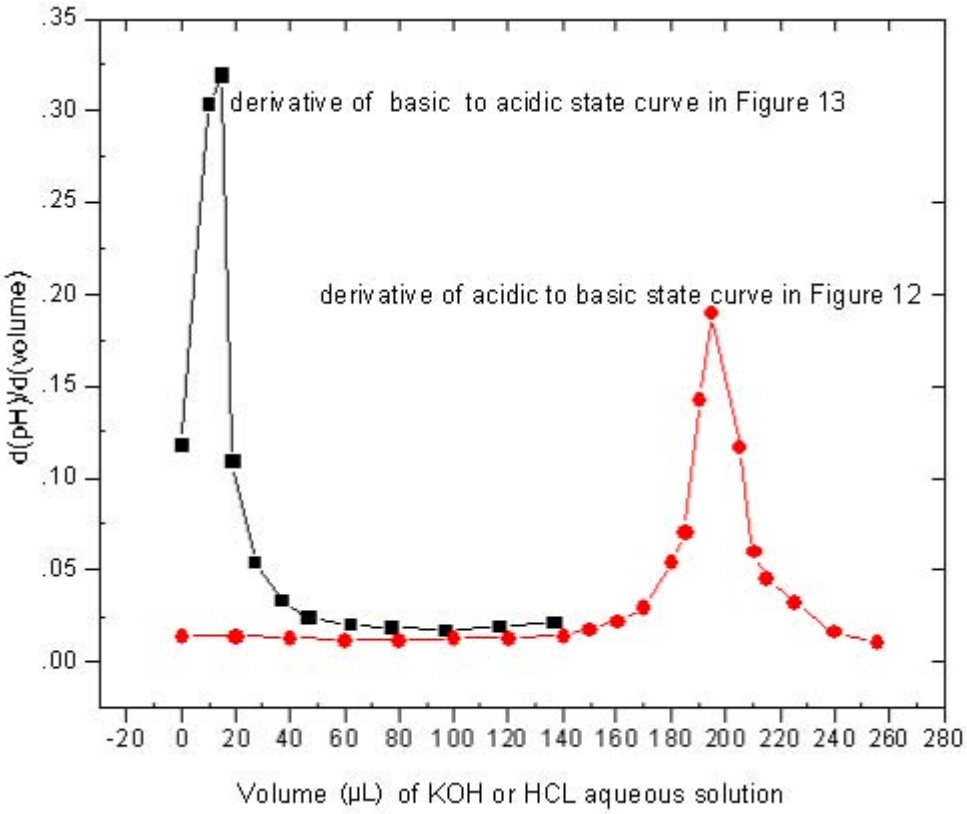

Figure 4. Derivatives of titration curves in figure 2 and 3.

4.9 Viscosity measurement

Polyampholyte solutions of samples B1-b and B2-b having a concentration 0.03 g/mL were prepared in deionized water. The starting pH for the B1-b aqueous solution was6.6 and for B2-b was 5.9. The viscosity of a 2 mL solution of B1-b and B2-b as a function of pH was measured by using the Contaves Low Shear 30 Viscometer at various shear speeds (all solutions were Newtonian) in Ralph Colby's laboratory at Pennsylvania State University. The viscosity of B2-b sample solution (2 mL) as a function of NaCl concentration of 0, 0.1 and 1 M, respectively was measured at a pH of 5.17. The dependences of pH on the viscosity of sample B1-b and B2-b are shown in Figure 5 and

Figure 6 respectively. The IEP of polyampholyte is 8.5 (Figure 5) which is comparable to the IEP measured by titration.

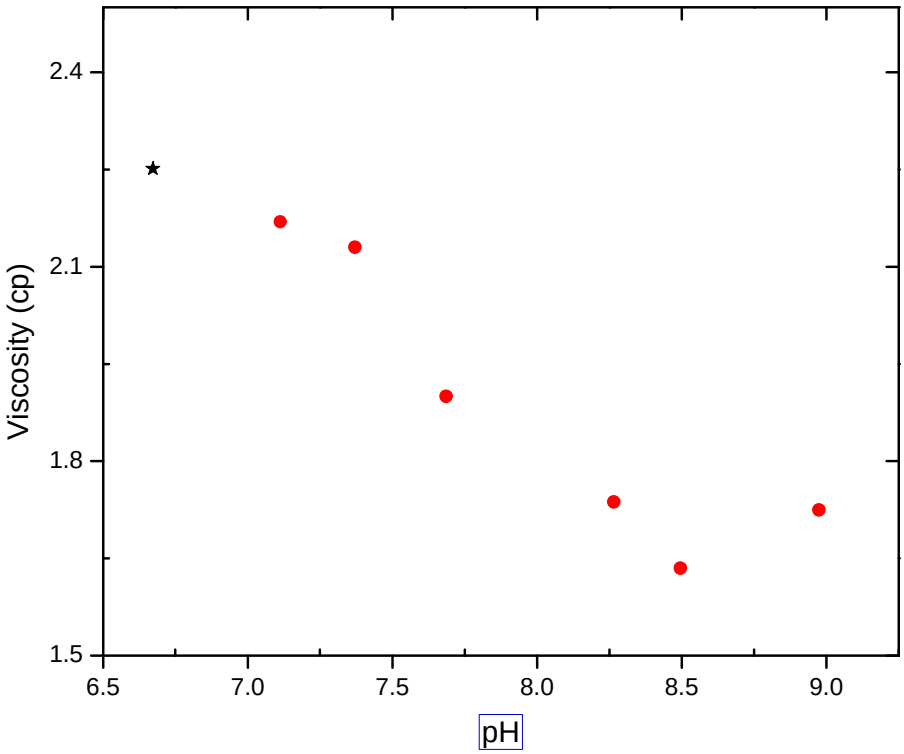

Figure 5. Viscosity of polyampholyte solution B1-b as a function of pH adjusted by adding aqueous KOH solution.

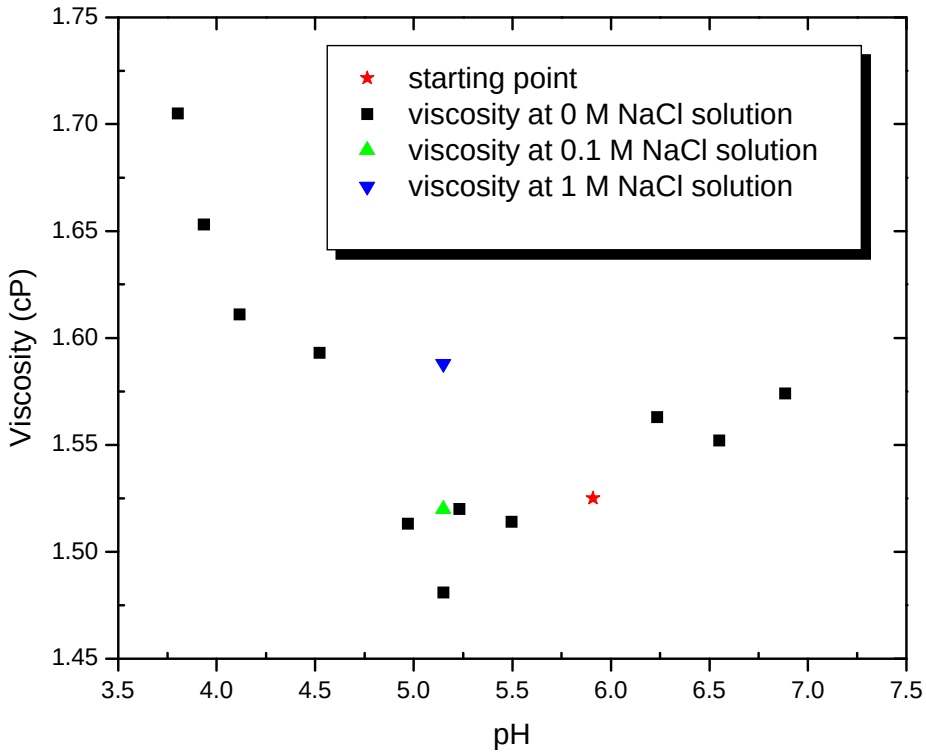

Figure 6. Viscosity of polyampholyte solution B2-b as a function of pH and NaCl concentration,with pH adjusted by adding aqueous KOH solution for pH >5.9 and by adding aqueous HCl solution at pH < 5.9.

The viscosity of the sample B1-b as a function of pH reveals that polyampholyte has a large net charge (or polyelectrolyte regime). As the pH is increased, the viscosity of the polyampholytes decreases and it acts like a polyelectrolyte. It is clear from Figure 5 that at around pH 8.0 methacrylic acid groups are fully neutralized and further addition of KOH simply increases the ionic strength of the solution. The IEP with the pH of minimum viscosity for the B1-b sample is 8.5. This decrease in viscosity with addition of salt or with pH increase indicates that the polyampholyte is clearly not charge-balanced and exhibits polyelectrolyte behavior (screening charge repulsion).

The real isoelectric point for the sample b2-b is at pH 5.2 corresponding to the lowest viscosity. Addition of NaCl to the polyampholyte solution B2-b at pH = 5.17

increases the viscosity of solution with salt concentration (Figure 6). This can be explained by screening of charge attraction by addition of salt, enlarging the coil size (polyampholyte effect). The viscosity measurement of both the polyampholyte solutions proved that the polyampholytes synthesized in this study are not charged-balance.

SEC analysis of isolated water soluble polyampholytes conducted at Eastman Kodak Company showed that the molecular weight distributions of polyampholytes are broad. The probable reason could be the cross-linking of polyampholytes during deprotection under acidic conditions.

The DLS study of aqueous solution of polyampholytes showed the aggregation of polyampholytes molecules due to hydrophobic interaction of the methacrylate polymer backbone. The interactions were overcome by dilution.

4.10 Conclusion

Terpolymers of SMA, DMAEMA and tBMA were synthesized by RAFT polymerization on 5.0 g scale in 1,4-dioxane. Terpolymers were characterized by SEC analysis and ^{1}H NMR spectroscopy. SEC analysis of the terpolymers showed narrow molecular weight distributions and ^{1}H NMR showed that there is no drift in composition of the terpolymers at higher conversion.

The terpolymers were successfully converted into water soluble polyampholytes by functional group conversion. The polyampholytes were characterized by SEC analysis, ^{1}H NMR spectroscopy, and Dynamic light scattering (DLS) study. The viscosity as a function of pH and added salt of polyampholyte solution showed that polyampholytes are not charge- balanced. In future we need to synthesize charged-

balanced random polyampholyte without the drift in composition to study the relationship between viscosity and pH value from pH 1-14. We also need to synthesize polyampholyte on a scale greater than 5.0 g to measure the viscosities over different salt and polyampholyte solution concentrations.

4.11 Experimental

Materials. Reagent grade *n*-hexane (Aldrich, 98 %), methyl iodide, and hydrochloric acid (Fisher Scientific) were used as received. 2-Methyl-2-(dodecylsulfanylthiocarbony)sulfanyl propanoic acid was provided by Dr. John Lai of the Lubrizol Corp. 4-Cyano-4-(dodecylsulfanylthiocarbony)sulfanyl pentanoic acid was purchased from Strem Chemicals. Cumyl dithiobenzoate and solketal methacrylate was synthesized in our lab. 2-(Dimethylamino)ethyl methacrylate (Polysciences, Inc.) and *tert*-butyl methacrylate (Aldrich) were purified before use by passing through a column of basic alumina. 2,2-Azobisisobutyronitrile (AIBN) (Aldrich) was recrystalized from methanol. Tetrahydrofuran (Aldrich, HPLC grade), 1,4-dioxane (Aldrich, anhydrous, 99.8%) and *p*-xylene (Eastman Chemicals) were used as received. $CDCl_3$ (Aldrich, 99.8 atom % D), 1,4-dioxane-d_8 (99 atom % D) and D_2O (99.9 atom % D) (Cambridge Isotope Laboratories, Inc.) were used as received.

Spectra/Por dialysis tubing (MWCO 1000, Spectrum) was washed with triply deionized water and was soaked in deionized water for 1 h before use to remove sodium azide added as a preservative.

Instrumentation. ^1H NMR spectra of all the terpolymers and water soluble polyampholytes were recorded on a 400 MH_Z NMR spectrometer. The relative molecular

weights of terpolymers were determined using an Agilent 1100 Series instrument equipped with two PLGEL 10 µm MIXED-B, 300 X 7.5 mm columns and a refractive index detector. Measurements were made in tertrahydrofuran as the mobile phase at 40 ^{o}C at a flow rate of 1.0 mL/min. All SEC samples were filtered through a Whatman polypropylene (0.2 µm) filter before injection. Absolute molecular weights were measured by light scattering detection in the lab of Thomas Mourey at Eastman Kodak Company. Particle size distributions of polyampholytes were measured by dynamic light scattering (Malvern HPPS 3.1 instrument equipped with a He-Ne, 3.0 mW, 633 nm laser). Polyampholyte (1 mg) was diluted with 1 mL of deionized water for DLS measurement. The particle size and size distribution were measured at 25 ^{o}C.

4.11.1 Purification of Cumyl Dithiobenzoate (CDB)

The ^{1}H NMR spectrum of CDB in $CDCl_3$ showed the signals corresponding to vinyl protons of α-methylstyrene, indicating that it was a mixture of cumyl dithiobenzoate and α-methylstyrene. The mixture was purified by chromatography using 200 g of alumina. Alumina of activity (III) was deactivated by adding 8.8 g of water and the mixture was rotated on rotary evaporator to mix it thoroughly for 3 hours before loading it onto the column. During elution with *n*-hexane the purple color CDB solution was separated into different color bands, with pale yellowish orange at the top, and purplish pink at the bottom. The purple color fractions were combined and evaporated by rotary evaporator using pump to get 1.26 g of CDB as dark purple viscous oil. ^{1}H NMR spectrum of pure CDB (Figure 2 in appendix) (400 MH_Z, $CDCl_3$) δ: 2.03 (s, 6H), 7.15-7.50 (m, 8H), 7.78 (m, 2H).

4.11.2 General Procedure for Large Scale Terpolymer Synthesis using Cumyl Dithiobenzoate as RAFT CTA

Terpolymers were synthesized in 1,4-dioxane at 75 ^{o}C. In a typical run (sample B1, DP=368), stock solutions of AIBN (0.038 g AIBN in 10 mL of 1,4-dioxane) and cumyl dithiobenzoate (0.192 g CDB in 10 mL 1,4-dioxane) were prepared. Monomers, SMA (8.40 g, 4.20 x 10^{-2} mol), DMAEMA (0.801 g, 5.1 x 10^{-2} mol) and tBMA (0.807 g, 5.7 x 10^{-2} mol) were weighed into a scintillation vial. The scintillation vial was rinsed with 1,4-dioxane and dried before use. AIBN (2.31 x 10^{-5} mol, 0.0038 g) and CDB (7.03 x 10^{-5} mol, 0.0192 g) were weighed out from the stock solutions and transfered to the scintillation vial. *p*-Xylene was used as the internal reference to measure monomer conversions from ^{1}H NMR spectral integrations of the initial mixture at room temperature (prior to polymerization) and at the end of polymerization. *p*-Xylene (0.405 g, 3.81 x 10^{-3} mol) and 1,4-dioxane (4.40 mL) were added to the scintillation vial The ternary reaction mixture (0.25 mL) was kept aside to get ^{1}H NMR spectrum at room temperature in 1,4-dioxane-d_8 (0.50 mL). The rest of the ternary mixture was transfered carefully from the scintillation vial to heavy walled glass tube by using a syringe with a long needle. The ternary mixture in heavy walled glass tube was degassed using freeze-pump-thaw cycles and the tube was flame sealed under vacuum. After sealing the tube was brought to room temperature and then was enclosed in an aluminum wire-mesh to prevent the content from splattering (in the event of an implosion). The polymerization was carried out by immersing the tube completely in an 8 L glass beaker filled with ethylene glycol pre-heated at 75 ^{o}C. ^{1}H NMR spectrum of the partially polymerized mixture (0.5 mL) was taken in 1,4-dioxane-d_8 (0.5 mL).

The terpolymer was isolated by precipitation into vigorously stirring *n*-hexane (800 mL). A pink colored polymer precipitated out of solution. The isolated terpolymer was filtered off and dried under vacuum at room temperature for 24 h (Sample B1 in Table 3, Figure 3 in appendix): ^{1}H NMR (400 MH_z, $CDCl_3$) δ: 6.10 and 5.60 (s, residual =C**H$_2$** of SMA monomer), 4.20 and 3.65 (residual SMA monomer), 4.31 (m, CH_2-C**H**), 4.16 (s, CO_2-C**H**-H), 4.15 (m, CO_2-CH-**H**), 4.04 (m, -CH-C**H**-H), 3.74 (-CH-CH-**H**), 3.60 (O-C**H$_2$**,DMAEMA), 2.55–2.70 (-N-C**H$_2$**, DMAEMA), 2.35 (-N**(CH$_3$)2**, DMAEMA), 1.93 (-CH_3's residual SMA monomer), 1.70-2.10 (backbone -C**H$_2$'s**), 1.50 (peak due to H_2O inCDCl3), 1.30-1.42 (-C(CH_3)3, tBMA and 2 -CH_3's, SMA), 0.70-1.15 (backbone -C**H$_3$'s**).

4.11.3 General Procedure for Small Scale Terpolymer Synthesis (A) 2-Methyl-2-(dodecylsulfanylthiocarbony)sulfanyl propanoic acid (MDSP) as RAFT CTA

Terpolymers of SMA, DMAEMA and tBMA were synthesized on NMR scale in the mole ratio of 80:10:10 using AIBN as initiator and MDSP as the RAFT agent. In a typical run (sample B6 with a DP of 270) , SMA (168 mg, 8.4 x 10^{-4} mol), DMAEMA (16 mg, 1.02 x 10^{-4} mol) and tBMA (16 mg, 1.12 x 10^{-4} mol) were weighed and transferred into a scintillation vial. Stock solutions of AIBN (8 mg of AIBN in 1.0 mL of 1,4-dioxane-d_8) and MDSP (0.51 mg MDSP in 1.0 mL of 1,4-dioxane-d_8) were prepared. AIBN and MDSP (0.1 mL) from prepared stock solutions, *p*-Xylene (50 mg, 4.71 x 10^{-4} mol) and 1,4-dioxane-d_8 (200 mg, 2.07 x 10^{-3} mol) were added to the scintillation vial. The ternary reaction mixture was transferred to a clean vacuum dried NMR tube. The polymerization was carried out at 85^{o}C for 2.45 h. The ^{1}H NMR spectra were acquired at

every 0.5 h. Quad probe was used, locked and shimmed to acquire a room temperature spectrum. The temperature was set to 85 ^{o}C, and the sample was left to equilibrate for 10 min. Then the probe was locked and shimmed at 85 ^{o}C. The spectra were arrayed to collect data every half hour.

After polymerization the reaction mixture was withdrawn from NMR tube using long pasteur pipette. The terpolymer was isolated by dropping ternary copolymer solution to a vigorously stirring solution of *n*-hexane (15.0). Terpolymer was filtered off and vacuum dried at room temperature for 48 h.

4.11.4 (B) 4-Methyl-4-(dodecylsulfanylthiocarbony)sulfanyl pentanoic acid (CDSP) as RAFT CTA

In a typical run (Sample B6 with a DP of 270), SMA (168 mg, 8.4 x 10^{-4} mol), DMAEMA (16 mg, 1.02 x 10^{-4} mol) and tBMA (16 mg, 1.12 x 10^{-4} mol) were weighed and transferred to a cleaned scintillation vial. Stock solution of AIBN (8 mg of AIBN in 1.0 mL of 1,4-dioxane-d_8) and CDSP (0.51 mg MDSP in 1.0 mL of 1,4-dioxane-d_8) were prepared. AIBN and CDSP (0.1 mL) from prepared stock solution, *p*-Xylene (50 mg, 4.71 x 10^{-4} mol), and 1,4-dioxane-d_8 (200 mg, 2.07 x 10^{-3} mol) were added to the scintillation vial. The ternary reaction mixture was transferred to a clean vacuum dried NMR tube. The polymerization was carried out at 85^{o}C for 2.0 h. The ^{1}H NMR spectra were acquired at every 0.5 h. Quad probe was used, locked and shimmed to acquire a room temperature spectrum. The temperature was set to 85 ^{o}C, and the sample was left to equilibrate for 10 min. Then the probe was locked and shimmed at 85 ^{o}C. The spectra were arrayed to collect data every 30 min.

4.11.5 General Procedure for Large Scale Terpolymer Synthesis using MDSP as RAFT CTA with DP = 1000. (A) Bulk Polymerization

MDSP was used as RAFT CTA to synthesize terpolymer with degree of polymerization of 1000 using the procedure reported above for the synthesis of large scale terpolymers using CDB as CTA except that the polymerization was done in the absence of 1,4-dioxane. The experimental data for the synthesized terpolymers is shown in Table 5.

4.11.6 Solution Polymerization

MDSP was used as RAFT CTA to synthesize terpolymer with degree of polymerization of 1000 using the procedure reported above for the synthesis of large scale terpolymers using CDB as CTA and polymerization was done in the absence of 1,4-dioxane. The experimental data for the synthesized terpolymers is shown in Table 6.

4.11.7 Quaternization of DMAEMA in RAFT Terpolymers

Quaternization of RAFT terpolymers were done in tertrahydrofuran at room temperature for 48 h. In a typical run 1 g of terpolymer (B1, DP =368 and 2.45 x 10^{-3} mol DMAEMA) was dissolved in 15 mL of tetrahydrofuran. Then a large excess of methyl iodide (19.8 mL, 0.318 mol) was added. The reaction mixture was stirred at room temperature for 48 h. Tetrahydrofuran and excess of methyl iodide were removed by rotary evaporation. The quaternized terpolymer was obtained after drying under vacuum at room temperature for 48. A ^{1}H NMR spectrum of the quaternized polymer is shown in Figure 7 in the Appendix: ^{1}H NMR(400 MHz, CDCl3) δ: 6.10 and 5.60 (s, residual =C**H$_2$**

of SMA monomer), 3.65–4.40 (m,-C**H$_2$**C**H**C**H$_2$**, 5 H from SMA, 2H from -O-C**H$_2$**, and 2H from -N-C**H$_2$**, DMAEMA), 3.60(m, br, -N+(C**H$_3$)$_3$**, DMAEMA), 3.30 (residual CH_3, CH_3I), 2.25 (-C**H$_3$**, *p*-xylene), 1.90 (-C**H$_3$'s** from monomer), 1.70-2.05 (backbone -C**H$_2$'s**), 1.50 (H_2O from $CDCl_3$), 1.34-1.42(-C(C**H$_3$)$_3$**, tBMA and 2 -C**H$_3$'s** SMA), 0.70-1.25 (backbone -C**H$_3$'s**).

4.11.8 Deprotection of Quaternized Polymers

The deprotection of quaternized polymers was carried out in 1:1 mixture of concentrated HCl and 1,4-dioxane at room temperature for 8 h. In a typical run (sample B1, DP = 368) 1.0 g of quaternized polymer was dissolved in 5 mL of 1,4-dioxane. Then 5 mL of concentrated HCl was added and the reaction mixture was stirred for 8 h at room temperature. The ^{1}H NMR spectrum of the sample was taken immediately after stirring. The sample was neutralized using 8M NaOH. The neutralized mixture was dialyzed in a dialysis membrane with molecular weight cut-off 1000 for 36 h by changing water after every 6 h to remove NaCl and iodide ion. The progress of dialysis was followed by measuring the conductivity of dialysate. The excess water in dialyzed mixture was rotary-evaporated under vacuum to a volume of 10 mL. The remaining water was lyophilized and pure polyampholyte was isolated after vacuum drying at room temperature for 24 h. The ^{1}H NMR spectra of purified water-soluble polyampholytes in D_2O are shown in Figures 8, 9, 10, and 11 in the Appendix: ^{1}H NMR (400 MHz, D_2O) 3.65–4.50 (m,-C**H$_2$**C**H**C**H$_2$**, 5 H from SMA, 2H from -O-C**H$_2$**, and 2H from -N-C**H$_2$**, DMAEMA), 3.40(m, br, -N+(C**H$_3$)$_3$**, DMAEMA), 1.70-2.05 (backbone -C**H$_2$'s**) and 0.70-1.25 (backbone -C**H$_3$'s**).

References:

(1) Batt-Coutrot, D.; Haddleton, D. M.; Jarvis, A, P.; Kelly, R. L. *Eur. Polym. J. 39*, **2003**, 2243-2252.

(2) Burguière, C.; Pascual, S.; Bui, C.; Vairon, J. P.; Charleux, B.; Davis, K. A.; Matyjaszewski, K.; Bétremieux, I. *Macromolecules*, **2001**, *34*, 4439-4450.

(3) Mori, H.; Hirao, A.; Nakahama, S. *Macromolecules* **1994**, *27*, 35-39.

(4) Li, Z.; Day, M.; Ding, J.; Faid, K. *Macromolecules* **2005**, *38*, 2620-2625.

(5) Miranda, L. N.; Ford, W. T. *J. Polym. Sci., Part A: Polym. Chem.* **2005**, *43*, 4666-4669.

(6) Miranda, L. N.; Kaur, B.; Ford, W. T. *Polymer Preprints* **2008**, *49*, 246-247.

(7) Nuopponen, M.; Ojala, J.; Tenhu, H. *Polymer* **2004**, *45*, 3643-3650.

(8) Sahnoun, M.; Charreyre, M.-T.; Veron, L.; Delair, T.; D'Agosto, F. *J. Polym. Sci., Part A: Polym. Chem.* **2005**, *43*, 3551-3565.

(9) Xiong, Q.; Ni, P.; Zhang, F.; Yu, Z. *Polym. Bull.* **2004**, *53*, 1-8.

(10) Moad, G.; Rizzardo, E.; Thang, S. H. *Aust. J. Chem.* **2005**. *58*, 379-410.

(11) Chong, Y. K.; Krstina, J.; Le, T. P. T.; Moad, G.; Postma, A.; Rizzardo, E.; Thang, S. H. *Macromolecules* **2003**, *36*, 2256-2272.

(12) Chiefari, J.; Mayadunne, R. T. A.; Moad, C. L.; Moad, G.; Rizzardo, E.;Postma, A.; Skidmore, M. A.; Thang, S. H. *Macromolecules* **2003**, *36*, 2273-2283.

(13) Plummer, R.; Goh, Y. K.; Whittaker, A. K.; Monteiro, M. J. *Macromolecules* **2005**, *38*, 5352-5355.

(14) Liu, Y.; Junpo, H.; Xu, J.; Fan, D.; Tang, W.; Yang, Y. *Macromolecule* **2005**, *38*, 10332-10335.

(15) Rudin A. *The Elements of Polymer Science and Engineering*; 2nd Ed.; Academic Press, San Diego, California, **1999**.

(16) Hagiopol, C.; Frangu, O. *J. Macromol. Sci., Pure Appl. Chem.* **2003**, *A40*, 571-584.

(17) Hagiopol, C. *Copolymerization: Toward a Systematic Approach*, Kluwer Academic: New York, **1999**, pp 1-47.

Appendix

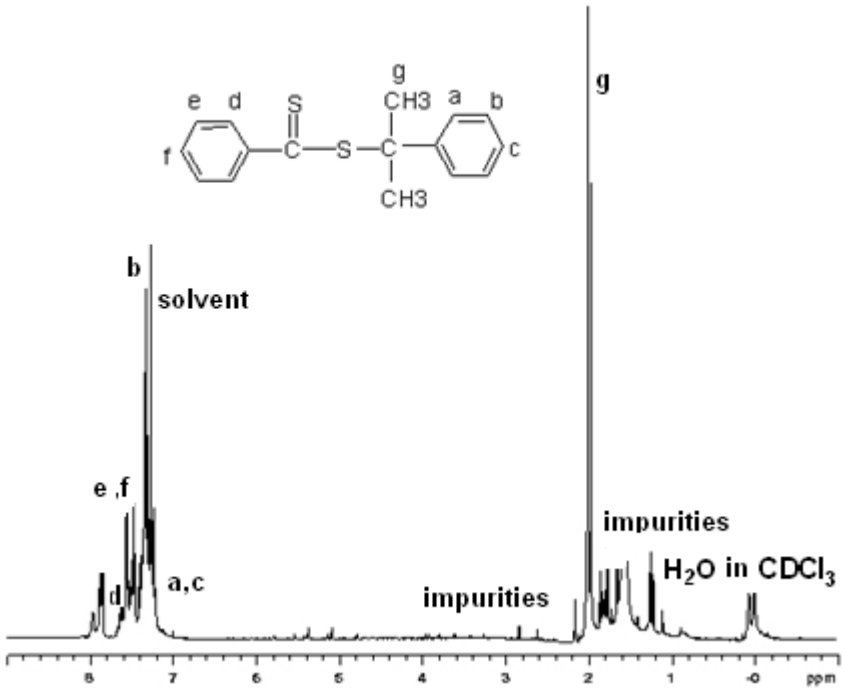

Figure 1. ^{1}H NMR spectrum of impure cumyl dithiobenzoate in $CDCl_3$

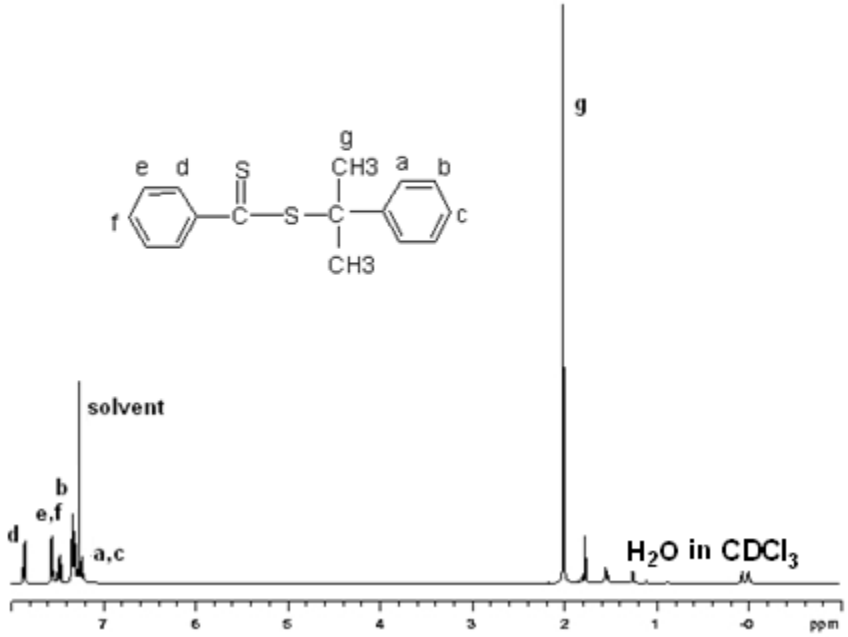

Figure 2. ^{1}H NMR spectrum of pure cumyl dithiobenzoate in $CDCl_3$.

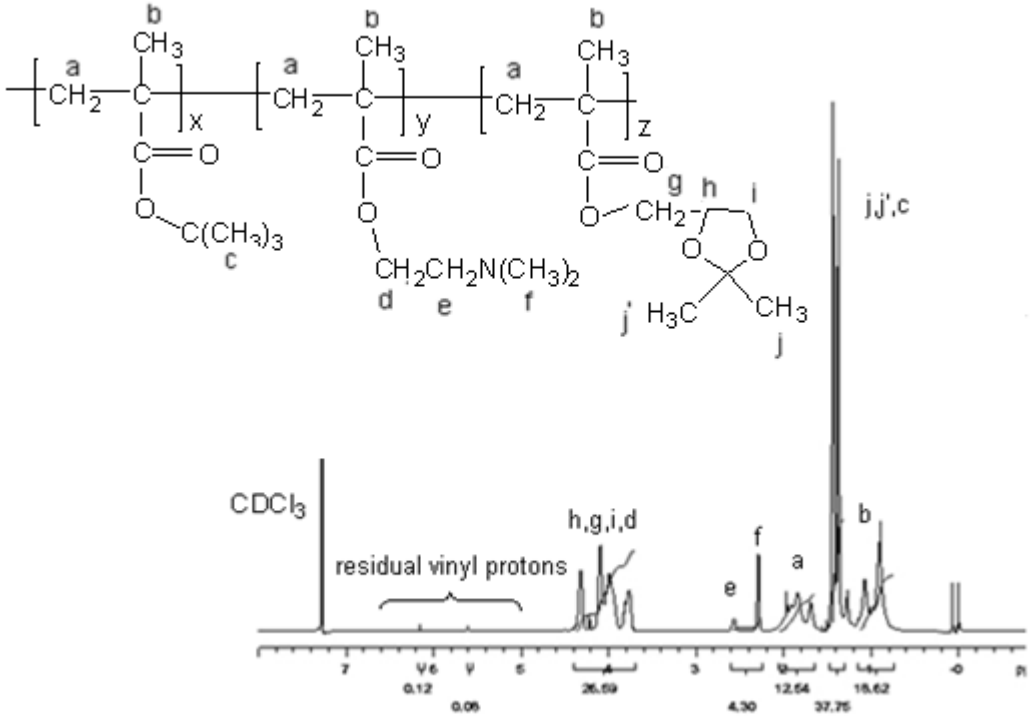

Figure 3. ^{1}H NMR spectrum of sample B1 terpolymer (DP =368) in $CDCl_3$.

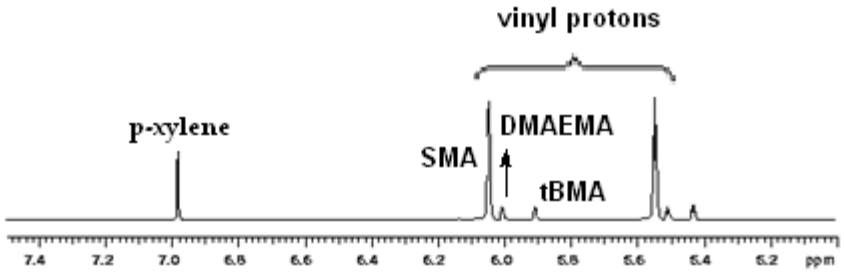

Figure 4. ^{1}H NMR spectrum for the determination of monomer conversions in 1,4-dioxane-d_8

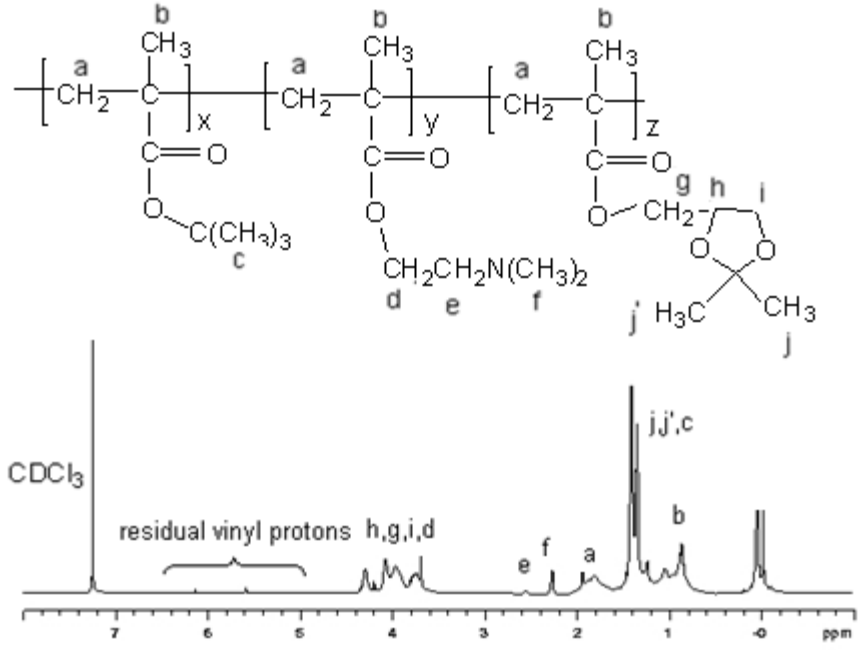

Figure 5. ^{1}H NMR spectrum of sample B10 terpolymer (DP =1825) in $CDCl_3$.

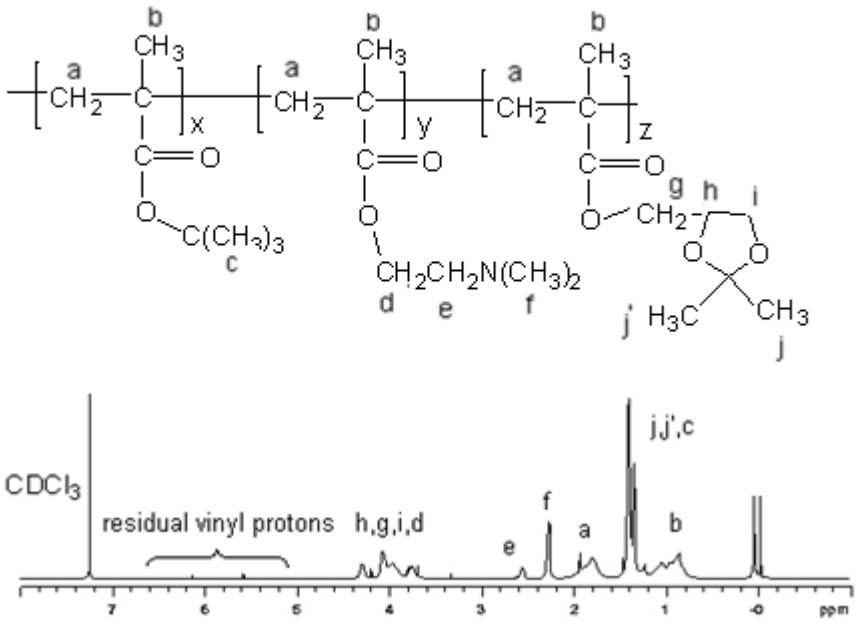

Figure 6. ^{1}H NMR spectrum of sample B11 terpolymer (DP =1075) in $CDCl_3$.

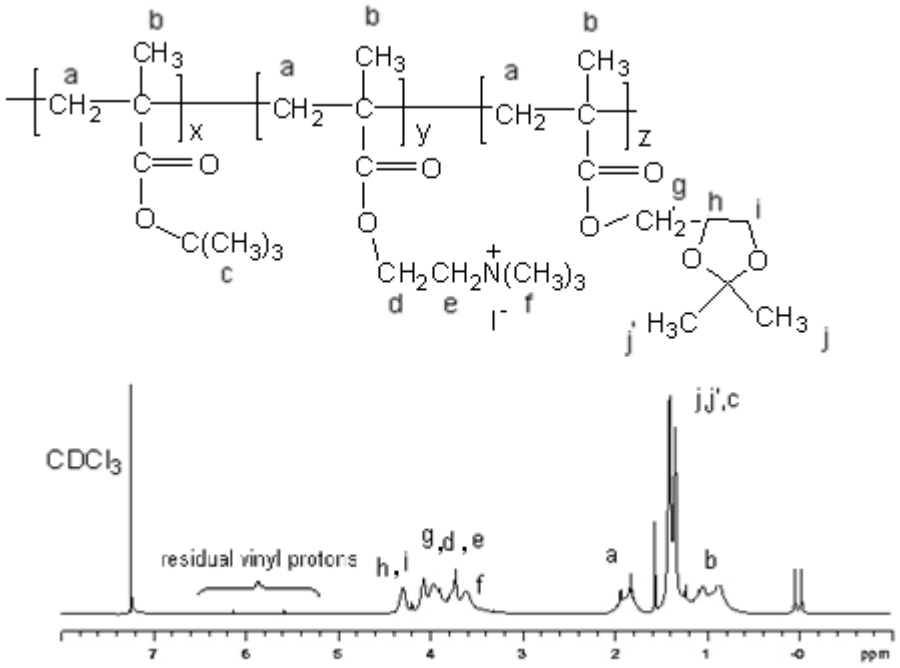

Figure 7. ^{1}H NMR spectrum of quaternized sample B1 terpolymer (DP 368) in $CDCl_3$.

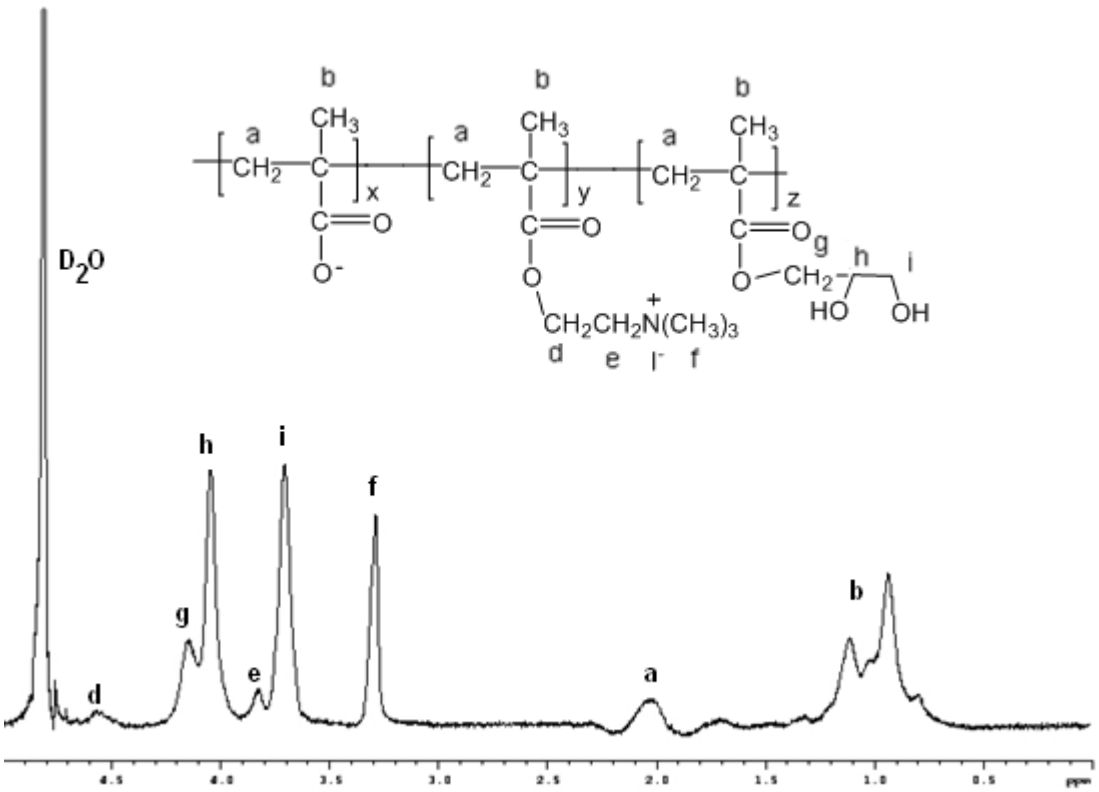

Figure 8. ^{1}H NMR spectrum of deprotected sample B1 quaternized polymer (DP 368) in D_2O.

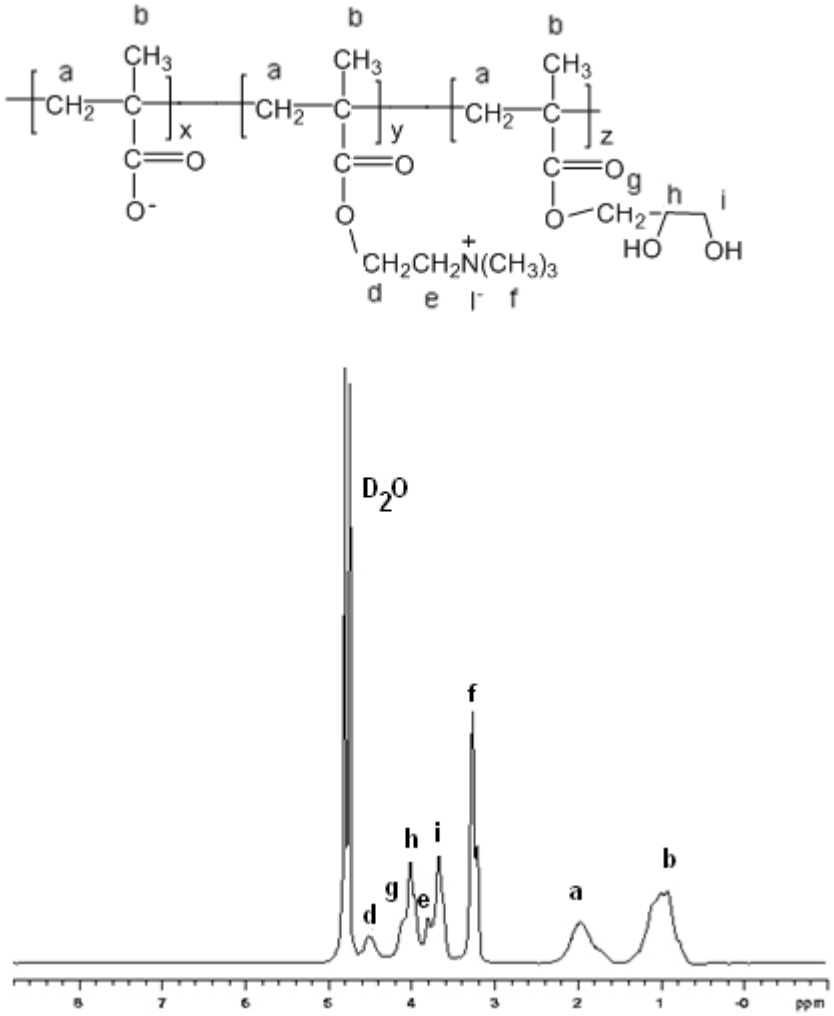

Figure 9. ^{1}H NMR spectrum of deprotected sample B4 quaternized polymer (DP 263) in D_2O.

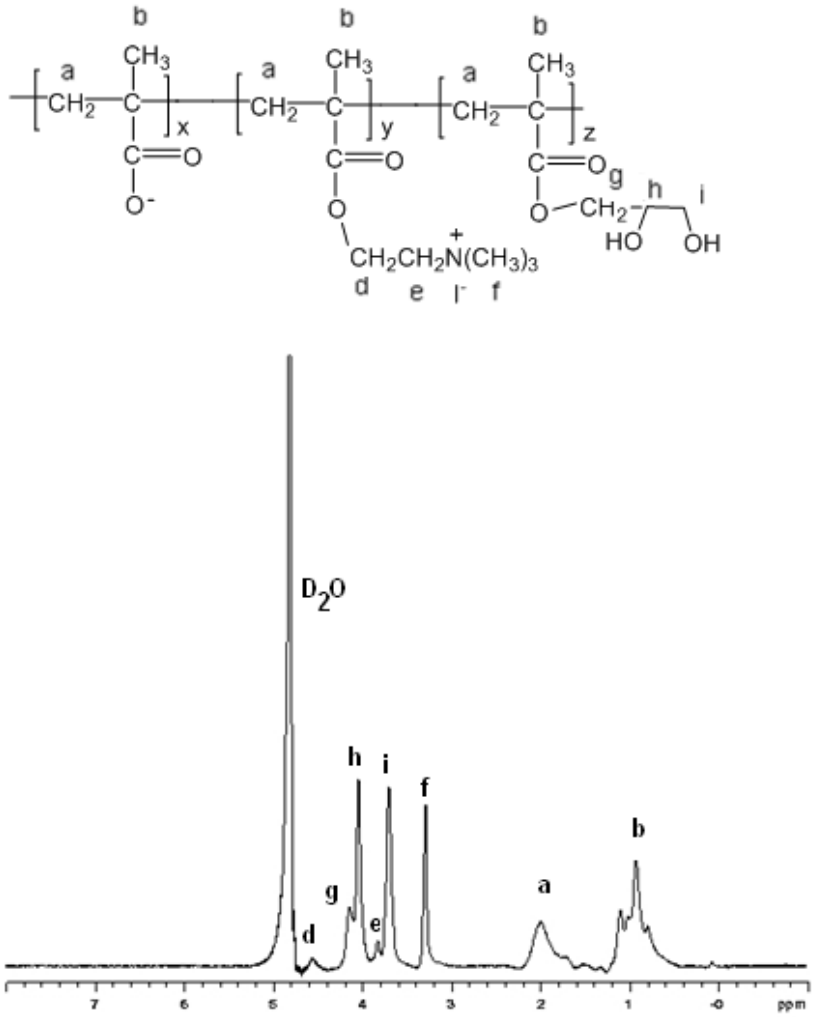

Figure 10. [1]H NMR spectrum of deprotected sample B10 quaternized polymer (DP 1825) in D_2O.

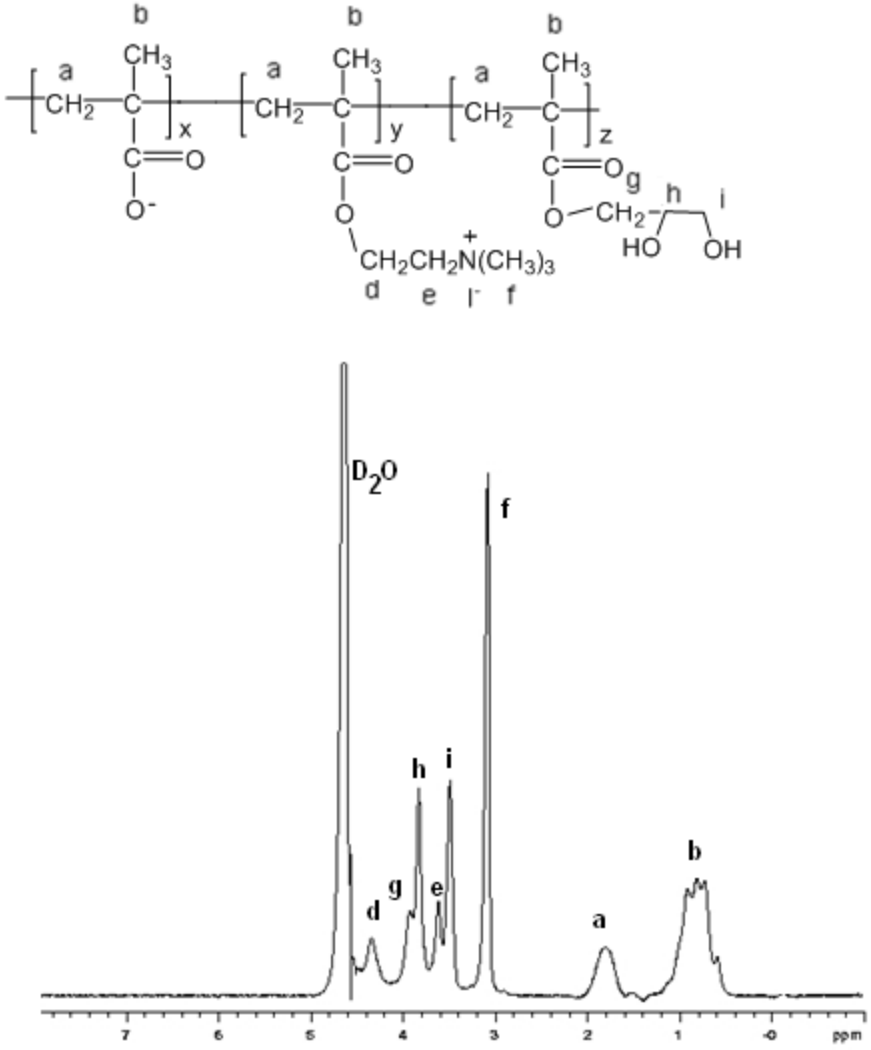

Figure 11. ^{1}H NMR spectrum of deprotected sample B11 quaternized polymer (DP 1075) in D_2O.

VITA

Baljinder Kaur

Candidate for the Degree of

Doctor of Philosophy

Thesis: SEMI-FLUORINATED CORE-SHELL LATEXES AND MODEL RANDOM POLYAMPHOLYTES

Major Field: Chemistry

Biographical:

Personal Data: Born in Gahot, INDIA, March, 1981. Daughter of Harkishan Singh and Shanti Devi. Married to Jagjit Singh Saini, July, 2006.

Education:

Completed the requirements for the Doctor of Philosophy in Chemistry at Oklahoma State University, Stillwater, Oklahoma in July, 2010.

Received the Master of Science in Organic Chemistry at Punjabi University, Patiala, India in 2003.

Received the Bachelor of Science in Chemistry at Punjab University, Chandigarh, India in 2001.

Experience: Lecturer of Chemistry at G.K.M.S College, Tanda Urmar, India, August, 2003 to May, 2005; Instructor of Chemistry at Khalsa Public School, India, August, 2005 to May, 2006; Teaching Assistant, Department of Chemistry, Oklahoma State University, January, 2007 to December, 2008, Research Assistant, Department of Chemistry, Oklahoma State University, January, 2009 to May, 2010

Professional Memberships: American Chemical Society

Name: BALJINDER KAUR Date of Degree: July, 2010

Institution: Oklahoma State University Location: Stillwater, Oklahoma

Title of Study: SEMI-FLUORINATED CORE-SHELL LATEXES AND MODEL RANDOM POLYAMPHOLYTES

Pages in Study: 147 Candidate for the Degree of Doctor of Philosophy

Major Field: Chemistry

Scope and Method of Study: Cationic polymer colloids in aqueous medium find applications in phase transfer catalysis. We have synthesized core shell latex particles with quaternary ammonium ion by emulsifier free shot growth emulsion polymerization. Model random polyampholytes are needed to test the modern theory of polyampholytes. We have synthesized random polyampholytes by living radical polymerization namely reversible-addition fragmentation chain transfer polymerization in order to understand dilute and semi-dilute solution properties of polyampholytes.

Findings and Conclusions: Hydrolysis of simulants of chemical warfare agents such as *p*-nitrophenyl hexanoate and Paraoxon was faster using cationic polymer dispersions than hydrolysis with coatings made from the aqueous dispersions. The aqueous solution properties of polyampholytes such as viscosity as function of pH and electrolyte concentration showed that the polyampholytes synthesized are charge imbalanced.

ADVISER'S APPROVAL: Warren T. Ford